Electronic Supplementary Material (ESI) for RSC Advances.
This journal is © The Royal Society of Chemistry 2019

# Synthesis, characterization, and photoluminescent studies of three-coordinate Cu(I)-NHC complexes bearing unsymmetrically-substituted dipyridylamine ligands

Kwame Glinton,[a] Reza Latifi,[a] David S. Cockrell,[a] Matthew Bardeaux,[a] Bachkhoa Nguyen,[a] and Laleh Tahsini,*[a]

[a] *Department of Chemistry, Oklahoma State University, Stillwater, Oklahoma 74078, United States.*

**Single-crystal X-ray crystallography.** A summary of crystal data and refinement details for all compounds is given in Table S1 and Table S2. For complexes **1-3**, **6-8**, and **12**, crystals were removed from the crystallization vial and immediately coated with Non-drying Immersion Oil for Microscopy (Type B, Formula Code: 1248) on a glass slide. A suitable crystal was mounted in oil on a MiTeGen loop and cooled to 100 K in a stream of cold $N_2$ using Bruker Kryoflex low temperature device. X-ray diffraction data for all complexes were collected on a Bruker Smart APEX II diffractometer with a CCD detector using combinations of ϕ and ω scans with Mo(Kα) radiation (λ = 0.71073 Å). Unit cell determination and data collection were done under APEX2 software package,[1] while data integration employed the Bruker SAINT software package.[2] Multi-scan absorption corrections were done by using SADABS.[3] All structures were solved by direct methods and refined by full-matrix least-squares on $F^2$ using the SHELXTL suite.[4] The non-hydrogen atoms were refined anisotropically and hydrogen atoms were placed geometrically and refined using the riding model. Images were generated by using ORTEP-3.[5] CCDC 1861502, 1865893, 1865901, 1866337, 1866344, 1866360, 1556652, and 1918545 contains the supplementary crystallographic data for this paper. These data can be obtained free of charge from The Cambridge Crystallographic Data Centre via www.ccdc.cam.ac.uk/data_request/cif.

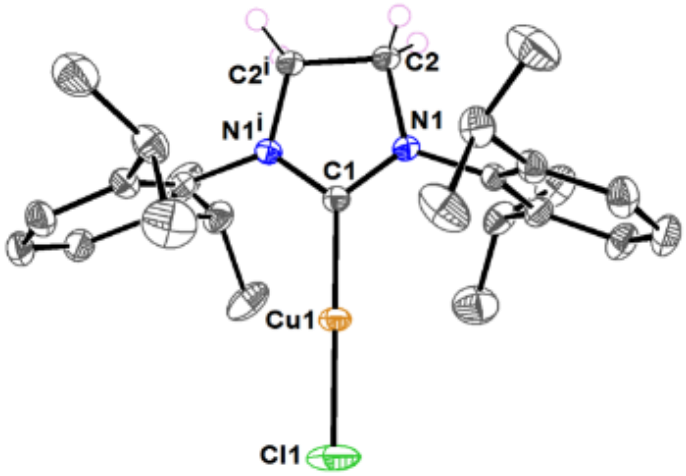


**Figure S1.** ORTEP diagrams of [Cu(SIPr)Cl]. Some hydrogen atoms are omitted for clarity. Ellipsoids are shown at the 55% probability level.

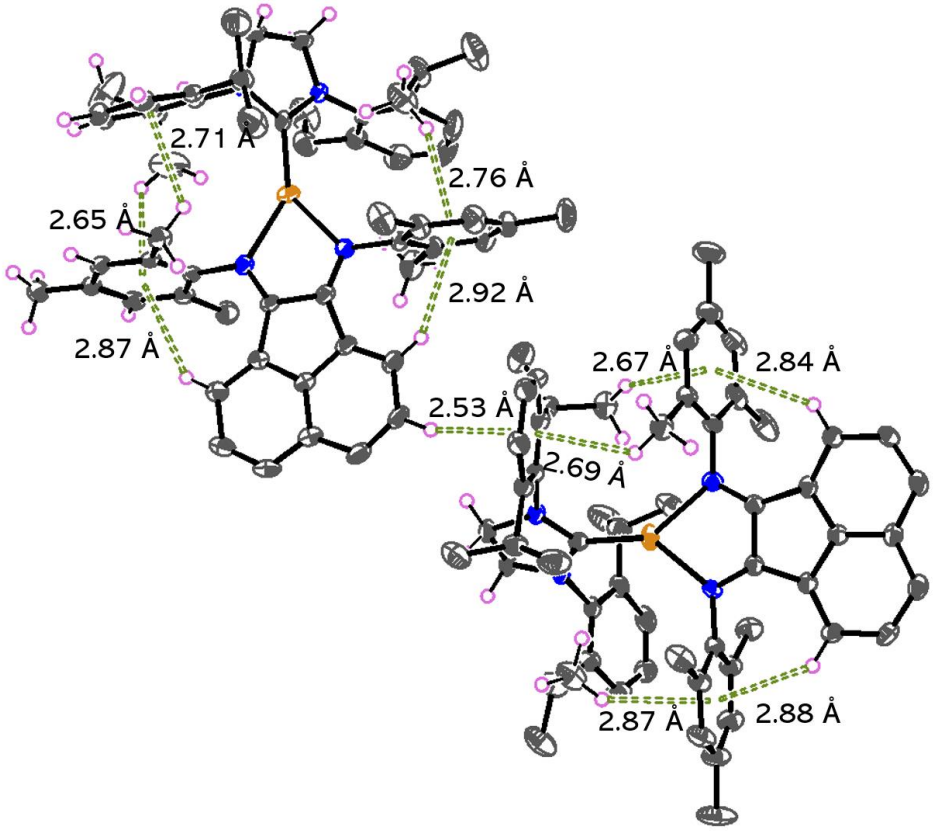


**Figure S2.** ORTEP diagram of [Cu(SIPr)(mesBIAN)]$PF_6$ (**12**) displaying two cation complexes in the unit cell. Anions and some hydrogen atoms are omitted for clarity. The hydrogen-bonding interactions with the anions are not shown. Ellipsoids are shown at the 55% probability level.

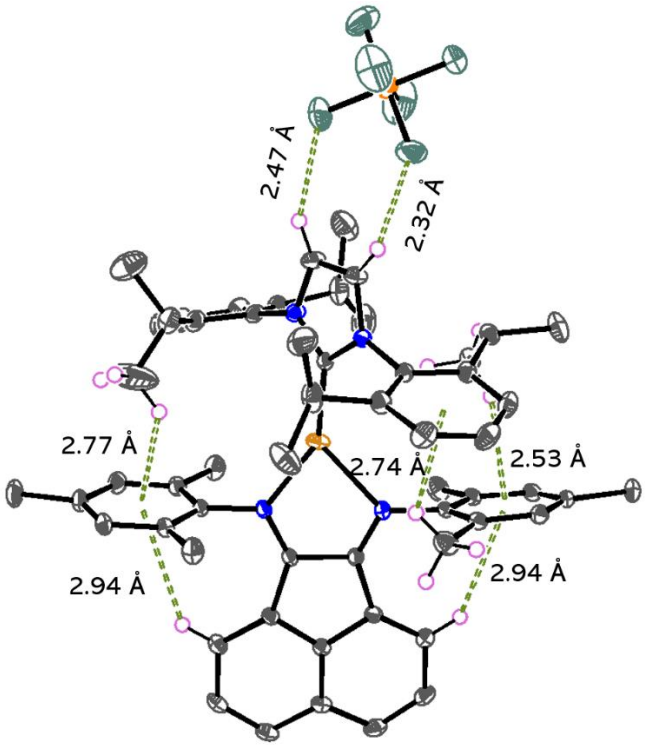


**Figure S3.** ORTEP diagram of [Cu(IPr)(mesBIAN)]$PF_6$ (**6**). Some hydrogen atoms are omitted for clarity and those involved in CH…π and CH…F interactions are displayed. Ellipsoids are shown at the 55% probability level.

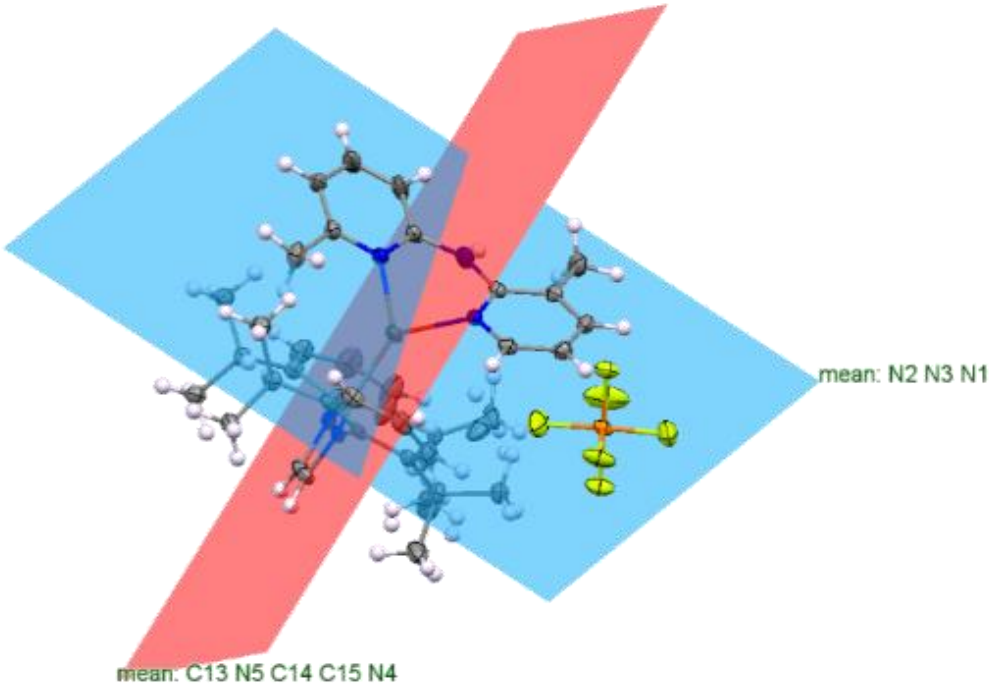


**Figure S4.** An exemplary representation of the angle formed between the NHC ring and the plane containing three N atoms of 3,6-$Me_2$Hdpa ligand in complex **3**.

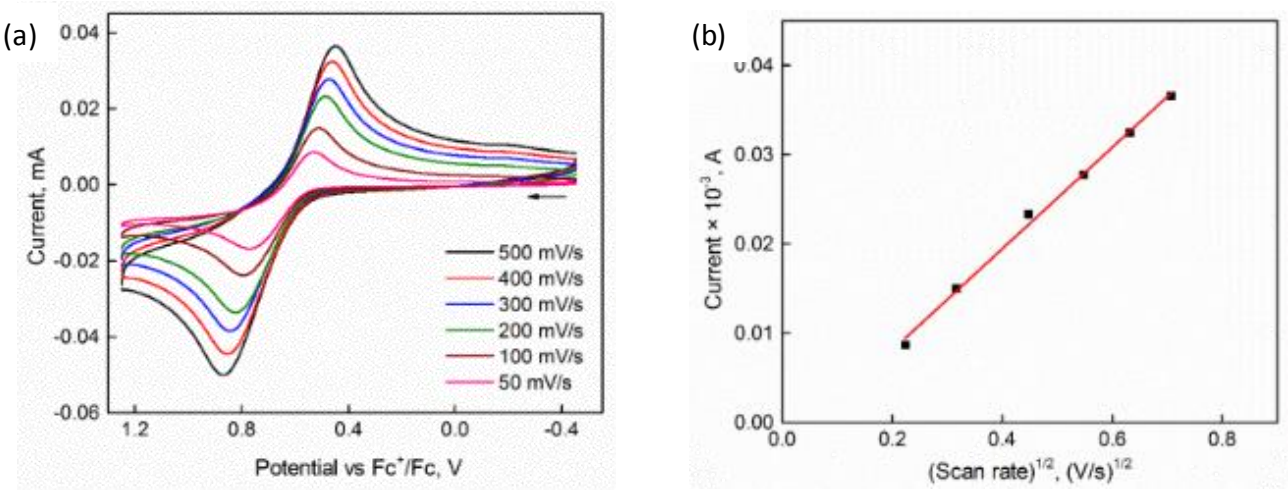


**Figure S5.** (a) Cyclic voltammograms of [Cu(IPr)(Hdpa)]$PF_6$, **4** (2.0 mM) at varying scan rates in de-aerated $CH_2Cl_2$ containing 0.1 M $^nBu_4PF_6$. (b) The plot of anodic peak current as a function of the square root of scan rate.

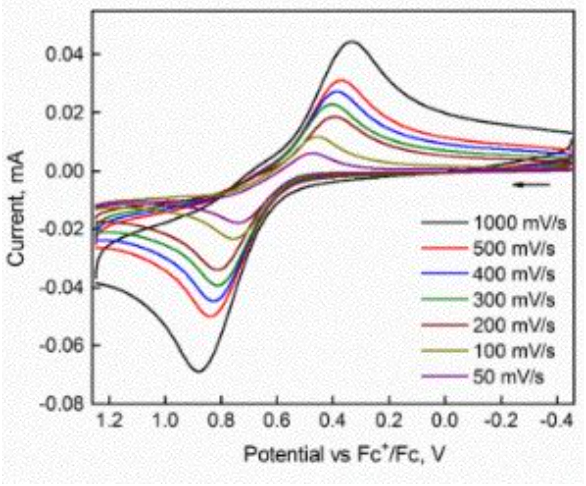


**Figure S6.** Cyclic voltammograms of [Cu(IPr)(3,3'-$Me_2$Hdpa)]$PF_6$, **5** (2.0 mM) at varying scan rates in de-aerated $CH_2Cl_2$ containing 0.1 M $^nBu_4PF_6$.

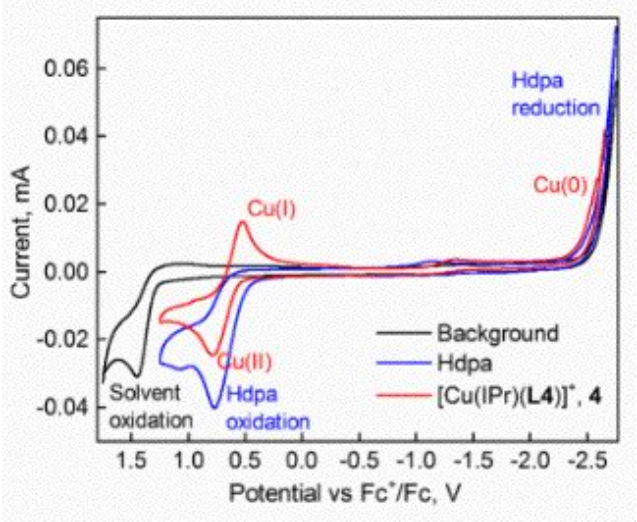


**Figure S7.** Cyclic voltammograms of [Cu(IPr)(**L4**)]$PF_6$, **4** (2.0 mM), Hdpa (2.0 mM), and the background in de-aerated $CH_2Cl_2$ containing 0.1 M $^nBu_4PF_6$.

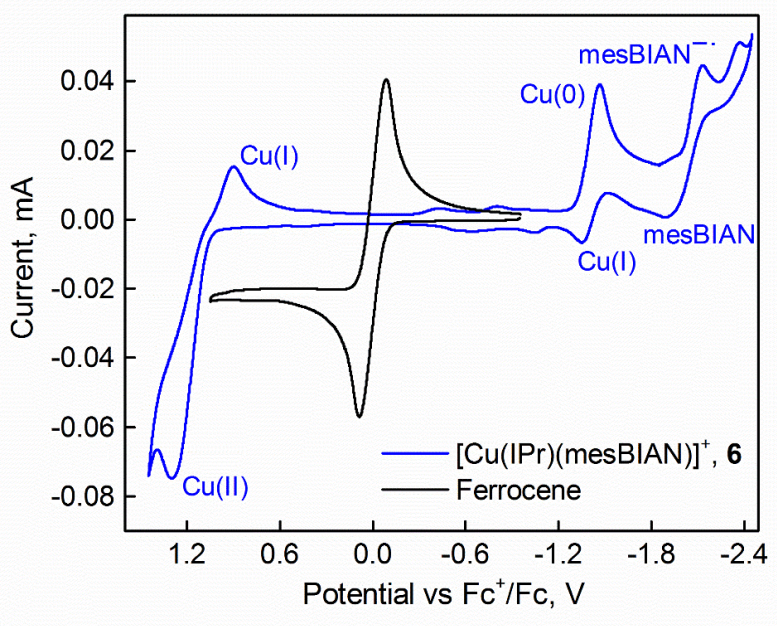


**Figure S8.** Cyclic voltammogram of [Cu(IPr)(mesBIAN)]$PF_6$, **6** (2.0 mM) superimposed on the CV of ferrocene (2.0 mM) in de-aerated $CH_2Cl_2$ containing 0.1 M $^nBu_4PF_6$ to indicate the possible one-electron oxidation and reduction waves.

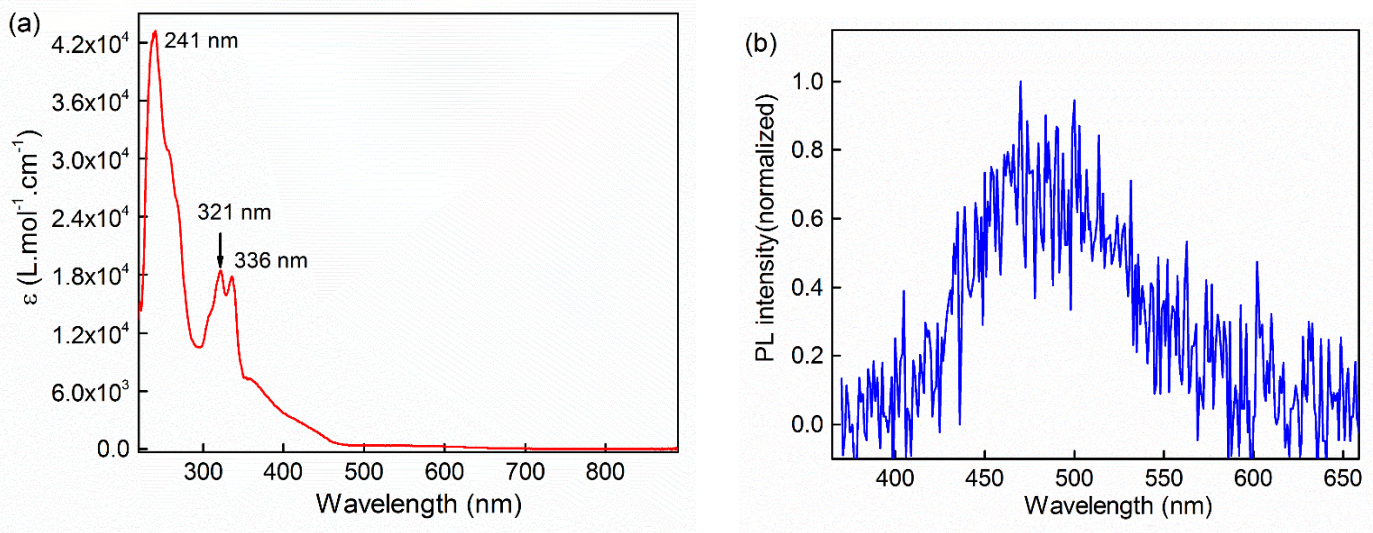


**Figure S9.** (a) Absorption spectra of complex **6** in $CH_2Cl_2$ solution at room temperature. (b) Photoluminescent (PL) spectra of **6** in the solid state.

**Table S1.** Summary of X-ray Crystallographic Data Collection Parameters for [Cu(IPr)(N^N)]$PF_6$ Complexes

| | [Cu(IPr)(**L1**)]$PF_6$ (**1**) | [Cu(IPr)(**L2**)]$PF_6$•0.5 $CH_3CN$ (**2**) | [Cu(IPr)(**L3**)]$PF_6$ (**3**) | [Cu(IPr)(**L6**)]$PF_6$ (**6**) |
|---|---|---|---|---|
| formula | $C_{39}H_{49}CuF_6N_5P$ | $C_{40}H_{50.50}CuF_6N_{5.50}P$ | $C_{39}H_{49}CuF_6N_5P$ | $C_{57}H_{64}CuF_6N_4P$ |
| Mr (g $mol^{-1}$) | 796.34 | 816.87 | 796.34 | 1013.63 |
| T (K) | 100 | 100 | 100 | 100 |
| λ (Å) | 0.71073 | 0.71073 | 0.71073 | 0.71073 |
| crystal system | monoclinic | monoclinic | monoclinic | monoclinic |
| space group | P 1 21/c 1 | P 1 21/n 1 | P 1 21/n 1 | P $2_1$/n |
| a (Å) | 9.6743(14) | 11.260(1) | 18.788(3) | 16.29(2) |
| b (Å) | 40.711(6) | 8.112(3) | 10.7257(15) | 14.23(2) |
| c (Å) | 20.576(3) | 12.5861(11) | 19.777(3) | 22.83(3) |
| α (deg) | 90 | 90 | 90 | 90 |
| β (deg) | 99.180(2) | 92.111(1) | 105.029(2) | 102.63(2) |
| γ (deg) | 90 | 90 | 90 | 90 |
| V ($Å^3$) | 8000(2) | 3981.3(6) | 3849.1(9) | 5162(13) |
| Z | 8 | 4 | 4 | 4 |
| ρcalc (g $cm^{-3}$) | 1.322 | 1.363 | 1.374 | 1.304 |
| μ ($mm^{-1}$) | 0.648 | 0.653 | 0.673 | 0.517 |
| F (000) | 3328.0 | 1708.0 | 1664.0 | 2128.0 |
| 2ϑ max (deg) | 28.700 | 28.282 | 28.282 | 29.187 |
| h,k,l max | 13,55,27 | 15,37,16 | 25,14,26 | 22,19,31 |
| no. of reflns collected | 131738 | 78856 | 58630 | 79683 |
| no. of unique reflns | 20652 | 9866 | 9548 | 13917 |
| R (int) | 0.0377 | 0.0442 | 0.0522 | 0.0297 |
| final R indices (I > 2σ) | 0.0436 | 0.0403 | 0.0409 | 0.0392 |
| R(F)[a] | 0.0515 | 0.0522 | 0.0533 | 0.0498 |
| R ($wF^2$)[b] | 0.0974 | 0.0987 | 0.1130 | 0.1066 |
| GOF on $F^2$ | 1.084 | 1.064 | 1.029 | 1.025 |

**Table S2.** Summary of X-ray Crystallographic Data Collection Parameters for [Cu(SIPr)Cl and [Cu(SIPr)(N^N)]$PF_6$ Complexes

| | [Cu(SIPr)Cl | [Cu(SIPr)(**L1**)]$PF_6$ (**7**) | [Cu(SIPr)(**L2**)]$PF_6$ (**8**) | [Cu(SIPr)(**L6**)]$PF_6$ (**12**) |
|---|---|---|---|---|
| formula | $C_{27}H_{38}ClCuN_2$ | $C_{39}H_{51}CuF_6N_5P$ | $C_{39}H_{51}CuF_6N_5P$ | $C_{58.50}H_{68.50}Cl_3CuF_6N_4P$ |
| Mr (g $mol^{-1}$) | 489.58 | 798.35 | 798.35 | 1142.53 |
| T (K) | 100 | 100 | 100 | 100 |
| λ (Å) | 0.71073 | 0.71073 | 0.71073 | 0.71073 |
| crystal system | orthorhombic | monoclinic | monoclinic | triclinic |
| space group | P c c n | P 1 21/c 1 | P 1 21/n 1 | P -1 |
| a (Å) | 10.8441(10) | 9.7826(10) | 14.048(4) | 12.683(11) |
| b (Å) | 12.6667(12) | 40.521(4) | 14.466(5) | 18.454(16) |
| c (Å) | 18.9978(18) | 20.629(2) | 19.223(6) | 25.59(2) |
| α (deg) | 90 | 90 | 90 | 87.913(15) |
| β (deg) | 90 | 99.209(2) | 92.497(5) | 80.698(14) |
| γ (deg) | 90 | 90 | 90 | 71.923(14) |
| V ($Å^3$) | 2609.5(4) | 8071.9(14) | 3903(2) | 5618(9) |
| Z | 4 | 4 | 4 | 4 |
| ρcalc (g $cm^{-3}$) | 1.246 | 1.314 | 1.359 | 1.351 |
| μ ($mm^{-1}$) | 0.955 | 0.642 | 0.664 | 0.621 |
| F (000) | 1040.0 | 3344.0 | 1672.0 | 2386.0 |
| 2ϑ max (deg) | 30.026 | 27.103 | 28.699 | 26.732 |
| h,k,l max | 15,17,26 | 12,51,26 | 18,19,25 | 16,23,32 |
| no. of reflns collected | 51307 | 118528 | 73056 | 97454 |
| no. of unique reflns | 3812 | 17833 | 10048 | 23779 |
| R (int) | 0.0404 | 0.0577 | 0.0597 | 0.0859 |
| final R indices (I > 2σ) | 0.0285 | 0.0449 | 0.0414 | 0.0625 |
| R(F)[a] | 0.0387 | 0.0592 | 0.0610 | 0.1067 |
| R ($wF^2$)[b] | 0.0790 | 0.0980 | 0.1303 | 0.1936 |
| GOF on $F^2$ | 1.037 | 1.067 | 1.066 | 1.042 |

**Table S3.** Correlation of the selected long-range interactions and quantum yields in [Cu(NHC)(N^N)]$PF_6$ complexes

| Complex | CH…π (Å) | NH/CH…F (Å)[a] | Plane angle θ (deg) | PLQY | Ref |
|---|---|---|---|---|---|
| [Cu(IPr)(**L1**)]$PF_6$ (**1**) | Cu1 2.78<br>Cu2 2.45<br>2.70 | Cu1 2.25 (NH)<br>2.48, 2.54 (CH)<br>Cu2 2.25 (NH)<br>2.31(CH) | Cu1 35.52<br>Cu2 59.76 | 0.48 | This work |
| [Cu(IPr)(**L2**)]$PF_6$ (**2**) | 2.58<br>2.95 | 2.43 (NH)<br>2.43 (CH) | 47.13 | 0.49 | This work |
| [Cu(IPr)(**L3**)]$PF_6$ (**3**) | | 2.68 (CH) | 76.06 | 0.64 | This work |
| [Cu(IPr)(**L4**)]$PF_6$ (**4**) | 2.43<br>2.48 | 2.15 (NH)<br>2.78 (NH)<br>2.54 (CH) | 19.95 | 0.22 | 35 (main) text |
| [Cu(IPr)(**L5**)]$PF_6$ (**5**) | Cu1 2.74<br>Cu2 2.42<br>2.74 | | 22.40 | 0.86 | 35 (main text) |
| [Cu(SIPr)(**L1**)]$PF_6$ (**7**) | Cu1 2.74<br>Cu2 2.42<br>2.74 | 2.26 (NH)<br>2.50 (CH)<br>2.28 (CH) | Cu1 38.77<br>Cu2 59.59 | 0.55 | This work |
| [Cu(SIPr)(**L2**)]$PF_6$ (**8**) | 2.46<br>2.94 | 2.24 (NH)<br>2.61 (CH) | 45.04 | 0.33 | This work |
| [Cu(SIPr)(**L4**)]$PF_6$ (**10**) | 2.59<br>2.69 | | 49.37 | 0.88 | 34 (main text) |

[a] only the hydrogen-bonding interactions of the pyridyl rings of the Hdpa ligands have been considered.

**DFT/TD-DFT Computational Studies**

The Gaussian 09 calculations[6] were performed with the non-local hybrid functional UB3LYP,[7] the standalone Truhlar functional M06,[8] and long-range corrected functional wB97XD.[9] The double zeta quality Los Almos ECP and valence basis set, LANL2DZ,[10] and Pople and Ahlrichs type basis set 6-31+G(d,p) were used.[11-19] The geometries of complexes were fully optimized at three levels using basis sets LANL2DZ and 6-31+G(d,p). All optimized geometries are characterized as stationary points on the potential energy surface (PES) with vibrational frequency calculations. TD-DFT calculations were performed on the equilibrium ground state geometries with the same DFT levels and 6-31+G(d,p) basis set. Molecular orbital compositions were determined by Mulliken contribution type (Tables S5-S6). The singlet and triplet states density were analyzed via natural transition orbital (NTO), an approach that determines the MO distribution of GS and ES by considering all the MOs involved in the electronic transition and weighing them by the CI coefficients (Tables S9-S10).[20] Visualization of HOMO and LUMO and the graphical representation of NTO analysis have been performed with ChemCraft and Chemissian programs, respectively.

**Table S4.** Calculated structural parameters and deviations of [Cu(IPr)(N^N)]$^+$ and [Cu(SIPr)(N^N)]$^+$ cations for various functionals and basis sets

| | $Cu–C_{NHC}$ (Å) | | $Cu–N_{N^N}$ (Å) | | $C_{NHC}–Cu–N_{N^N}$ (°) | | $N_{N^N}–Cu–N_{N^N}$ (°) | | CH…π (Å)[a] | | Functional/basis set |
|---|---|---|---|---|---|---|---|---|---|---|---|
| [Cu(IPr)(**L1**)]$^+$ (**1**) | 1.929 | 1.2% | 2.042<br>2.048 | 1.3%<br>0.2% | 133.59<br>134 | -0.4%<br>-0.9% | 91.35 | 1.2% | 2.539<br>2.578 | 3.7%<br>-4.5% | M06/LANL2DZ |
| | 1.96 | 2.8% | 2.082<br>2.093 | 3.3%<br>2.4% | 134.68<br>134.86 | 0.4%<br>-0.3% | 90.26 | -0.1% | 2.546<br>2.648 | 4.0%<br>-1.9% | UB3LYP/LANL2DZ |
| | 1.94 | 1.8% | 2.051<br>2.063 | 1.8%<br>0.9% | 133.84<br>133.92 | -0.2%<br>-1.0% | 91.09 | 0.9% | 2.426<br>2.644 | -0.9%<br>-2.0% | wB97XD/LANL2DZ |
| | 1.925 | 1.0% | 2.062<br>2.07 | 2.3%<br>1.3% | 134.33<br>134.91 | 0.2%<br>-0.2% | 89.85 | -0.5% | 2.575<br>2.641 | 5.2%<br>-2.1% | M06/6-31+G(d,p) |
| | 1.945 | 2.0% | 2.094<br>2.109 | 3.9%<br>3.2% | 135.47<br>135.49 | 1.0%<br>0.2% | 88.87 | -1.6% | 2.59<br>2.716 | 5.8%<br>0.6% | UB3LYP/6-31+G(d,p) |
| | 1.921 | 0.8% | 2.059<br>2.069 | 2.2%<br>1.2% | 134.38<br>134.76 | 0.2%<br>-0.4% | 89.94 | -0.4% | 2.427<br>2.67 | -0.9%<br>-1.1% | wB97XD/6-31+G(d,p) |
| [Cu(IPr)(**L2**)]$^+$(**2**) | 1.93 | 1.6% | 2.047<br>2.048 | 0.7%<br>0.3% | 133.58<br>134.42 | -0.5%<br>-1.3% | 91.38 | 3.0% | 2.44<br>2.754 | -5.5%<br>-6.6% | M06/LANL2DZ |
| | 1.959 | 3.1% | 2.078<br>2.083 | 2.3%<br>2.1% | 133.98<br>134.35 | -0.2%<br>-1.4 | 91.59 | 3.2% | 2.581 | 0.0% | UB3LYP/LANL2DZ |
| | 1.937 | 1.9% | 2.049<br>2.062 | 0.8%<br>1.0% | 132.91<br>134.57 | -1.0%<br>-1.2% | 91.19 | 2.7% | 2.438<br>2.809 | -5.6%<br>-4.7% | wB97XD/LANL2DZ |
| | 1.926 | 1.4% | 2.057<br>2.077 | 1.2%<br>1.8% | 134.05<br>135.57 | -0.1%<br>-0.5% | 89.74 | 1.1% | 2.542<br>2.775 | -1.5%<br>-5.9% | M06/6-31+G(d,p) |
| | 1.942 | 2.2% | 2.093<br>2.108 | 3.0%<br>3.3% | 135.06<br>135.9 | 0.6%<br>-0.2% | 88.71 | -0.1% | 2.576 | -0.2% | UB3LYP/6-31+G(d,p) |
| | 1.918 | 0.9% | 2.056<br>2.07 | 1.2%<br>1.4% | 133.48<br>135.17 | -0.5%<br>-0.8% | 89.99 | 1.4% | 2.458<br>2.833 | -4.8%<br>-3.9% | wB97XD/6-31+G(d,p) |
| [Cu(IPr)(**L3**)]$^+$ (**3**) | 1.939 | 2.8% | 2.052<br>2.064 | 1.6%<br>1.7% | 132.56<br>136.81 | -1.1%<br>1.8% | 88.97 | -0.1% | 2.445 | -34.5% | M06/LANL2DZ |
| | 1.945 | 3.1% | 2.064<br>2.098 | 2.2%<br>3.4% | 134.37<br>135.64 | 0.3%<br>0.9% | 89.29 | 0.3% | 2.94 | -21.2% | UB3LYP/LANL2DZ |
| | 1.943 | 3.0% | 2.059<br>2.072 | 1.9%<br>2.1% | 132.02<br>136.36 | -1.5%<br>1.4% | 89.16 | 0.1% | 2.497 | -33.1% | wB97XD/LANL2DZ |
| | 1.934 | 2.5% | 2.083<br>2.088 | 3.1%<br>2.9% | 132.73<br>139.18 | -1.0%<br>3.5% | 86.54 | -2.8% | 2.523 | -32.4% | M06/6-31+G(d,p) |
| | 1.929 | 2.2% | 2.08<br>2.121 | 3.0%<br>4.5% | 135.42<br>137.1 | 1.0%<br>2.0% | 86.82 | -2.5% | 2.987 | -20.0% | UB3LYP/6-31+G(d,p) |
| | 1.923 | 1.9% | 2.072<br>2.082 | 2.6%<br>2.6% | 132.35<br>137.83 | -1.2%<br>2.5% | 87.64 | -1.6% | 2.521 | -32.5% | wB97XD/6-31+G(d,p) |
| [Cu(IPr)(**L4**)]$^+$ (**4**) | 1.947 | 1.2% | 2.06<br>2.061 | 0.5%<br>-0.1% | 133.92<br>134.01 | 0.0%<br>-1.6% | 92.05 | 2.3% | 2.32<br>2.385 | -4.0%<br>-6.9% | M06/LANL2DZ |
| | 1.963 | 2.1% | 2.084 | 1.7%<br>1.0% | 134.08<br>134.36 | 0.2%<br>-1.3% | 91.56 | 1.8% | 2.659<br>2.709 | 10.0%<br>5.7% | UB3LYP/LANL2DZ |
| | 1.939 | 0.8% | 2.056<br>2.061 | 0.3%<br>-0.1% | 133.46<br>133.98 | -0.3%<br>-1.6% | 91.19 | 1.3% | 2.434<br>2.658 | 0.7%<br>3.7% | wB97XD/LANL2DZ |
| | 1.944 | 1.1% | 2.078<br>2.083 | 1.4%<br>1.0% | 134.56<br>134.85 | 0.5%<br>-0.9% | 90.58 | 0.7% | 2.345<br>2.415 | -3.0%<br>-5.8% | M06/6-31+G(d,p) |
| | 1.947 | 1.2% | 2.097<br>2.102 | 2.3%<br>1.9% | 134<br>136.13 | 0.1%<br>0.0% | 89.83 | -0.2% | 2.509<br>2.868 | 3.8%<br>11.9% | UB3LYP/6-31+G(d,p) |
| | 1.919 | -0.2% | 2.063<br>2.068 | 0.6%<br>0.2% | 127.45<br>128.74 | -4.8%<br>-5.4% | 89.96 | 0.0% | 2.473<br>2.691 | 2.3%<br>5.0% | wB97XD/6-31+G(d,p) |
| [Cu(IPr)(**L5**)]$^+$ (**5**) | 1.931 | 0.5% | 2.046<br>2.047 | -0.6%<br>-0.6% | 128.2<br>128.44 | 0.1%<br>-0.6% | 91.96 | 2.6% | 2.496<br>2.567 | 2.6%<br>3.4% | M06/LANL2DZ |
| | 1.958 | 1.9% | 2.086<br>2.087 | 1.4%<br>1.4% | 134.87<br>134.89 | 5.3%<br>4.4% | 89.97 | 0.4% | 2.638 | 8.4% | UB3LYP/LANL2DZ |
| | 1.94 | 1.0% | 2.055<br>2.057 | -0.1%<br>-0.1% | 133.65<br>133.82 | 4.4%<br>3.6% | 91.18 | 1.7% | 2.441<br>2.709 | 0.3%<br>9.1% | wB97XD/LANL2DZ |
| | 1.926 | 0.3% | 2.064<br>2.069 | 0.3%<br>0.5% | 134.2<br>134.26 | 4.8%<br>3.9% | 90.42 | 0.9% | 2.551<br>2.628 | 4.8%<br>5.9% | M06/6-31+G(d,p) |
| | 1.942 | 1.1% | 2.101 | 2.1% | 135.73 | 6.0% | 88.31 | -1.5% | 2.722 | 11.9% | UB3LYP/6-31+G(d,p) |
| | 1.918 | -0.2% | 2.06<br>2.068 | 0.1%<br>0.4% | 133.91<br>134.52 | 4.6%<br>4.1% | 89.98 | 0.4% | 2.522<br>2.68 | 3.7%<br>8.0% | wB97XD/6-31+G(d,p) |

[a] Distance between the hydrogen and the phenyl ring center.

**Table S4 (continued).**

| | Cu–$C_{NHC}$ (Å) | | Cu–$N_{N^N}$ (Å) | | $C_{NHC}$–Cu–$N_{N^N}$ (°) | | $N_{N^N}$–Cu–$N_{N^N}$ (°) | | CH…π (Å)[a] | | Functional/basis set |
|---|---|---|---|---|---|---|---|---|---|---|---|
| [Cu(IPr)(**L6**)]$^+$(**6**) | 1.93 | 0.4% | 2.039<br>2.221 | -1.1%<br>-0.4% | 132.79<br>147.34 | -0.8%<br>-0.2% | 79.76 | 1.7% | 2.469<br>2.641<br>2.772<br>2.773<br>2.85 | -2.5%<br>-4.6%<br>1.2%<br>-5.6%<br>-4.5% | M06/LANL2DZ |
| | 1.958 | 1.9% | 2.154<br>2.167 | 4.5%<br>-2.9% | 139.78<br>140.5 | 4.4%<br>-4.9% | 79.72 | 1.7% | 2.689<br>2.694<br>3.016<br>2.806<br>2.807 | 6.2%<br>-2.7%<br>10.1%<br>-4.5%<br>-5.9% | UB3LYP/LANL2DZ |
| | 1.934 | 0.6% | 2.097<br>2.121 | 1.7%<br>-4.9% | 137.66<br>141.7 | 2.8%<br>-4.1% | 80.65 | 2.9% | 2.488<br>2.526<br>2.767<br>2.859<br>2.865 | -1.7%<br>-8.7%<br>1.0%<br>-2.7%<br>-4.0% | wB97XD/LANL2DZ |
| | 1.93 | 0.4% | 2.015<br>2.312 | -2.3%<br>3.6% | 125.52<br>130.73 | -6.2%<br>-11.5% | 78.05 | -0.4% | 2.659<br>2.671<br>2.791<br>2.735<br>2.78 | 5.0%<br>-3.5%<br>1.9%<br>-6.9%<br>-6.8% | M06/6-31+G(d,p) |
| | 1.94 | 0.9% | 1.998<br>2.548 | -3.1%<br>14.2% | 128.42<br>156.54 | -4.1%<br>6.0% | 75.03 | -4.3% | 2.734<br>2.773<br>2.658<br>2.755 | 8.0%<br>0.2%<br>-9.5%<br>-7.6% | UB3LYP/6-31+G(d,p) |
| | 1.916 | -0.3% | 2.084<br>2.138 | 1.1%<br>-4.2% | 136.9<br>143.2 | 2.3%<br>-3.0% | 79.9 | 1.9% | 2.49<br>2.499<br>2.723<br>2.779<br>2.794 | -1.7%<br>-9.7%<br>-0.6%<br>-5.4%<br>-6.3% | wB97XD/6-31+G(d,p) |
| [Cu(SIPr)(**L1**)]$^+$ (**7**) | 1.927 | 0.5% | 2.022<br>2.045 | 0.0%<br>-0.3% | 128.39<br>140.66 | -4.4%<br>4.0% | 90.9 | 0.9% | 2.456 | 1.5% | M06/LANL2DZ |
| | 1.972 | 2.9% | 2.074<br>2.091 | 2.6%<br>1.9% | 133.72<br>134.9 | -0.4%<br>-0.3% | 91.37 | 1.4% | 2.635<br>2.773 | 8.9%<br>1.3% | UB3LYP/LANL2DZ |
| | 1.949 | 1.7% | 2.056<br>2.068 | 1.7%<br>0.8% | 133.66<br>134.21 | -0.5%<br>-0.8% | 90.68 | 0.6% | 2.418<br>2.663 | -0.1%<br>-2.7% | wB97XD/LANL2DZ |
| | 1.94 | 1.2% | 2.068<br>2.079 | 2.3%<br>1.3% | 134.73<br>134.78 | 0.3%<br>-0.4% | 89.66 | -0.5% | 2.422<br>2.722 | 0.1%<br>-0.6% | M06/6-31+G(d,p) |
| | 1.948 | 1.6% | 2.079<br>2.103 | 2.9%<br>2.5% | 133.35<br>136.94 | -0.7%<br>1.2% | 89.64 | -0.5% | 2.588 | 6.9% | UB3LYP/6-31+G(d,p) |
| | 1.926 | 0.5% | 2.058<br>2.077 | 1.8%<br>1.2% | 133.94<br>135.14 | -0.2%<br>-0.1% | 89.25 | -0.9% | 2.466<br>2.757 | 1.9%<br>0.7% | wB97XD/6-31+G(d,p) |
| [Cu(SIPr)(**L2**)]$^+$ (**8**) | 1.943 | 1.3% | 2.053<br>2.056 | 0.4%<br>0.5% | 133.97<br>134.09 | -0.1%<br>-1.1% | 91.12 | 1.8% | 2.454<br>2.716 | -0.3%<br>-7.6% | M06/LANL2DZ |
| | 1.968 | 2.6% | 2.079<br>2.083 | 1.7%<br>1.8% | 134.15<br>134.28 | 0.0%<br>-1.0% | 91.45 | 2.2% | 2.583 | 5.0% | UB3LYP/LANL2DZ |
| | 1.948 | 1.6% | 2.055<br>2.068 | 0.5%<br>1.1% | 132.84<br>134.89 | -1.0%<br>-0.5% | 90.77 | 1.4% | 2.425<br>2.811 | -1.5%<br>-4.4% | wB97XD/LANL2DZ |
| | 1.939 | 1.1% | 2.069<br>2.081 | 1.2%<br>1.7% | 134.81<br>135.14 | 0.5%<br>-0.3% | 89.4 | -0.1% | 2.467<br>2.796 | 0.2%<br>-4.9% | M06/6-31+G(d,p) |
| | 1.948 | 1.6% | 2.089<br>2.101 | 2.2%<br>2.7% | 134.55<br>135.88 | 0.3%<br>0.2% | 89.38 | -0.1% | 2.585 | 5.0% | UB3LYP/6-31+G(d,p) |
| | 1.926 | 0.4% | 2.062<br>2.073 | 0.8%<br>1.3% | 133.6<br>135.38 | -0.4%<br>-0.1% | 89.63 | 0.1% | 2.416<br>2.85 | -1.8%<br>-3.0% | wB97XD/6-31+G(d,p) |
| [Cu(SIPr)(**L4**)]$^+$ (**10**) | 1.952 | 2.7% | 2.058<br>2.061 | 1.4%<br>1.5% | 133.6<br>134.32 | 1.2%<br>-1.1% | 92.06 | 2.2% | 2.313<br>2.46 | -10.6%<br>-8.6% | M06/LANL2DZ |
| | 1.971 | 3.7% | 2.084<br>2.085 | 2.7%<br>2.7% | 134.27 | 1.8%<br>-1.2% | 91.46 | 1.5% | 2.73 | 5.5%<br>1.4% | UB3LYP/LANL2DZ |
| | 1.95 | 2.6% | 2.061<br>2.068 | 1.5%<br>1.8% | 133.39<br>134.24 | 1.1%<br>-1.2% | 90.81 | 0.8% | 2.417<br>2.648 | -6.6%<br>-1.6% | wB97XD/LANL2DZ |
| | 1.949 | 2.6% | 2.073<br>2.084 | 2.1%<br>2.6% | 133.86<br>135.54 | 1.4%<br>-0.2% | 90.55 | 0.5% | 2.331<br>2.529 | -9.9%<br>-6.0% | M06/6-31+G(d,p) |
| | 1.956 | 2.9% | 2.097 | 3.3% | 134.83 | -0.7% | 90.33 | 0.3% | 2.802 | 4.1% | UB3LYP/6-31+G(d,p) |
| | 1.928 | 1.5% | 2.068<br>2.073 | 1.9%<br>2.1% | 134.13<br>134.84 | 1.6%<br>-0.7% | 89.68 | -0.5% | 2.423<br>2.711 | -6.4%<br>0.7% | wB97XD/6-31+G(d,p) |

[a] Distance between the hydrogen and the phenyl ring center.

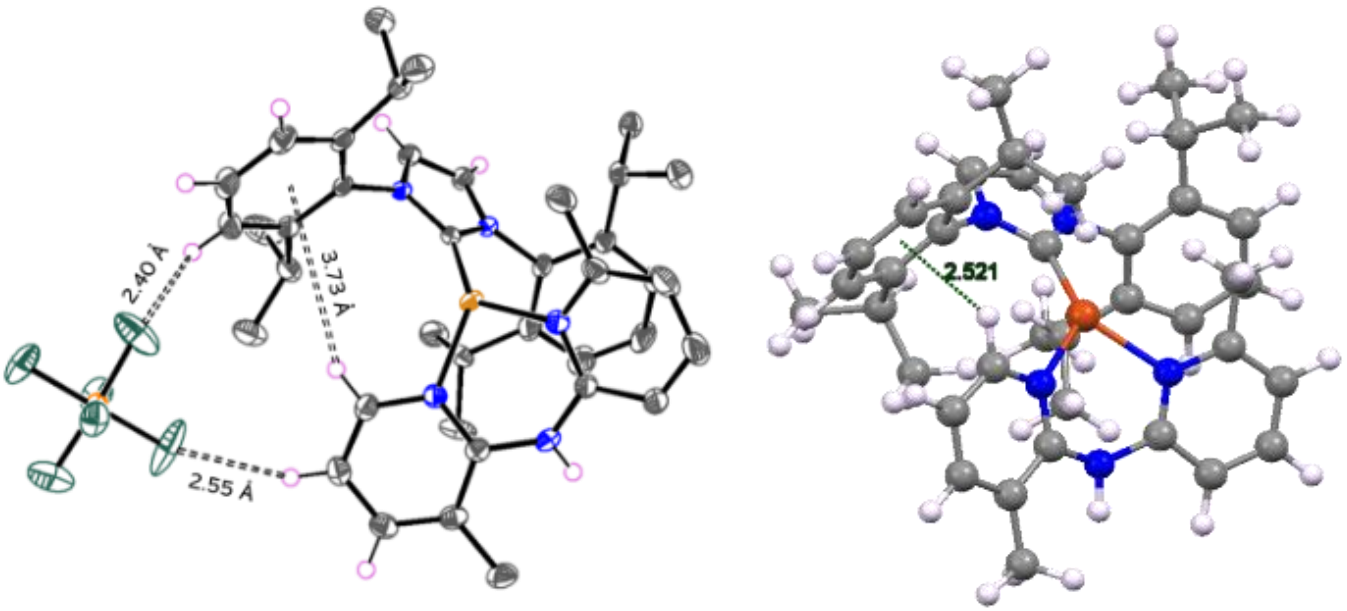


**Figure S10.** ORTEP diagram of [Cu(IPr)(3,6'-$Me_2$Hdpa)]$PF_6$ (**3**), left. Some hydrogen atoms are omitted for clarity and those involved in CH…π and CH…F interactions are displayed. Ellipsoids are shown at the 55% probability level. The optimized structure for [Cu(IPr)(3,6'-$Me_2$Hdpa)]$^+$ ion at wB97XD/6–31+G(d,p) is shown on the right.

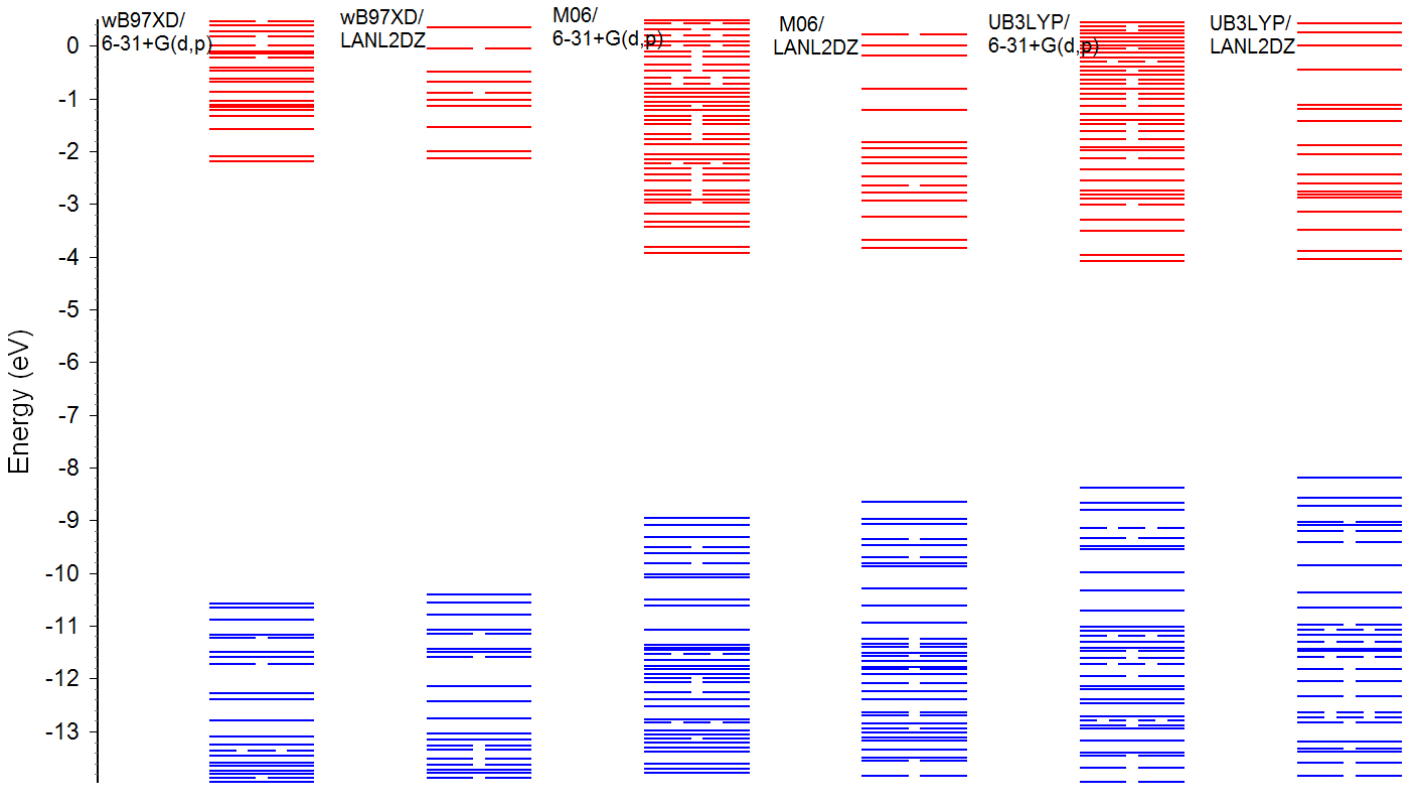


**Figure S11.** Molecular orbital energy diagrams for [Cu(IPr)(Hdpa)]$PF_6$ (**4**) calculated at three levels of theory and two basis sets.

**Table S5.** HOMO, LUMO, HOMO-LUMO levels and gaps and MO composition for the copper complexes calculated with UB3LYP

| | UB3LYP/6-31+G(d,p) | | | MO Composition [%] | | |
|---|---|---|---|---|---|---|
| | Orbital | Energy (eV) | Gap (eV) | Cu | N^N | NHC |
| [Cu(IPr)(**L1**)]$^+$ (**1**) | HOMO | -8.28 | -4.41 | 71 | 27 | 2 |
| | LUMO | -3.87 | | 1 | 99 | 1 |
| [Cu(IPr)(**L2**)]$^+$ (**2**) | HOMO | -8.29 | -4.36 | 70 | 27 | 4 |
| | LUMO | -3.94 | | 2 | 98 | 0 |
| [Cu(IPr)(**L3**)]$^+$ (**3**) | HOMO | -8.28 | -4.31 | 61 | 24 | 15 |
| | LUMO | -3.97 | | 2 | 98 | 0 |
| [Cu(IPr)(**L4**)]$^+$ (**4**) | HOMO | -8.38 | -4.30 | 67 | 26 | 7 |
| | LUMO | -4.08 | | 1 | 99 | 0 |
| [Cu(IPr)(**L5**)]$^+$ (**5**) | HOMO | -8.29 | -4.39 | 73 | 26 | 1 |
| | LUMO | -3.91 | | 1 | 99 | 0 |
| [Cu(IPr)(**L6**)]$^+$ (**6**) | HOMO | -8.06 | -2.83 | 22 | 76 | 2 |
| | LUMO | -5.23 | | 1 | 98 | 1 |
| [Cu(SIPr)(**L1**)]$^+$ (**7**) | HOMO | -8.30 | -4.40 | 68 | 27 | 5 |
| | LUMO | -3.90 | | 1 | 99 | 0 |
| [Cu(SIPr)(**L2**)]$^+$ (**8**) | HOMO | -8.34 | -4.38 | 68 | 28 | 4 |
| | LUMO | -3.96 | | 1 | 99 | 0 |
| [Cu(SIPr)(**L4**)]$^+$ (**10**) | HOMO | -8.44 | -4.34 | 70 | 27 | 3 |
| | LUMO | -4.10 | | 1 | 99 | 0 |

**Table S6.** HOMO, LUMO, HOMO-LUMO levels and gaps and MO composition for the copper complexes calculated with M06 and wB97XD

| | M06/6-31+G(d,p) | | | MO Composition [%] | | | wB97XD/6-31+G(d,p) | | | MO Composition [%] | | |
|---|---|---|---|---|---|---|---|---|---|---|---|---|
| | Orbital | Energy (eV) | Gap (eV) | Cu | N^N | NHC | Orbital | Energy (eV) | Gap (eV) | Cu | N^N | NHC |
| [Cu(IPr)(**L1**)]$^+$ (**1**) | HOMO | -8.84 | -5.08 | 66 | 31 | 2 | HOMO<br>(HOMO – 1)[a] | -10.45<br>(-10.41) | -8.41<br>(-8.38) | 55<br>(26) | 40<br>(69) | 5<br>(4) |
| | LUMO | -3.76 | | 2 | 97 | 1 | LUMO | -2.03 | | 1 | 98 | 1 |
| [Cu(IPr)(**L2**)]$^+$ (**2**) | HOMO | -8.82 | -5.01 | 49 | 47 | 4 | HOMO | -10.41 | -8.33 | 28 | 68 | 3 |
| | LUMO | -3.82 | | 3 | 97 | 0 | LUMO | -2.08 | | 2 | 98 | 1 |
| [Cu(IPr)(**L3**)]$^+$ (**3**) | HOMO | -8.88 | -5.08 | 57 | 34 | 9 | HOMO | -10.44 | -8.36 | 31 | 58 | 10 |
| | LUMO | -3.80 | | 2 | 97 | 1 | LUMO | -2.08 | | 2 | 98 | 0 |
| [Cu(IPr)(**L4**)]$^+$ (**4**) | HOMO | -8.96 | -5.04 | 66 | 30 | 4 | HOMO | -10.59 | -8.39 | 59 | 35 | 6 |
| | LUMO | -3.92 | | 1 | 99 | 0 | LUMO | -2.20 | | 1 | 99 | 0 |
| [Cu(IPr)(**L5**)]$^+$ (**5**) | HOMO | -8.86 | -5.05 | 65 | 32 | 2 | HOMO<br>(HOMO – 1) | -10.45<br>(-10.41) | -8.38<br>(-8.34) | 29<br>(50) | 66<br>(40) | 5<br>(4) |
| | LUMO | -3.81 | | 2 | 98 | 0 | LUMO | -2.07 | | 1 | 98 | 1 |
| [Cu(IPr)(**L6**)]$^+$ (**6**) | HOMO | -8.38 | -3.25 | 20 | 78 | 2 | HOMO | -10.00 | -6.51 | 25 | 68 | 7 |
| | LUMO | -5.14 | | 3 | 97 | 1 | LUMO | -3.49 | | 2 | 98 | 0 |
| [Cu(SIPr)(**L1**)]$^+$ (**7**) | HOMO<br>(HOMO – 1) | -8.86<br>(-8.81) | -5.12<br>(-5.06) | 63<br>(11) | 34<br>(84) | 3<br>(5) | HOMO<br>(HOMO – 1) | -10.46<br>(-10.41) | -8.43<br>(-8.39) | 33<br>(49) | 63<br>(46) | 4<br>(5) |
| | LUMO | -3.75 | | 1 | 98 | 1 | LUMO | -2.02 | | 1 | 99 | 0 |
| [Cu(SIPr)(**L2**)]$^+$ (**8**) | HOMO<br>(HOMO – 1) | -8.85<br>(-8.81) | -5.04<br>(-5.00) | 19<br>(54) | 79<br>(43) | 2<br>(4) | HOMO | -10.42 | -8.36 | 18 | 80 | 2 |
| | LUMO | -3.81 | | 3 | 96 | 1 | LUMO | -2.06 | | 2 | 97 | 1 |
| [Cu(SIPr)(**L4**)]$^+$ (**10**) | HOMO | -8.98 | -5.07 | 65 | 31 | 3 | HOMO | -10.61 | -8.44 | 57 | 37 | 6 |
| | LUMO | -3.91 | | 1 | 99 | 0 | LUMO | -2.17 | | 1 | 99 | 0 |

[a] Molecular orbitals at a slightly lower energy (< 0.05 eV) than HOMO, thus can be considered nearly degenerate.

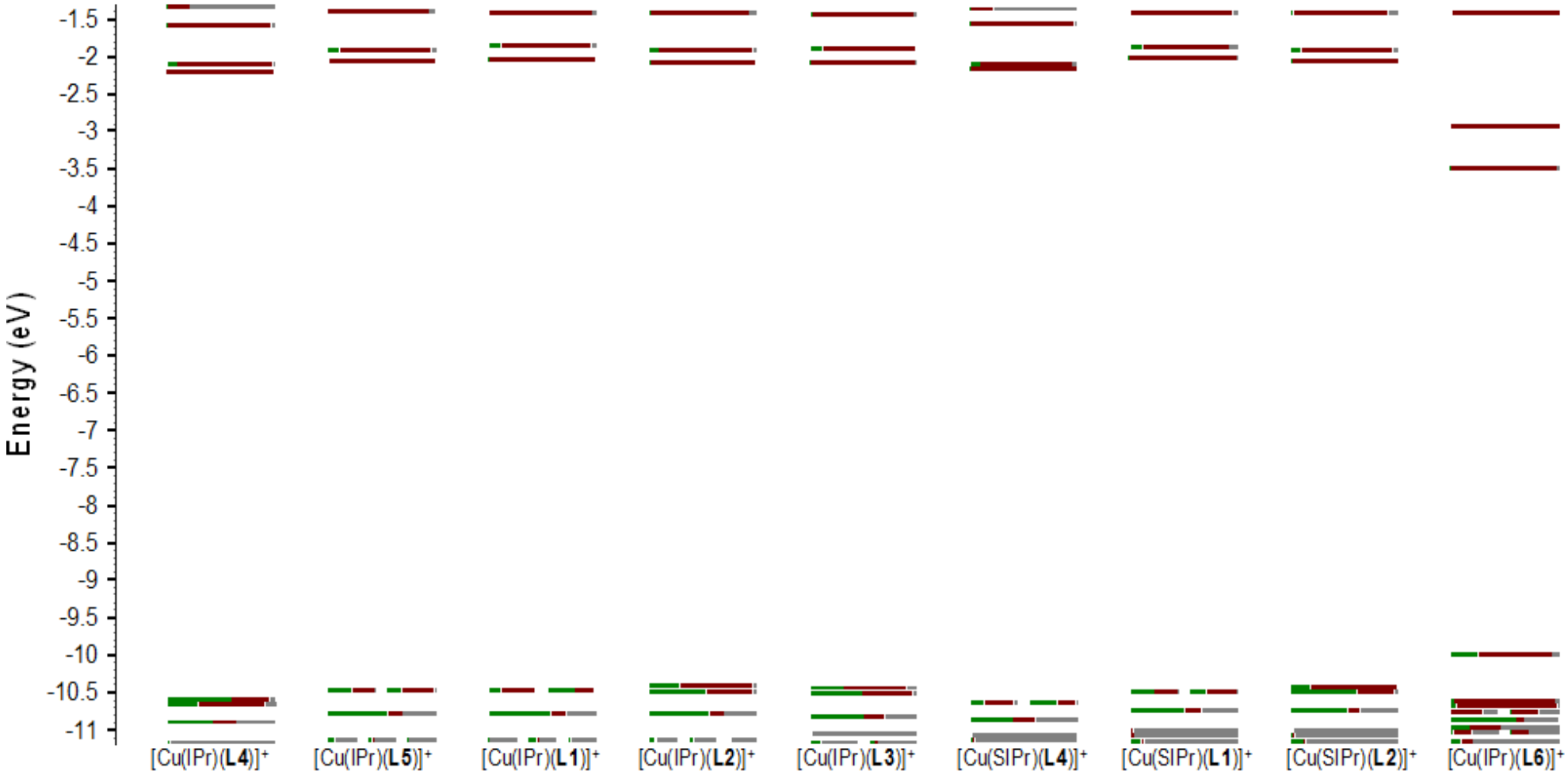


**Figure S12.** Molecular orbital energy diagrams for the copper complexes calculated at the wB97XD level using 6-31+G(d,p) basis set. The color coding of levels refers to the MO composition with corresponding contributions from Cu (green), Hdpa ligand (brown), and NHC ligand (gray). Note: HOMO and HOMO-1 with energy difference of < 0.05 eV are shown at the same level as nearly degenerate orbitals.

**Table S7.** Vertical transition energies, absorption wavelength (λ in nm), oscillator strengths (*f*), and main MO contribution for three singlet−singlet ($S_0 \rightarrow S_n$) and singlet−triplet ($S_0 \rightarrow T_1$) transitions calculated with **wB97XD/6-31+G(d,p)**

| | **$S_0 \rightarrow S_n$ (n = 1, 2, 3)** | | | | **$S_0 \rightarrow T_1$** [a] | | |
|---|---|---|---|---|---|---|---|
| Complex | Transition Type (Weight, %) [b] | E (eV) | λ (nm) | *f* | Transition Type (Weight, %) | E (eV) | λ (nm) |
| [Cu(IPr)(**L1**)]$^+$ (**1**) | H ->L+1 (45)<br>H ->L (68)<br>H-1 ->L (72) | 4.25<br>4.34<br>4.52 | 291.8<br>285.8<br>274.6 | 0.003<br>0.002<br>0.158 | H-1 ->L (40) | 3.52 | 351.8 |
| [Cu(IPr)(**L2**)]$^+$ (**2**) | H-1 ->L (29)<br>H ->L (28)<br>H ->L (45) | 4.23<br>4.31<br>4.45 | 293.0<br>287.9<br>278.9 | 0.002<br>0.012<br>0.141 | H ->L (43) | 3.49 | 355.7 |
| [Cu(IPr)(**L3**)]$^+$ (**3**) | H-1 ->L (32)<br>H-1 ->L (26)<br>H ->L (55) | 4.29<br>4.34<br>4.42 | 289.2<br>285.6<br>280.2 | 0.012<br>0.001<br>0.108 | H ->L (38) | 3.51 | 353.7 |
| [Cu(IPr)(**L4**)]$^+$ (**4**) | H ->L+1 (58)<br>H ->L (84)<br>H-1 ->L (82) | 4.24<br>4.29<br>4.50 | 292.4<br>289.3<br>275.3 | 0.001<br>0.004<br>0.112 | H-1 ->L (37) | 3.55 | 349.7 |
| [Cu(IPr)(**L5**)]$^+$ (**5**) | H-1 ->L+1 (41)<br>H-1 ->L (50)<br>H ->L (50) | 4.23<br>4.28<br>4.47 | 292.8<br>289.4<br>277.5 | 0.000<br>0.006<br>0.143 | H ->L (39) | 3.49 | 355.5 |
| [Cu(IPr)(**L6**)]$^+$ (**6**) | H ->L (87)<br>H-5 ->L (78)<br>H-1 ->L (61) | 2.42<br>3.15<br>3.37 | 511.4<br>393.6<br>367.5 | 0.001<br>0.002<br>0.010 | H ->L (85) | 2.23 | 556.5 |
| [Cu(SIPr)(**L1**)]$^+$ (**7**) | H-1 ->L+1 (36)<br>H ->L (48)<br>H-2 ->L+1 (30) | 4.14<br>4.36<br>4.41 | 299.3<br>284.7<br>281.1 | 0.001<br>0.006<br>0.028 | H ->L (34) | 3.53 | 351.8 |
| [Cu(SIPr)(**L2**)]$^+$ (**8**) | H-1 ->L+1 (40)<br>H-1 ->L (58)<br>H-2 ->L+1 (24) | 4.15<br>4.34<br>4.42 | 299.1<br>285.8<br>280.8 | 0.002<br>0.008<br>0.031 | H ->L (50) | 3.49 | 354.8 |
| [Cu(SIPr)(**L4**)]$^+$ (**10**) | H ->L+1 (49)<br>H ->L (84)<br>H-2 ->L+3 (24) | 4.15<br>4.16<br>4.52 | 298.7<br>286.5<br>274.2 | 0.001<br>0.003<br>0.115 | H-1 ->L (36) | 3.56 | 348.5 |

[a] The oscillator strength for the singlet to triplet transitions is 0 due to them being forbidden by the spin selection rule. [b] For each excitation energy, the corresponding most relevant molecular orbital transitions are shown with the relative weight.

**Table S8.** Vertical transition energies, absorption wavelength (λ in nm), oscillator strengths (f), and main MO contribution for three singlet−singlet ($S_0 \rightarrow S_n$) and singlet−triplet ($S_0 \rightarrow T_1$) transitions calculated with **M06/6-31+G(d,p)**

| | $S_0 \rightarrow S_n$ (n = 1, 2, 3) | | | | $S_0 \rightarrow T_1$ [a] | | |
|---|---|---|---|---|---|---|---|
| **Complex** | **Transition Type (Weight, %)** [b] | **E (eV)** | **λ (nm)** | ***f*** | **Transition Type (Weight, %)** | **E (eV)** | **λ (nm)** |
| [Cu(IPr)(**L1**)]$^+$ (**1**) | H ->L (88) | 3.80 | 326.5 | 0.003 | H-1 ->L (46)<br>H-1 ->L+3 (12)<br>H-1 ->L+4 (8) | 3.56 | 369.5 |
| | H ->L+1 (84) | 4.12 | 301.1 | 0.085 | | | |
| | H-1 ->L+1 (52)<br>H-2 ->L+1 (30) | 4.24 | 292.4 | 0.066 | | | |
| [Cu(IPr)(**L2**)]$^+$ (**2**) | H ->L (78)<br>H-1 ->L (18) | 3.76 | 329.8 | 0.001 | H-1 ->L (38)<br>H ->L (24) | 3.31 | 375.2 |
| | H ->L+1 (70)<br>H-1 ->L+1 (20) | 3.86 | 321.3 | 0.006 | | | |
| | H-1 ->L (70)<br>H ->L (16) | 4.05 | 306.4 | 0.097 | | | |
| [Cu(IPr)(**L3**)]$^+$ (**3**) | H ->L (86)<br>H-1 ->L (10) | 3.83 | 323.9 | 0.004 | H-1 ->L (46)<br>H-1 ->L+3 (14) | 3.36 | 369.2 |
| | H ->L+1 (84) | 3.93 | 315.9 | 0.003 | | | |
| | H-1 ->L (80)<br>H ->L (10) | 4.05 | 305.8 | 0.065 | | | |
| [Cu(IPr)(**L4**)]$^+$ (**4**) | H ->L (97) | 3.77 | 328.9 | 0.000 | H-1 ->L (54)<br>H-1 ->L+3 (25) | 3.39 | 365.8 |
| | H ->L+1 (91) | 3.89 | 318.9 | 0.002 | | | |
| | H-1 ->L (90) | 4.17 | 297.3 | 0.153 | | | |
| [Cu(IPr)(**L5**)]$^+$ (**5**) | H ->L (97) | 3.77 | 328.7 | 0.002 | H-1 ->L (54)<br>H-1 ->L (20) | 3.31 | 374.8 |
| | H ->L+1 (89) | 3.83 | 323.5 | 0.000 | | | |
| | H-1 ->L (85) | 4.07 | 304.4 | 0.091 | | | |
| [Cu(IPr)(**L6**)]$^+$ (**6**) | H ->L (95) | 2.04 | 608.8 | 0.001 | H ->L (93) | 1.90 | 654.0 |
| | H-1 ->L (86)<br>H ->L+1 (11) | 2.65 | 468.7 | 0.002 | | | |
| | H-2 ->L (36)<br>H-4 ->L (36)<br>H-3 ->L (16) | 2.96 | 419.3 | 0.005 | | | |
| [Cu(SIPr)(**L1**)]$^+$ (**7**) | H ->L (60)<br>H ->L+1 (28) | 3.83 | 324.1 | 0.002 | H-1 ->L (44)<br>H-1 ->L+3 (14) | 3.35 | 370.1 |
| | H ->L+1 (54)<br>H ->L (36) | 3.89 | 319.0 | 0.001 | | | |
| | H-1 ->L (80)<br>H-2 ->L (10) | 4.14 | 299.8 | 0.103 | | | |
| [Cu(SIPr)(**L2**)]$^+$ (**8**) | H-1 ->L+1 (56)<br>H ->L+1 (20) | 3.86 | 320.9 | 0.004 | H ->L (52)<br>H-1 ->L (10) | 3.30 | 375.8 |
| | H ->L (62)<br>H-1 ->L (24) | 4.05 | 305.9 | 0.111 | | | |
| | H ->L+1 (40)<br>H-1 ->L+1 (24)<br>H ->L+1 (12) | 4.17 | 297.2 | 0.068 | | | |
| [Cu(SIPr)(**L4**)]$^+$ (**10**) | H ->L (98) | 3.80 | 326.6 | 0.001 | H-1 ->L (53)<br>H-1 ->L+3 (27) | 3.40 | 364.9 |
| | H ->L+1 (87) | 3.88 | 319.9 | 0.001 | | | |
| | H-1 ->L (85) | 4.18 | 296.7 | 0.129 | | | |

[a] The oscillator strength for the singlet to triplet transitions is 0 due to them being forbidden by the spin selection rule. [b] For each excitation energy, the corresponding most relevant molecular orbital transitions are shown with the relative weight.

**Table S9.** Graphic representation of electronic states for $S_0 \rightarrow S_1$ and $S_0 \rightarrow T_1$ transitions calculated at **M06/6-31+G(d,p)**

| Complex | $S_0 \rightarrow S_1$ | | $S_0 \rightarrow T_1$ | |
|---|---|---|---|---|
| | **Ground State (GS)** | **Excited State (ES)** | **GS** | **ES** |
| [Cu(IPr)(**L1**)]$^+$ (**1**) | 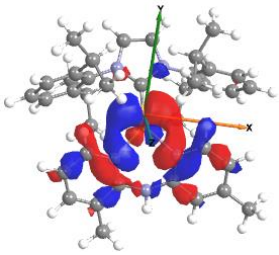 | 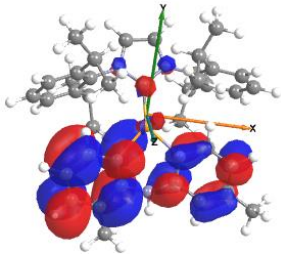 | 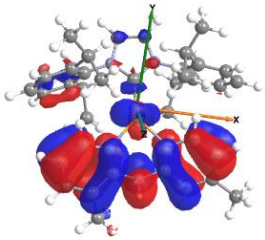 | 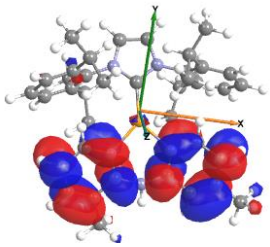 |
| [Cu(IPr)(**L2**)]$^+$ (**2**) | 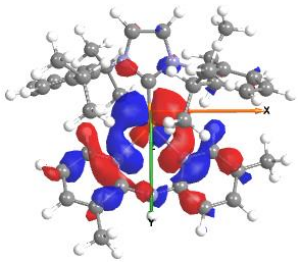 | 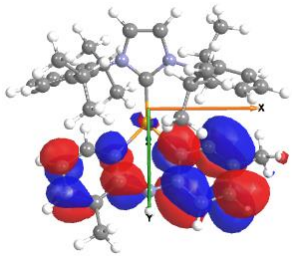 | 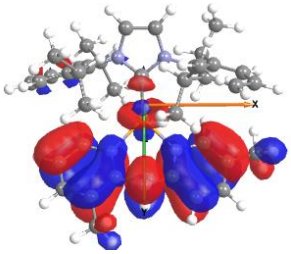 | 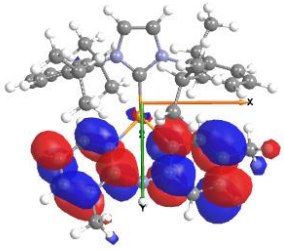 |
| [Cu(IPr)(**L3**)]$^+$ (**3**) | 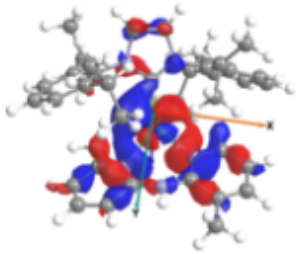 | 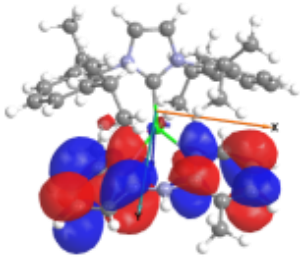 | 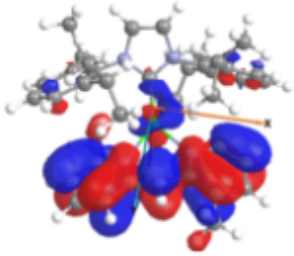 | 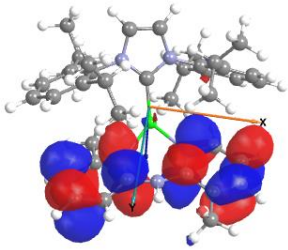 |
| [Cu(IPr)(**L4**)]$^+$ (**4**) | 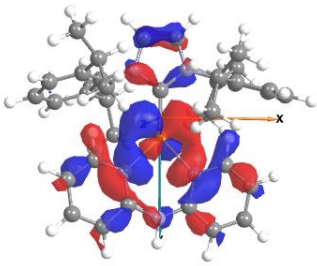 | 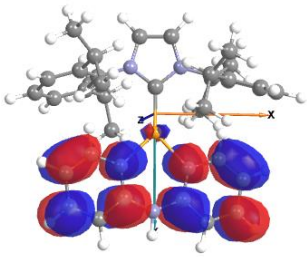 | 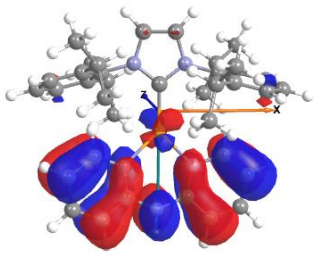 | 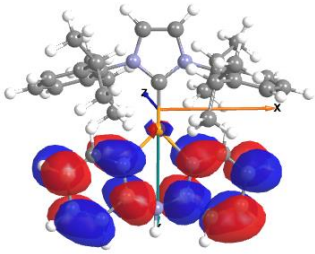 |
| [Cu(IPr)(**L5**)]$^+$ (**5**) | 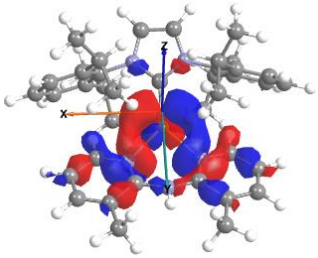 | 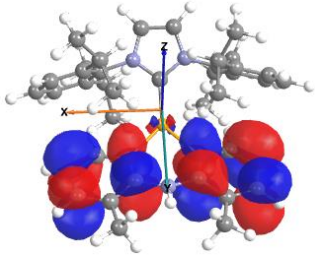 | 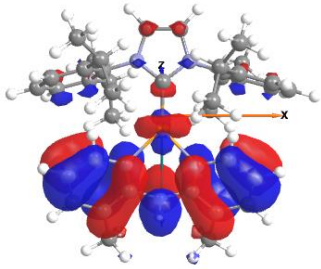 | 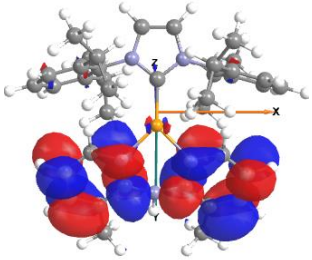 |

**Table S9 (continued).** Graphic representation of electronic states for $S_0 \rightarrow S_1$ and $S_0 \rightarrow T_1$ transitions calculated at **M06/6-31+G(d,p)**

| Complex | $S_0 \rightarrow S_1$ | | $S_0 \rightarrow T_1$ | |
|---|---|---|---|---|
| | **Ground State (GS)** | **Excited State (ES)** | **GS** | **ES** |
| [Cu(IPr)(**L6**)]$^+$ (**6**) | 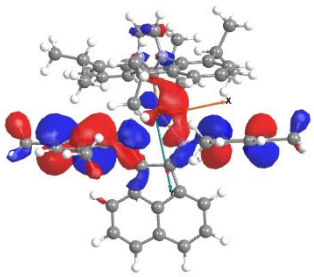 | 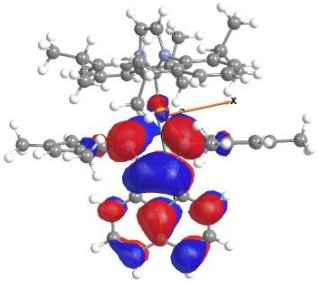 | 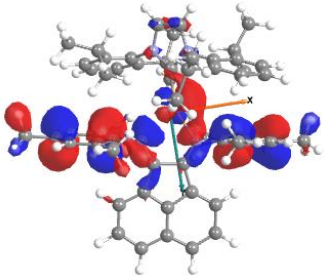 | 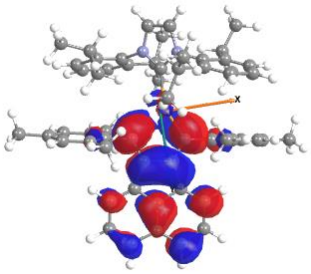 |
| [Cu(SIPr)(**L1**)]$^+$ (**7**) | 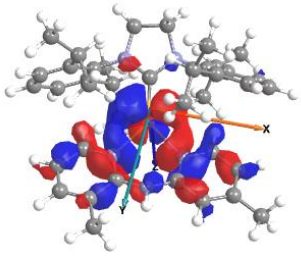 | 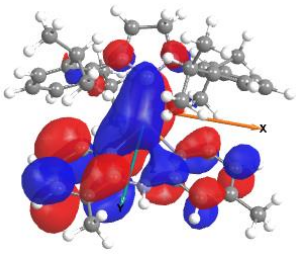 | 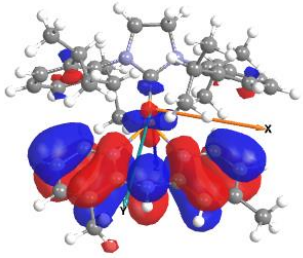 | 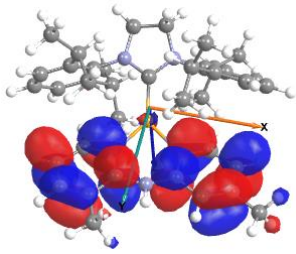 |
| [Cu(SIPr)(**L2**)]$^+$ (**8**) | 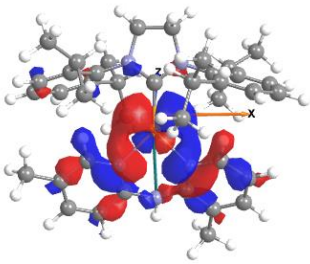 | 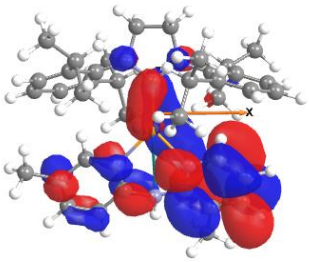 | 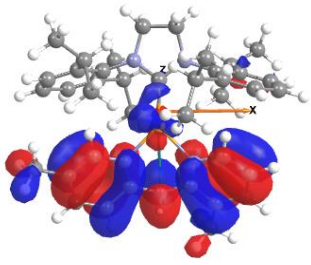 | 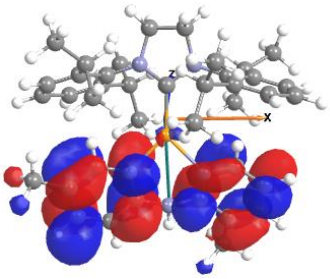 |
| [Cu(SIPr)(**L4**)]$^+$ (**10**) | 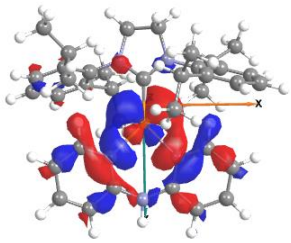 | 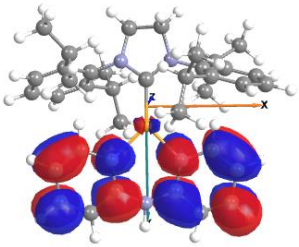 | 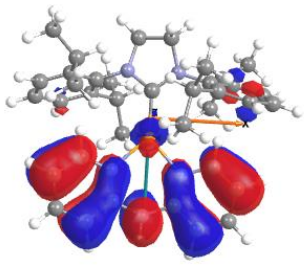 | 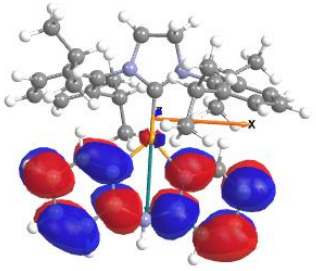 |

**Table S10.** Graphic representation of electronic states for $S_0 \rightarrow S_1$ transitions calculated at **wB97XD/6-31+G(d,p)**

| Complex | $S_0 \rightarrow S_1$ | | $S_0 \rightarrow T_1$ | |
|---|---|---|---|---|
| | **Ground State (GS)** | **Excited State (ES)** | **GS** | **ES** |
| [Cu(IPr)(**L1**)]$^+$ (**1**) | 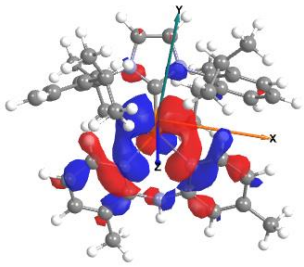 | 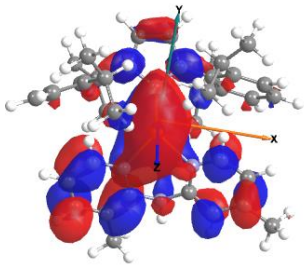 | 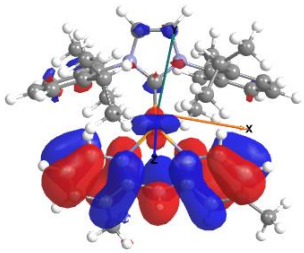 | 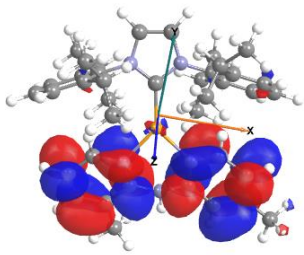 |
| [Cu(IPr)(**L2**)]$^+$ (**2**) | 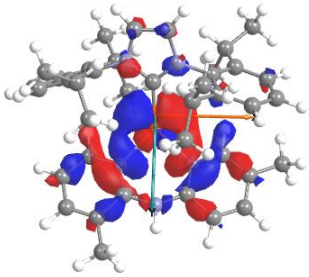 | 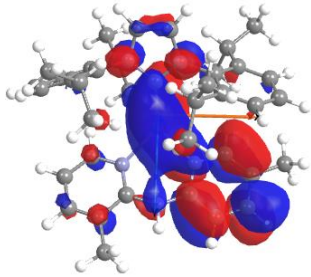 | 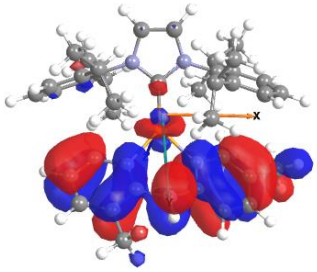 | 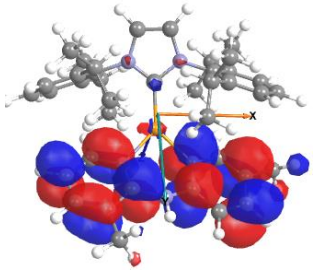 |
| [Cu(IPr)(**L3**)]$^+$ (**3**) | 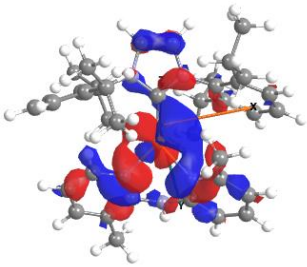 | 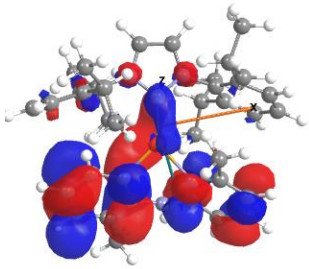 | 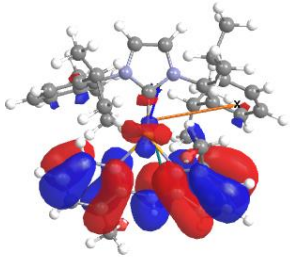 | 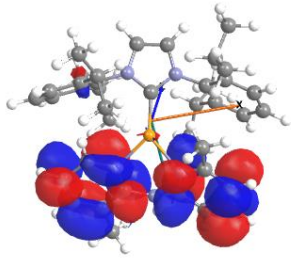 |
| [Cu(IPr)(**L4**)]$^+$ (**4**) | 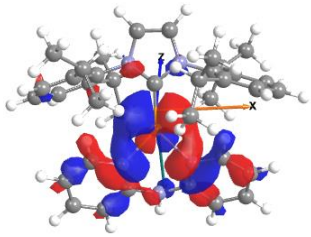 | 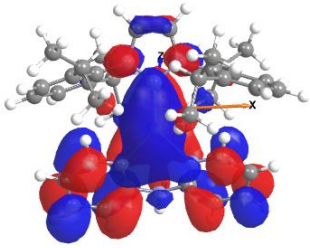 | 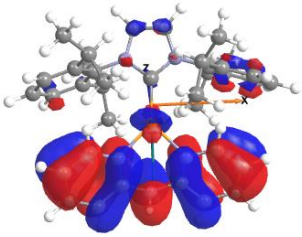 | 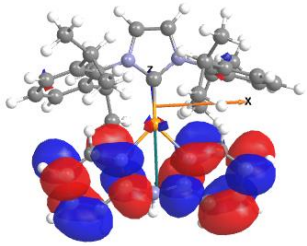 |
| [Cu(IPr)(**L5**)]$^+$ (**5**) | 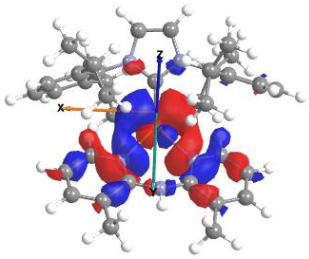 | 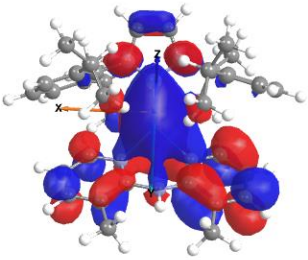 | 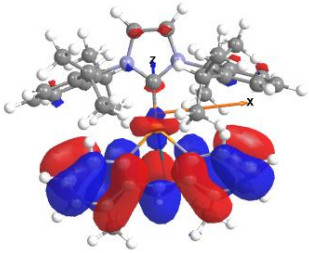 | 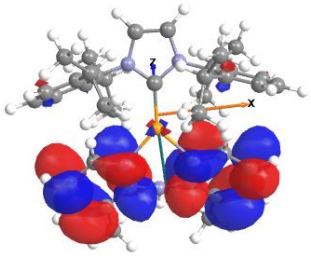 |

**Table S10 (continued).** Graphic representation of electronic states for $S_0 \rightarrow S_1$ transitions calculated at **wB97XD/6-31+G(d,p)**

| Complex | $S_0 \rightarrow S_1$ | | $S_0 \rightarrow T_1$ | |
|---|---|---|---|---|
| | **Ground State (GS)** | **Excited State (ES)** | **GS** | **ES** |
| [Cu(IPr)(**L6**)]$^+$ (**6**) | 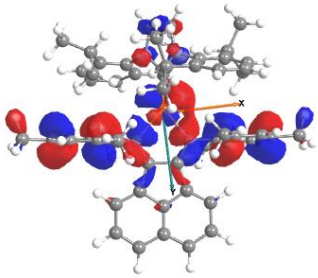 | 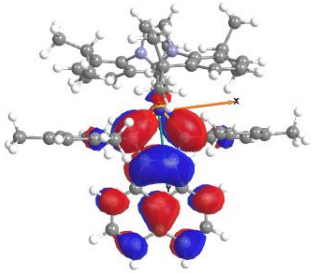 | 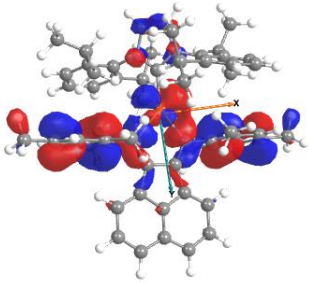 | 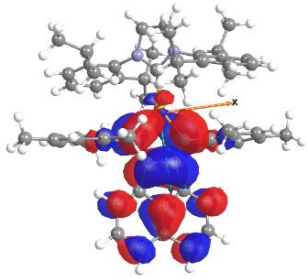 |
| [Cu(SIPr)(**L1**)]$^+$ (**7**) | 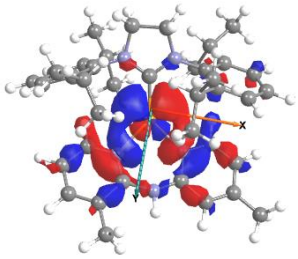 | 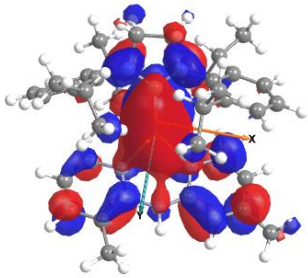 | 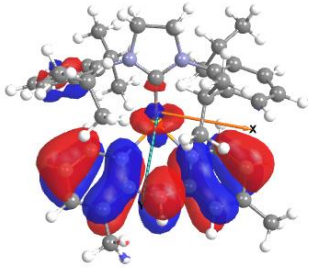 | 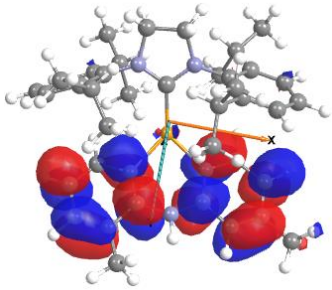 |
| [Cu(SIPr)(**L2**)]$^+$ (**8**) | 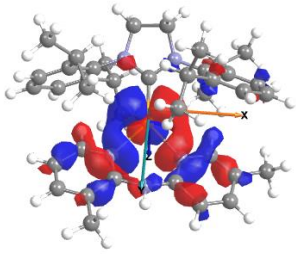 | 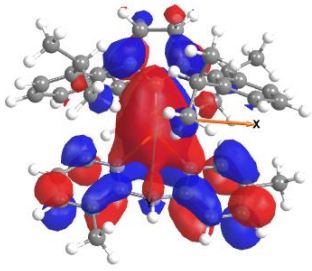 | 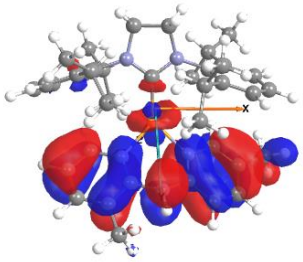 | 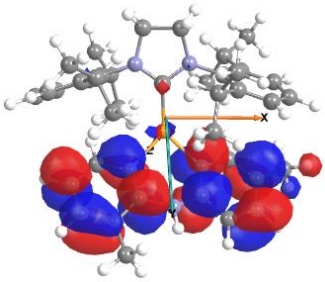 |
| [Cu(SIPr)(**L4**)]$^+$ (**10**) | 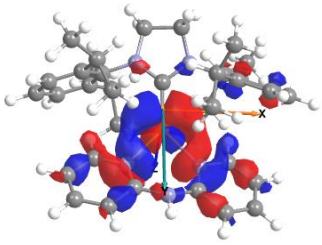 | 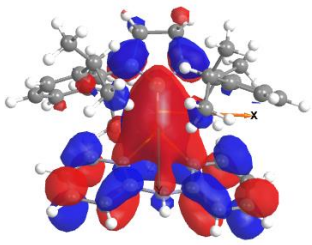 | 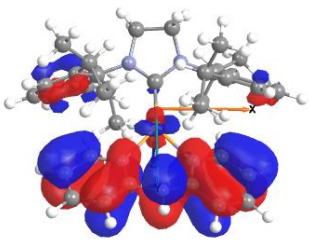 | 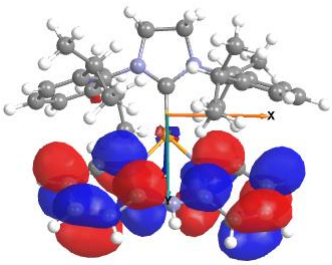 |

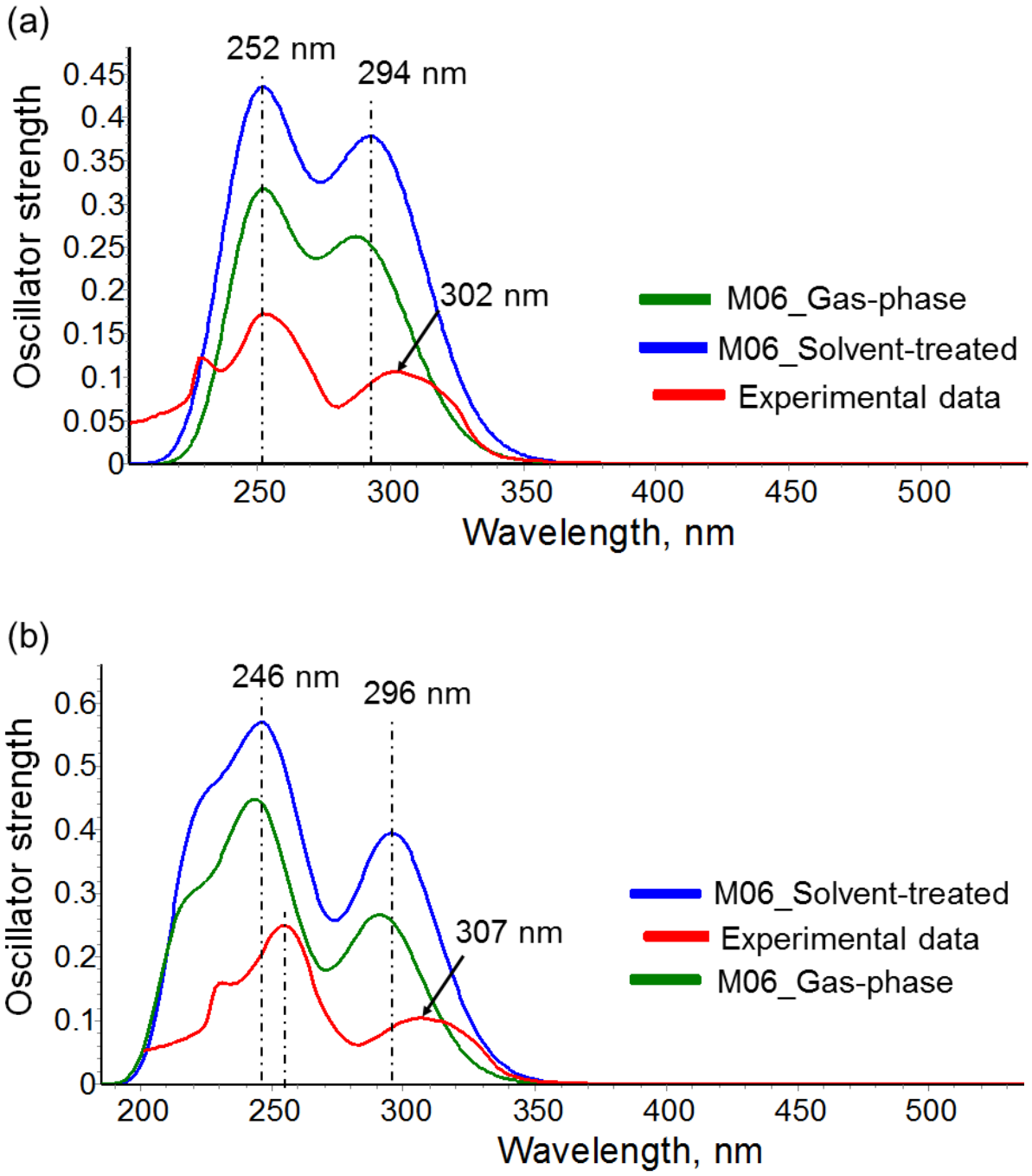


**Figure S13.** Experimental and TD-DFT simulated UV-Vis absorption spectra of (a) [Cu(IPr)(**L1**)]$^+$ and (b) [Cu(SIPr)(**L4**)]$^+$ in gas-phase and in $CH_2Cl_2$ calculated at M06/6-31+G(d,p).

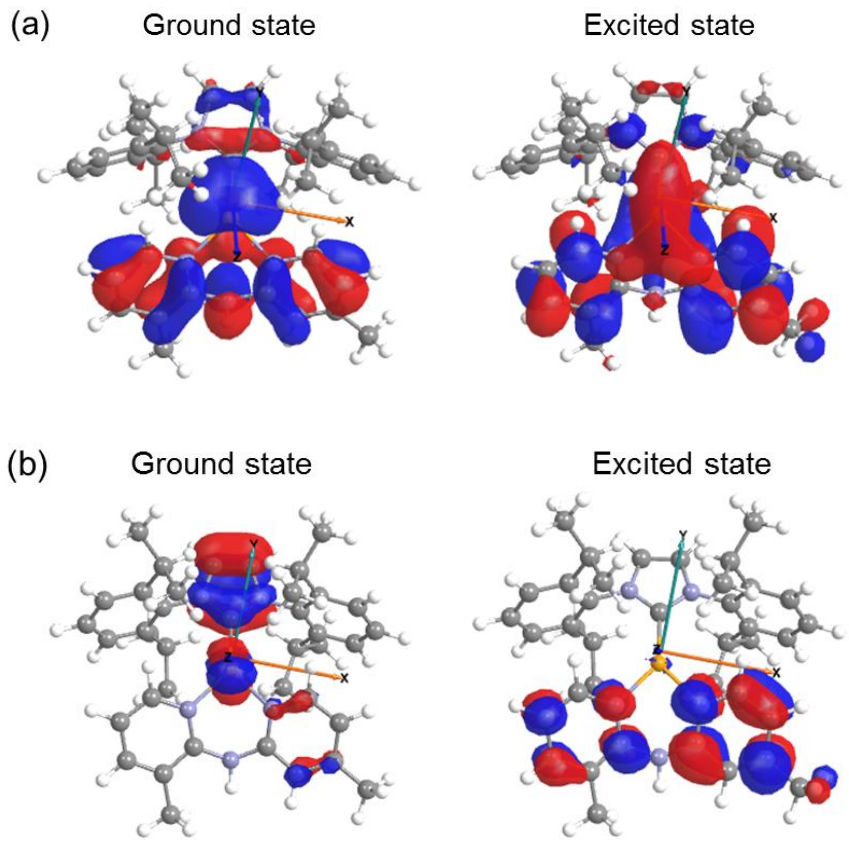


**Figure S14.** Graphical representation of the ground and excited states for the electronic transitions at (a) 294 nm and (b) 252 nm in the simulated UV-Vis spectrum of [Cu(IPr)(**L1**)]$^{+}$ calculated at M06/6-31+G(d,p)

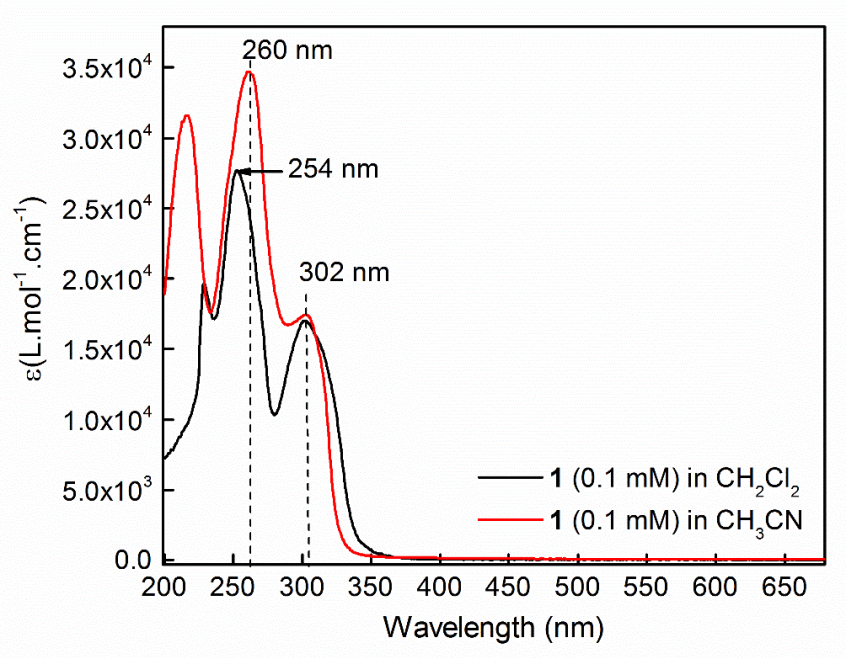


**Figure S15.** Absorption spectra of [Cu(IPr)(**L1**)]$PF_6$ (**1**) in $CH_2Cl_2$ and $CH_3CN$ solution at room temperature

**Synthesis of [Cu(IPr)Cl]**

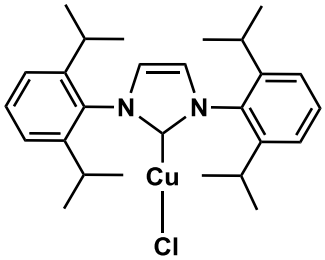

Under Ar atmosphere, IPr·HCl salt (0.70 mmol, 0.300 g), CuCl (1.05 mmol, 0.104 g) and $K_2CO_3$ (2.1 mmol, 0.290 g) were combined in a reaction vial. The vial was charged with 5 mL acetone forming a green/orange suspension instantly. The reaction mixture was stirred at 60°C for 48 hours, and then filtered through a plug of Celite to separate an orange solid from a clear solution. The solid was rinsed with acetone and dichloromethane and the colorless filtrate was concentrated under vacuum. The product was formed as white solid after adding hexanes which was then filtered and kept under vacuum. The material was recrystallized from THF and hexane to afford an off-white solid in 74% yield (0.255 g). $^1$H NMR ($CDCl_3$, 400 MHz) δ 7.49 (t, *J* = 7.8 Hz, 1H), 7.30 (d, *J* = 7.8 Hz, 2H), 7.13 (s, 1H), 2.57 (sept, *J* = 6.9 Hz, 2H), 1.31 (d, *J* = 6.9 Hz, 6H), 1.23 (d, *J* = 6.9 Hz, 6H). $^{13}$C NMR ($CDCl_3$, 400MHz): δ 145.72, 134.53, 130.73, 124.36, 123.27 28.89, 24.96, 24.02.

**Synthesis of [Cu(IPr)]$PF_6$**

Under Ar atmosphere, [Cu(IPr)Cl] (0.160 mmol, 0.078 g) and $KPF_6$ (1.60 mmol, 0.294 g) were combined in a reaction vial. The vial was charged with 6 mL acetone forming a green/orange suspension instantly. The reaction mixture was stirred at room temperature for 4 hours and then filtered through a plug of Celite. The solid was rinsed with acetone and THF and the solution was kept under vacuum to remove the solvent completely. The solid material was recrystallized from a mixture of THF and hexanes to afford an off-white solid in 65% yield (0.062 g). $^1$H NMR ($CD_3CN$, 400 MHz) δ 7.56 (t, *J* = 7.8 Hz, 2H), 7.46-7.36 (m, 6H), 2.56 (sept, *J* = 6.9 Hz, 4H), 1.24 (dd, *J* = 6.9, 9.0 Hz, 24H). Elemental analysis (%) calcd. for $C_{27}H_{36}CuF_6N_2P$: C, 54.31; H, 6.08; N, 4.69; found: C 56.64; H, 5.94; N, 4.66.

**Synthesis of [Cu(SIPr)Cl]**

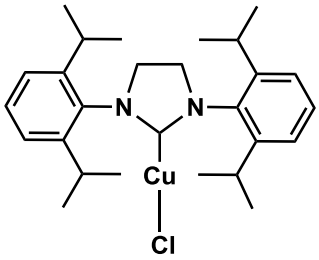

Under Ar atmosphere, SIPr·HCl salt (0.70 mmol, 0.300 g), CuCl (1.05 mmol, 0.104g) and $K_2CO_3$ (2.1 mmol, 0.290g) were combined in a reaction vial. The vial was charged with 5 mL acetone forming a green/orange suspension instantly. The reaction mixture was stirred at 60°C for 48 hours, and then filtered through a plug of Celite to separate an orange solid from a clear solution. The solid was rinsed with acetone and dichloromethane and the colorless filtrate was concentrated under vacuum. The product was formed as white solid after adding hexanes which was then filtered and kept under vacuum. The material was recrystallized from DCM and hexane to afford an off-white solid in 78% yield (0.268 g). $^1$H NMR ($CDCl_3$, 400MHz δ 7.40 (t, *J* = 7.8 Hz, 1H), 7.24 (d, *J* = 7.8 Hz, 2H), 4.02 (s, 2H), 3.07 (sept, *J* = 6.9 Hz, 2H), 1.36 (dd, *J* = 9.7, 6.9 Hz, 12H). $^{13}$C NMR ($CDCl_3$, 400MHz): δ 203.16 ($C_{NHC}$), 146.75, 134.50, 130.04, 124.72, 53.87, 29.08, 25.64, 24.05.

**Synthesis of MesBIAN**

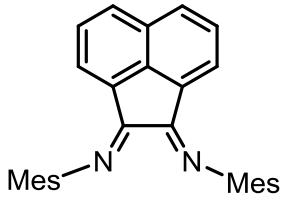


Acenaphthenequinone (5.49 mmol, 1.00 g) was suspended in 50 ml MeOH and then mixed with formic acid (1 ml) to create a cloudy orange solution. 2,4,6-trimethylaniline (13.2 mmol, 1.79 g) was added to the mixture affording a red solution instantly. The reaction mixture was heated at reflux for 24 hours, after which time the cherry red solution was transferred into a 100 ml beaker and left open for ~24 hours. The red/orange solid was then filtered through a glass frit and rinsed with dichloromethane, methanol, and diethyl ether. The product was collected as a red powder in 76% yield (1.74 g) $^{1}$HNMR ($CDCl_3$, 400MHz): 7.89 (d, *J* = 8.3 Hz, 2H), 7.40 (dd, *J* = 8.3, 7.2 Hz, 2H), 6.97 (s, 4H), 6.78 (d, *J* = 7.2 Hz, 2H), 2.38 (s, 6H), 2.09 (s, 12H). $^{13}$C NMR ($CDCl_3$, 400MHz): δ 161.20, 146.93, 140.69, 132.94, 131.15, 129.87, 129.07, 128.89, 128.36, 124.73, 122.62, 21.08, 17.86.

**General Procedure for the synthesis of dimethyl dipyridylamine ligands**

Under Ar atmosphere, the reaction vial was charged with $Pd_2(dba)_3$ (0.0174 mmol, 0.0213 g), dppp (0.0697 mmol, 0.0288 g), 2-bromomethyl pyridine derivative (1.74 mmol, 0.300 g), 2-aminomethyl pyridine derivative (2.09 mmol, 0.226 g), $KO^tBu$ (2.44 mmol, 0.274 g) and 5 ml toluene subsequently. The cherry red mixture was removed from the glovebox and heated at 120°C for 24 hours. The mixture was then filtered through a plug of Celite and washed with ethyl acetate. The solvent was then removed under vacuum affording a yellow solid. The residual material was loaded on a silica gel column and eluted with appropriate mixtures of hexanes and ethyl acetate to afford a yellow solid.

**3,3'-dimethyl-2,2'-dipyridial amine,** (3,3'-$Me_2$Hdpa; **L5**)

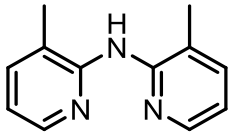


Following the general procedure, a yellow solid was isolated in 67% yield (0.232 g); $^{1}$H NMR ($CDCl_3$, 400MHz): δ 8.15 (m, 2H), 7.46 (dd, *J* = 7.5, 1.8 Hz, 2H), 6.88 (dd, *J* = 7.4, 4.9 Hz, 2H), 6.40 (s, 1H), 2.23 (s, 6H). $^{13}$C NMR ($CDCl_3$, 400MHz): δ 153.62, 145.77, 138.79, 123.54, 118.24, 18.26. m/z calcd. for $C_{12}H_{13}N_3$: 199.11; found: 199.11.

**3,4'-dimethyl-2,2'-dipyridial amine (**3,4'-$Me_2$Hdpa; **L1)**

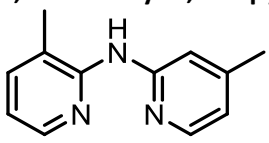


Following the general procedure, a yellow oil was isolated in 93% yield (0.323 g), $^{1}$H NMR ($CDCl_3$, 400MHz): δ 8.23 (dt, *J* = 1.6, 0.8 Hz, 1H), 8.16 (dd, *J* = 5.0, 1.8 Hz, 1H), 8.07 (d, *J* = 5.1 Hz, 1H), 7.37 (ddd, *J* = 7.3, 1.8, 0.9 Hz, 1H), 7.04 (s, 1H), 6.76 (dd, *J* = 7.3, 5.0 Hz, 1H), 6.70 (dd, *J* = 5.2, 1.5 Hz, 1H), 2.35 (s, 3H), 2.27 (s, 3H). $^{13}$C NMR ($CDCl_3$, 400MHz): δ 153.86, 152.74, 149.25, 147.43, 145.19, 138.13, 118.98, 118.41, 116.15, 112.56, 21.65, 17.48. m/z calcd. for $C_{12}H_{13}N_3$: 199.11; found: 199.11.

**3,5'-dimethyl-2,2'-dipyridial amine (**3,5'-$Me_2$Hdpa; **L2**)

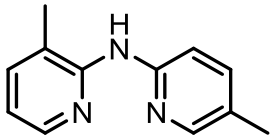

Following the general procedure a yellow oil was isolated in 74% yield (0.257 g), $^1$H NMR ($CDCl_3$, 400MHz): δ 8.31 (d, *J* = 8.5 Hz, 1H), 8.13 (dd, *J* = 5.1, 1.9 Hz, 1H), 8.04 (m, 1H), 7.46 (dd, *J* = 8.6, 2.3 Hz, 1H), 7.36 (dq, *J* = 7.3, 1.0 Hz, 1H), 6.98 (s, 1H), 6.74 (ddd, *J* = 6.4, 4.9, 1.3 Hz, 1H), 2.26 (d, *J* = 2.1 Hz, 6H). $^{13}$C NMR ($CDCl_3$, 400MHz): δ 152.87, 151.70, 147.59, 145.18, 138.63, 138.01, 126.11, 118.63, 115.89, 112.06, 17.76, 17.47. m/z calcd. for $C_{12}H_{13}N_3$: 199.11; found: 199.11.

**3,6'-dimethyl-2,2'-dipyridial amine (**3,6'-$Me_2$Hdpa; **L3**)

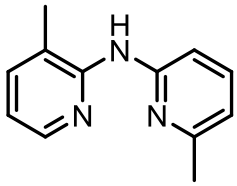

Following the general procedure a yellow oil was isolated in 98% yield (0.340 g), $^1$H NMR ($CDCl_3$, 400MHz): δ 8.24-8.12 (m, 2H), 7.55 (dd, *J* = 8.3, 7.4 Hz, 1H), 7.39 (ddd, *J* = 7.3, 1.9, 1.0 Hz, 1H), 7.01 (s, 1H), 6.81 – 6.71 (m, 2H), 2.45 (s, 3H), 2.30 (s, 3H). $^{13}$C NMR ($CDCl_3$, 400MHz): δ 156.64, 153.25, 152.85, 145.26, 138.37, 138.16, 119.01, 116.52, 116.19, 109.19, 24.31, 17.64. m/z calcd for $C_{12}H_{13}N_3$: 199.11; found: 199.11.

**Synthesis of the Cu(NHC)(N^N)]$PF_6$ Complexes**

**Note on $^{13}$C NMR data:** The peak of the NHC ligand's carbene was only detectable for a few Cu-IPr complexes (δ ~ 183 ppm) and Cu-SIPr complexes (δ ~ 203 ppm) due to a low intensity. In these complexes, the assignment has been shown in parenthesis following the chemical shift.

**[Cu(IPr)(Hdpa)]$PF_6$ (4)**

Following the general procedure, a white solid was isolated in 70% yield (0.086 g). $^1$H NMR ($CDCl_3$, 400MHz): δ 8.09 (s, 1H), 7.58 (t, *J* = 7.8 Hz, 2H), 7.47 (ddd, *J* = 8.9, 7.2, 1.9 Hz, 2H), 7.33 (d, *J* = 7.8 Hz, 4H), 7.22 (s, 2H), 7.15 (dt, *J* = 8.5, 1.1 Hz, 2H), 6.31 (ddd, *J* = 7.0, 5.6, 1.1 Hz, 2H), 6.17 (dd, *J* = 5.8, 1.9 Hz, 2H), 5.30 (s, dichloromethane), 2.65 (sept, *J* = 6.9 Hz, 4H), 1.23 (d, *J* = 6.9 Hz, 13H), 1.08 (d, *J* = 6.8 Hz, 12H). $^{13}$C NMR ($CDCl_3$, 400MHz): δ 153.17, 147.44, 146.16, 139.27, 136.08, 130.78, 124.85, 123.46, 116.44, 115.45, 28.90, 24.30, 24.14.

**[Cu(IPr)(3,3'-$Me_2$Hdpa)]$PF_6$ (5)**

Following the general procedure, a pale-yellow solid was isolated in 53% yield (0.067 g). $^1$H NMR ($CDCl_3$, 400MHz): 7.59 (t, *J* = 7.8 Hz, 2H), 7.50 – 7.43 (m, 2H), 7.33 (d, *J* = 7.8 Hz, 4H), 7.26 (s, 2H), 6.72 (s, 1H), 6.41 (dd, *J* = 7.4, 5.5 Hz, 2H), 6.21 (dd, *J* = 5.5, 1.9 Hz, 2H), 2.66 (sept, *J* = 6.9 Hz, 4H), 2.33 (s, 6H), 1.23 (d, *J* = 6.9 Hz, 13H), 1.08 (d, *J* = 6.9 Hz, 13H). $^{13}$C NMR ($CDCl_3$, 400MHz): δ 151.01, 146.11, 146.05, 140.28, 136.01, 130.86, 124.85, 123.67, 121.73, 117.43, 28.87, 24.32, 24.13, 17.29.

**[Cu(IPr)(3,4'-$Me_2$Hdpa)]$PF_6$ (1)**

Following the general procedure, a pale-yellow solid was isolated in 77% yield (0.095 g). $^1$H NMR ($CDCl_3$, 400MHz): δ 7.57 (t, *J* = 7.8 Hz, 2H), 7.33 (d, *J* = 7.8 Hz, 5H), 7.23 (d, *J* = 8.3 Hz, 4H), 7.17 (s, 1H), 6.30 – 6.16 (m, 3H), 6.05 (d, *J* = 5.7 Hz, 1H), 5.30 (dichloromethane), 2.66 (sept, *J* = 7.0 Hz, 4H), 2.34 (s, 3H), 2.25 (s, 3H), 1.23 (d, *J* = 6.9 Hz, 12H), 1.09 (d, *J* = 6.9 Hz, 12H). $^{13}$C NMR ($CDCl_3$, 400MHz): δ 152.78, 151.74, 146.93, 146.12, 145.63, 143.62, 139.66, 136.06, 130.75, 124.80, 123.47, 122.49, 118.59, 116.35, 116.00, 53.58 ($CH_2Cl_2$), 28.89, 24.30, 24.18, 20.95, 17.50. Elemental analysis (%) calcd. for $C_{39}H_{50}CuN_5$: C, 56.49; H, 6.12; N, 8.34; found: C 56.54; H, 6.17; N, 8.34.

**[Cu(IPr)(3,5'-$Me_2$Hdpa)]$PF_6$ (2)**

Following the general procedure a pale yellow solid was isolated in 83% yield (0.102 g).$^1$H NMR ($CDCl_3$, 400MHz): δ 7.54 (t, *J* = 7.8 Hz, 2H), 7.41 (dd, *J* = 8.6, 2.3 Hz, 1H), 7.31 (d, *J* = 7.8 Hz, 5H), 7.22 (d, *J* = 8.5 Hz, 4H), 6.38 – 6.32 (m, 1H), 6.32 – 6.22 (m, 2H), 2.68 (hept, *J* = 6.8 Hz, 4H), 2.34 (s, 3H), 1.96 (s, 3H), 1.25 (hexanes), 1.22 (d, *J* = 6.9 Hz, 12H), 1.10 (d, *J* = 6.9 Hz, 12H).$^{13}$C NMR ($CDCl_3$, 400MHz): δ 183.45 ($C_{NHC}$), 151.72, 150.94, 146.32, 146.01, 145.44, 141.03, 139.63, 135.96, 130.74, 126.70, 124.64, 123.49, 122.30, 116.54, 116.04, 28.88, 24.25, 24.18, 18.02, 17.41. Elemental analysis (%) calcd. for $C_{39}H_{50}CuN_5$: C, 58.74; H, 6.35; N, 9.42; found: C, 58.63: H, 6.33: N, 9.36.

**[Cu(IPr)(3,6'-$Me_2$Hdpa)]$PF_6$ (3)**

Following the general procedure, except for stirring for 48 hours, a pale-yellow solid was isolated in 62% yield (0.076 g). $^1$H NMR ($CDCl_3$, 400MHz): δ 7.54 (t, *J* = 7.8 Hz, 2H), 7.41 (dd, *J* = 8.6, 2.3 Hz, 1H), 7.31 (d, *J* = 7.8 Hz, 5H), 7.21 (q, *J* = 2.5 Hz, 4H), 6.38 – 6.32 (m, 1H), 6.32 – 6.22 (m, 2H), 2.68 (sept, *J* = 6.8 Hz, 4H), 2.34 (s, 3H), 1.96 (s, 3H), 1.22 (d, *J* = 6.9 Hz, 12H), 1.10 (d, *J* = 6.9 Hz, 12H). $^{13}$C NMR ($CDCl_3$, 400MHz): δ 183.44 ($C_{NHC}$), 151.71, 150.94, 146.32, 146.01, 145.45, 141.02, 139.63, 135.96, 130.74, 126.70, 124.64, 123.49, 122.28, 116.54, 116.03, 28.88, 24.25, 24.18, 18.02, 17.40. Elemental analysis (%) calcd. for $C_{39}H_{50}CuN_5$: C, 58.81; H, 6.28; N, 8.80; found: C 58.89; H, 6.32; N, 8.20.

**[Cu(IPr)(mesBIAN)]$PF_6$•0.5$CH_2Cl_2$ (6)**

Following the general procedure, a dark green/black solid was isolated in 68% yield (0.110 g). $^1$H NMR ($CDCl_3$, 400MHz): δ 8.06 (d, *J* = 8.3 Hz, 2H), 7.51 (t, *J* = 7.8 Hz, 2H), 7.43 (dd, *J* = 8.3, 7.3 Hz, 2H), 7.18 – 7.10 (m, 6H), 6.89 (s, 4H), 6.40 (d, *J* = 7.3 Hz, 2H), 2.60 (sept, *J* = 6.8 Hz, 4H), 2.42 (s, 6H), 1.59 (s, 11H), 1.08 (d, *J* = 6.8 Hz, 11H), 0.89 (d, *J* = 6.9 Hz, 11H).$^{13}$C NMR ($CDCl_3$, 400MHz): δ 167.46, 145.14, 143.13,142.74, 136.36, 135.46, 132.30, 131.06, 130.69, 129.94, 129.28, 126.78, 125.98, 124.86, 124.62, 124.46, 28.84, 24.33, 23.63, 21.07, 17.70 Elemental analysis (%) calcd. for $C_{57.5}H_{65}ClCuF_6N_4P$: C, 65.39; H, 6.20; N, 5.30; found: C 65.42; H, 6.16; N, 5.51.

**[Cu(SIPr)(Hdpa)]$PF_6$ (10)**

Following the general procedure, a white solid was isolated in 63% yield (0.077 g). $^1$H NMR ($CDCl_3$, 400MHz): δ 8.03 (s, 1H), 7.50 – 7.40 (m, 4H), 7.26 (d, *J* = 7.8 Hz, 4H), 7.12 (d, *J* = 8.5 Hz, 2H), 6.29 (t, *J* = 6.4 Hz, 2H), 6.16 (dd, *J* = 5.6, 1.9 Hz, 2H), 4.07 (s, 4H), 3.48 (Et2O), 3.14 (sept, *J* = 6.9 Hz, 4H), 1.34 (d, *J* = 6.9 Hz, 12H), 1.15 (d, *J* = 6.8 Hz, 12H). $^{13}$C NMR ($CDCl_3$, 400MHz) δ 153.08, 147.53, 147.07, 139.24, 136.23, 130.02, 125.16, 116.41, 115.30, 53.84 ($CH_2Cl_2$), 29.02, 24.86, 24.42. Elemental analysis (%) calcd. for $C_{37}H_{46}CuN_5$: C, 57.69; H, 6.15; N, 9.09; found: C 57.53; H, 6.31; N, 8.93.

**[Cu(SIPr)(3,3'-$Me_2$Hdpa)] $PF_6$ (11)**

Following the general procedure an off-white solid was isolated in 78% yield (0.099 g). $^{1}$H NMR ($CDCl_3$, 400MHz): 7.50-7.39 (m, 4H), 7.26 (d, *J* = 7.8 Hz, 4H), 6.67 (s, 1H), 6.39 (dd, *J* = 7.4, 5.5 Hz, 2H), 6.20 (dd, *J* = 5.6, 1.8 Hz, 2H), 4.10 (s, 4H), 3.15 (sept, J= 6.9 Hz, 4H), 2.31 (s, 6H), 1.34 (d, *J* = 6.9 Hz, 12H), 1.15 (d, *J* = 6.8 Hz, 12H). $^{13}$C NMR ($CDCl_3$, 400MHz): δ 150.93, 147.10, 146.17, 140.23, 136.24, 130.01, 125.12, 121.59, 117.36, 53.92 ($CH_2Cl_2$), 28.97, 24.90, 24.41, 17.28. Elemental analysis (%) calcd. for $C_{39}H_{52}CuN_5$: C, 58.67; H, 6.51; N, 8.77; found: C 58.25; H, 6.61; N, 8.64.

**[Cu(SIPr)(3,4'-Me$_2$Hdpa)]PF$_6$ (7)**

Following the general procedure, a pale-yellow solid was isolated in 69% yield (0.088 g). $^{1}$HNMR ($CDCl_3$, 400MHz): δ 7.44 (t, *J* = 7.8 Hz, 2H), 7.29 (ddd, *J* = 7.3, 1.9, 1.0 Hz, 1H), 7.24 (s, 4H), 7.16 (s, 1H), 7.12 – 7.07 (m, 1H), 6.30 – 6.15 (m, 3H), 6.05 (d, *J* = 5.7 Hz, 1H), 5.30 (dichloromethane), 4.08 (s, 4H), 3.14 (sept, *J* = 6.9 Hz, 4H), 2.30 (s, 3H), 2.23 (s, 3H), 1.33 (d, *J* = 6.9 Hz, 12H), 1.15 (d, *J* = 6.8 Hz, 12H). $^{13}$C NMR ($CDCl_3$, 400MHz): δ 152.67, 151.69, 147.04, 147.02, 145.73, 139.64, 136.22, 129.95, 125.10, 122.33, 118.55, 116.32, 115.86, 68.13, 53.86 ($CH_2Cl_2$), 29.00, 25.76, 24.84, 24.48, 20.92, 17.44. Elemental analysis (%) calcd. for $C_{39}H_{52}CuN_5PF_6$: C, 56.36; H, 6.35; N, 8.32; found: C, 56.48; H, 6.35, N, 8.33.

**[Cu(SIPr)(3,5'-Me$_2$Hdpa)]PF$_6$ (8)**

Following the general procedure, a pale-yellow solid was isolated in 85% yield (0.108 g) was formed. $^{1}$H NMR ($CDCl_3$, 400MHz): δ 7.46 – 7.34 (m, 3H), 7.34 – 7.20 (m, 5H), 7.16 (d, *J* = 8.5 Hz, 2H), 6.32 – 6.21 (m, 3H), 4.08 (s, 4H), 3.15 (sept, *J* = 6.9 Hz, 4H), 2.30 (s, 3H), 1.95 (s, 3H), 1.33 (d, *J* = 6.9 Hz, 12H), 1.18 (d, *J* = 6.9 Hz, 12H). $^{13}$C NMR ($CDCl_3$, 400MHz): 206.08($C_{NHC}$), 151.58,150.84, 146.98, 146.43, 145.59, 141.00, 139.62, 136.15, 129.90, 126.69, 124.96, 122.13, 116.48, 115.88, 53.87 ($CH_2Cl_2$), 28.99, 24.79, 24.56, 17.94, 17.37. Elemental analysis (%) calcd. for $C_{39}H_{52}CuN_5PF_6$: C, 51.80; H, 5.92; N, 7.42; found: C, 51.83; H, 5.75, N, 7.78.

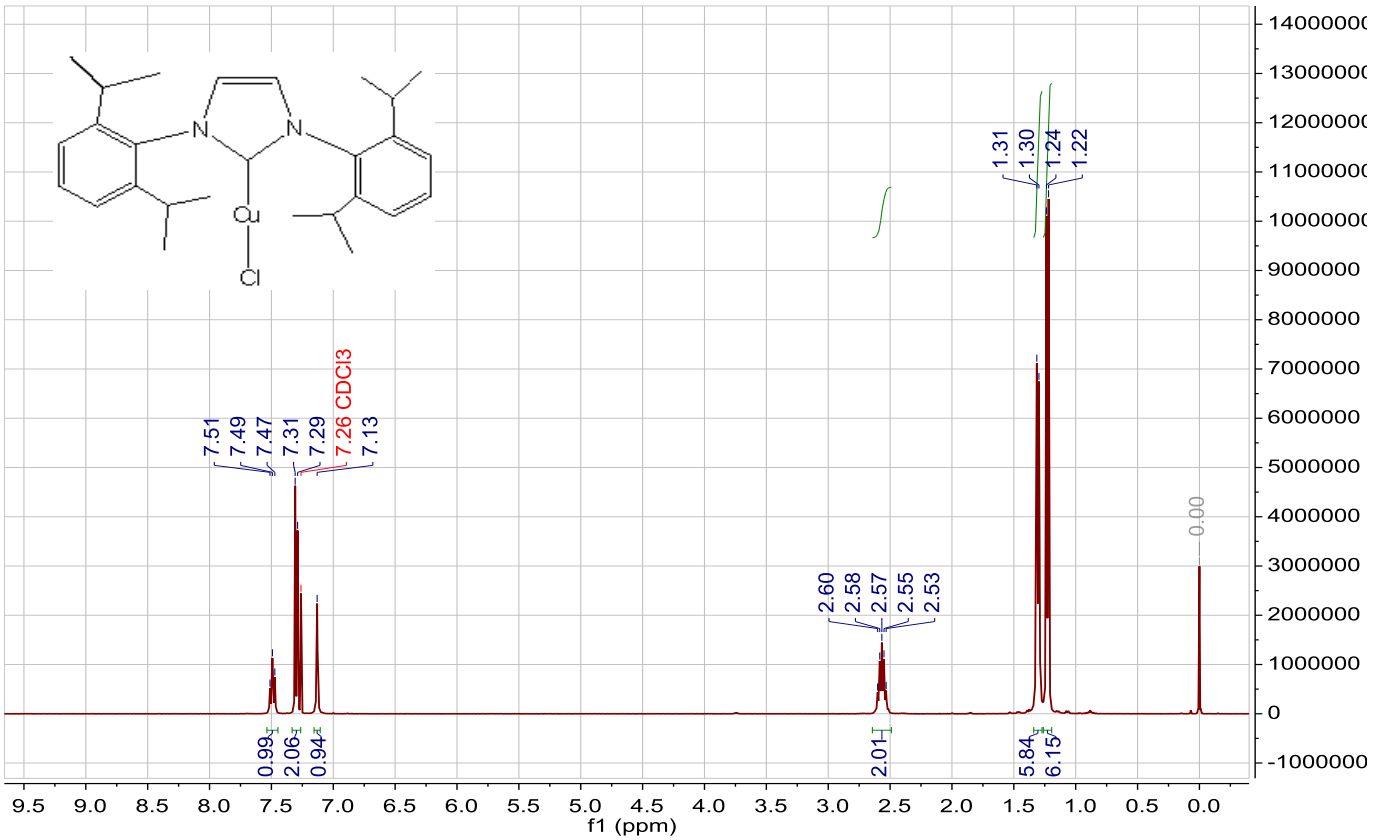


**Figure S16**. $^{1}$H NMR spectrum of [Cu(IPr)Cl] in $CDCl_3$

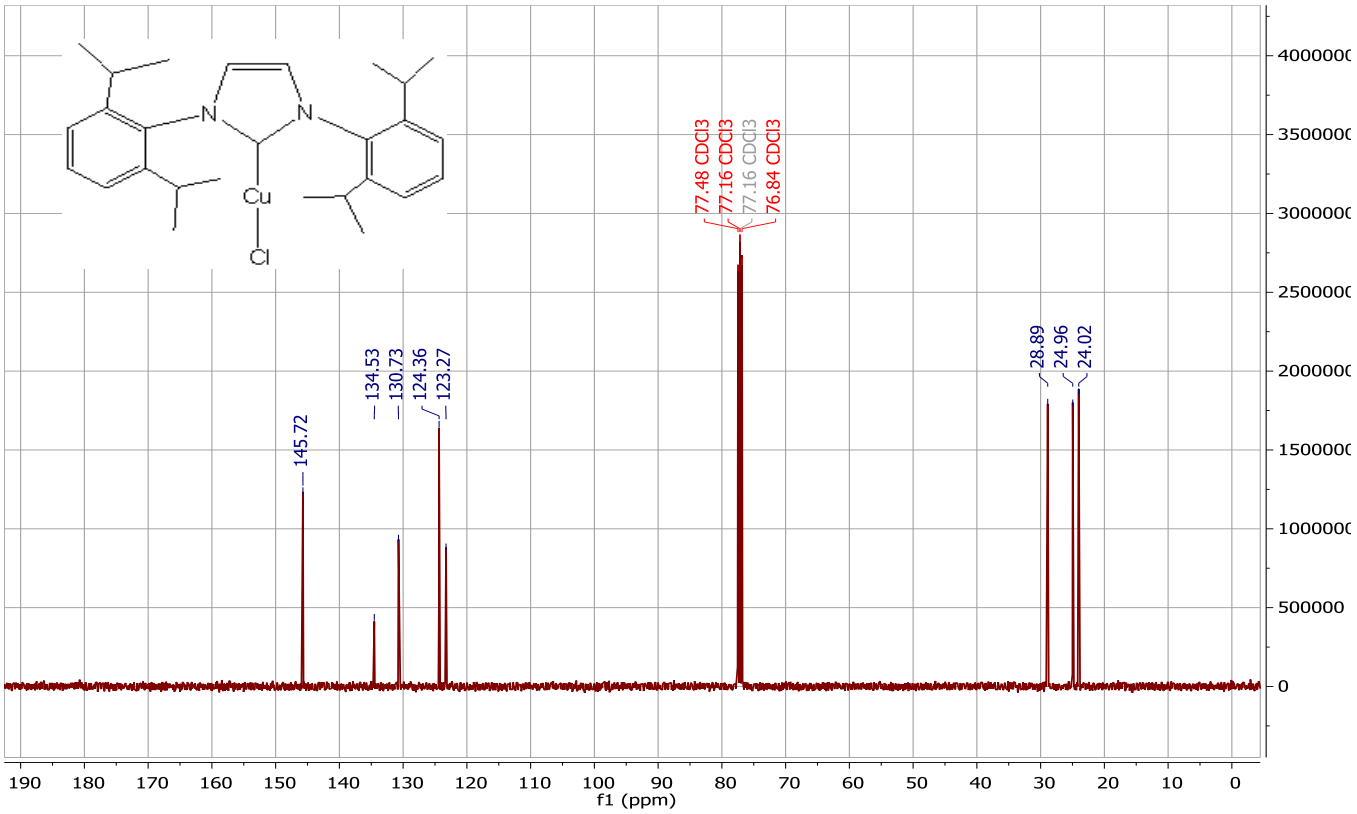


**Figure S17**. $^{13}$C NMR spectrum of [Cu(IPr)Cl] in $CDCl_3$

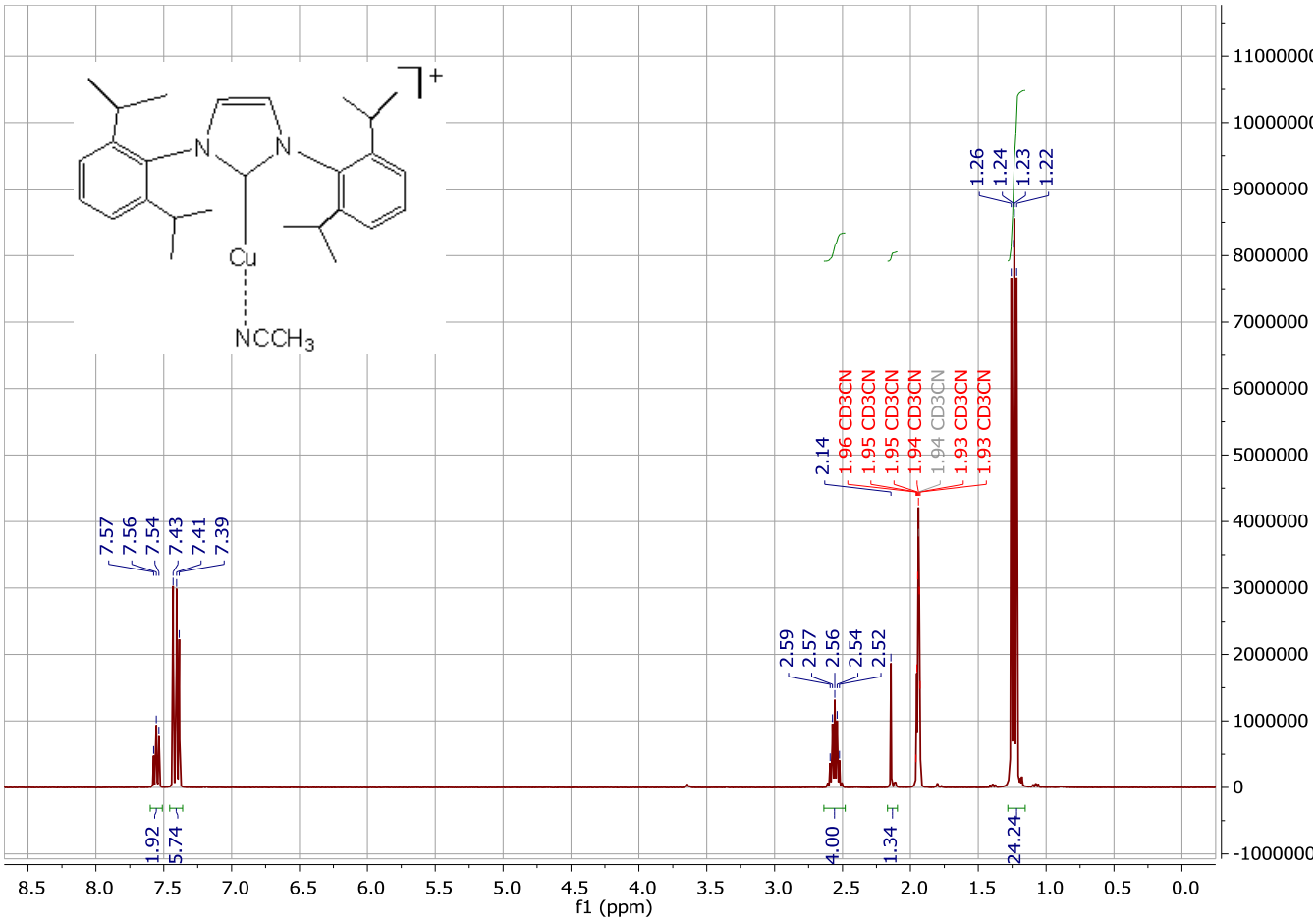


**Figure S18**. $^{1}H$ NMR spectrum of [Cu(IPr)]$PF_6$ in $CD_3CN$

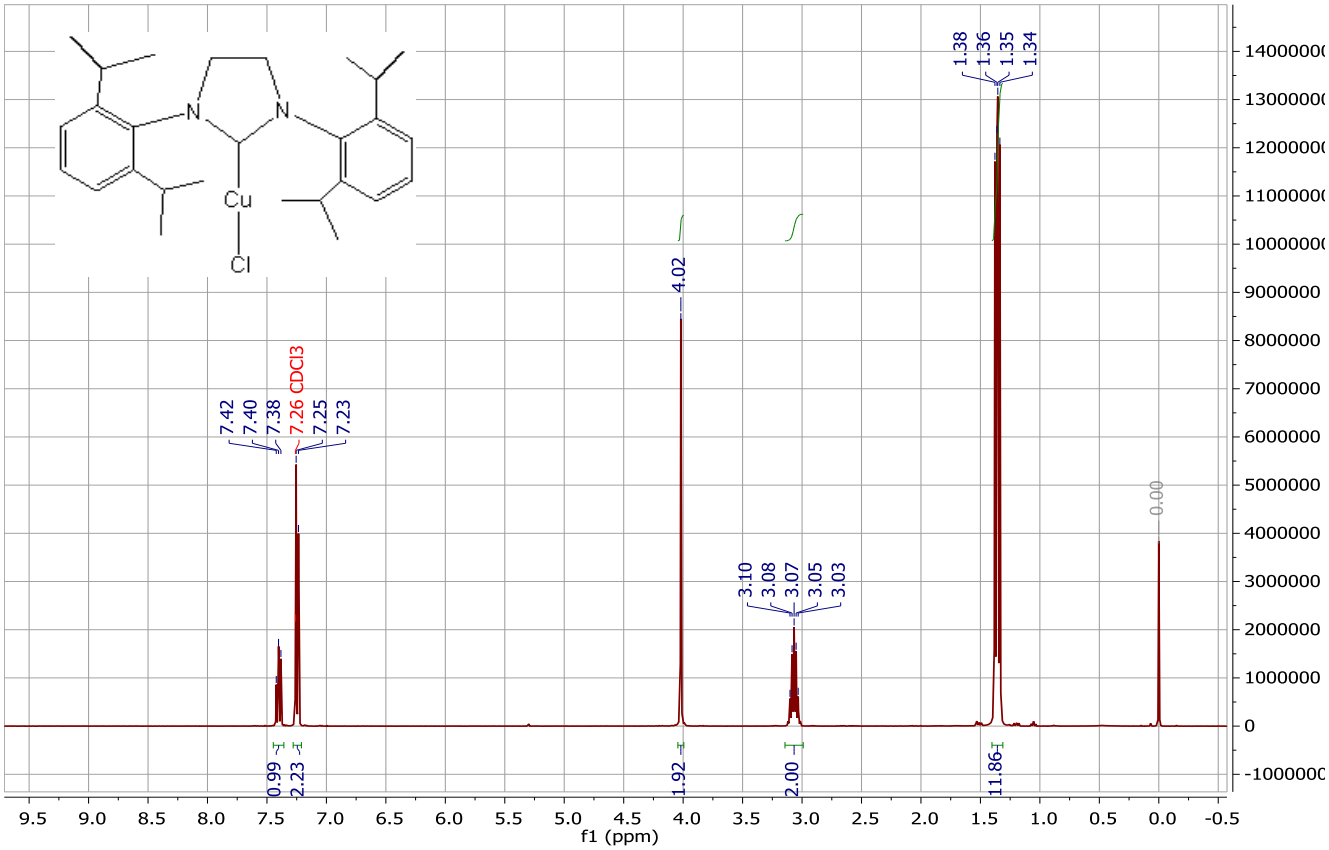


**Figure S19**. $^{1}$H NMR spectrum of [Cu(SIPr)Cl] in $CDCl_3$

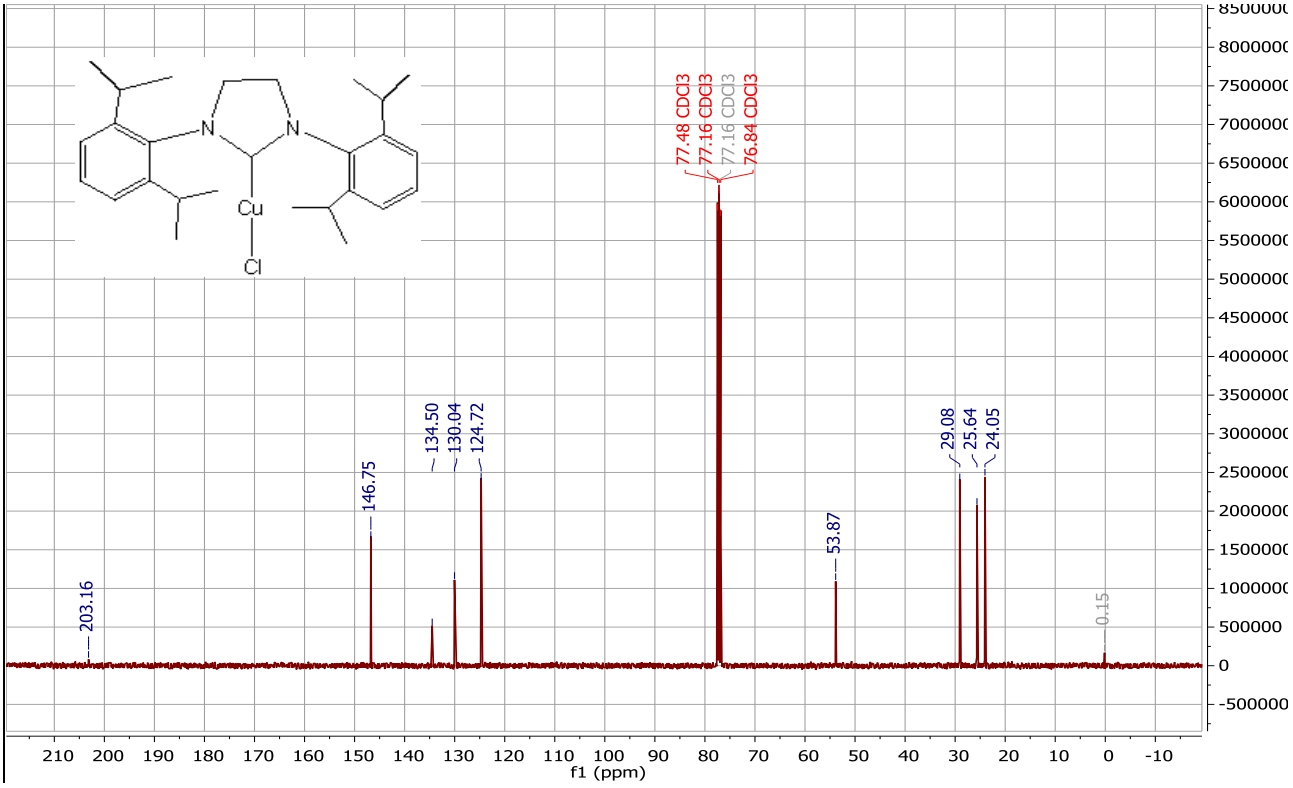


**Figure S20**. $^{13}$C NMR spectrum of [Cu(SIPr)Cl] in $CDCl_3$

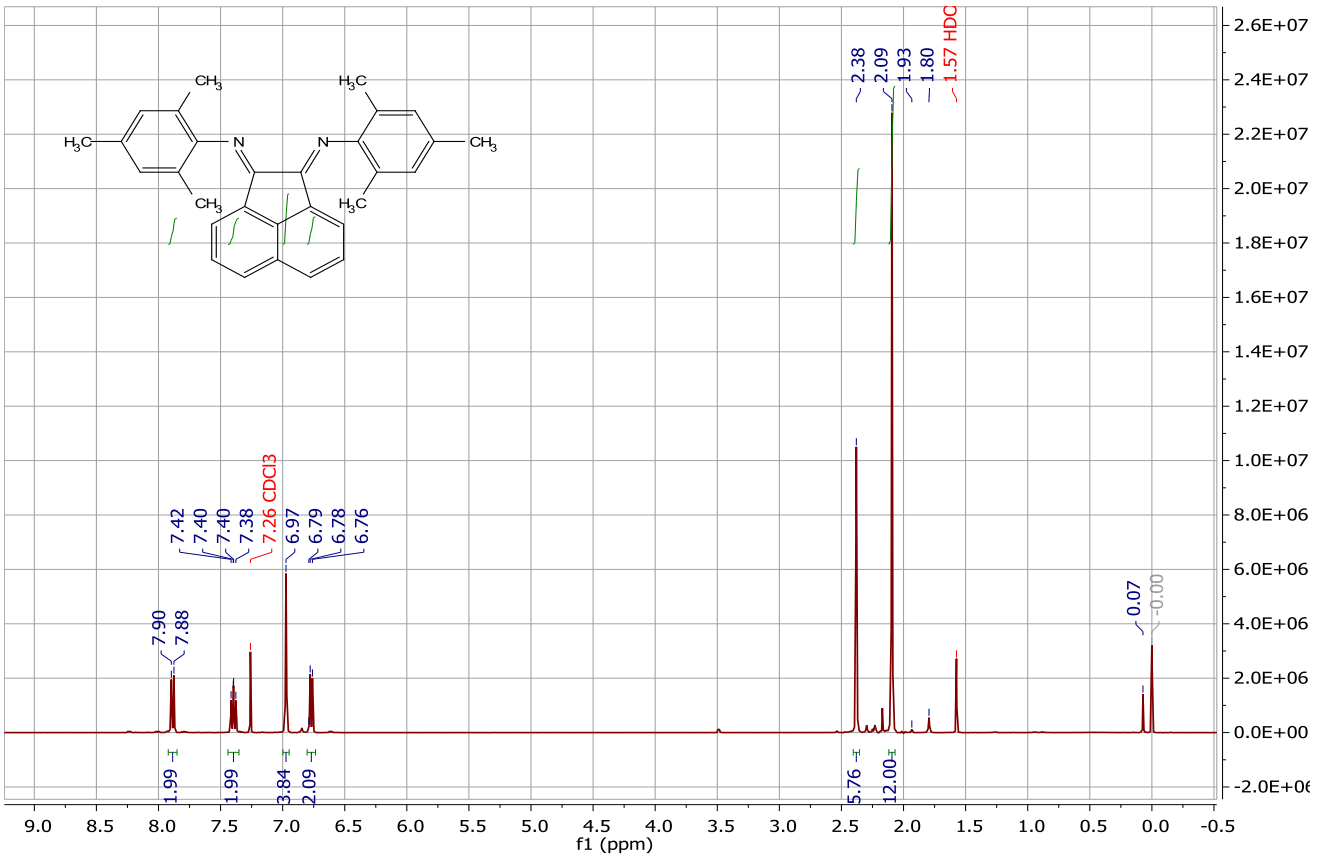


**Figure S21**. $^{1}$H NMR spectrum of mesBIAN in $CDCl_3$

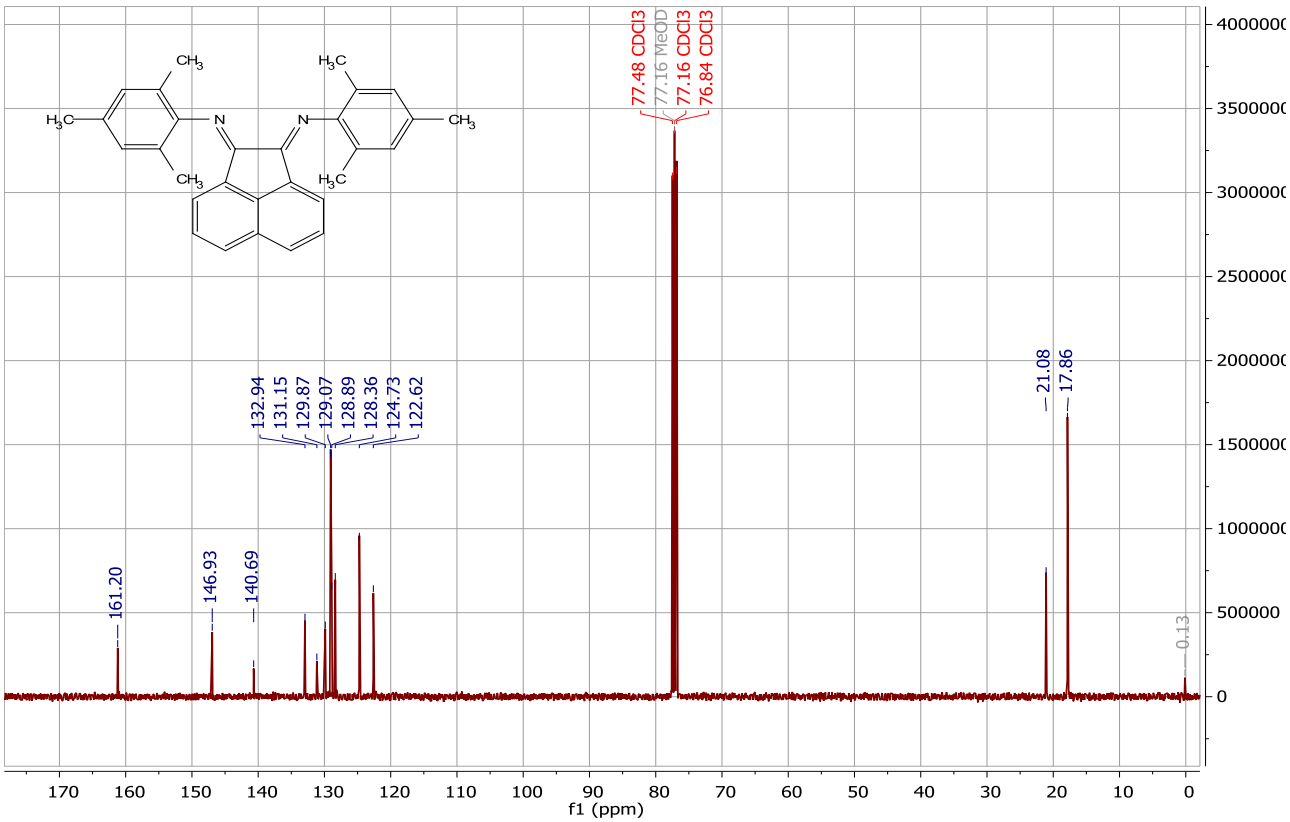


**Figure S22**. $^{13}$C NMR spectrum of mesBIAN in $CDCl_3$

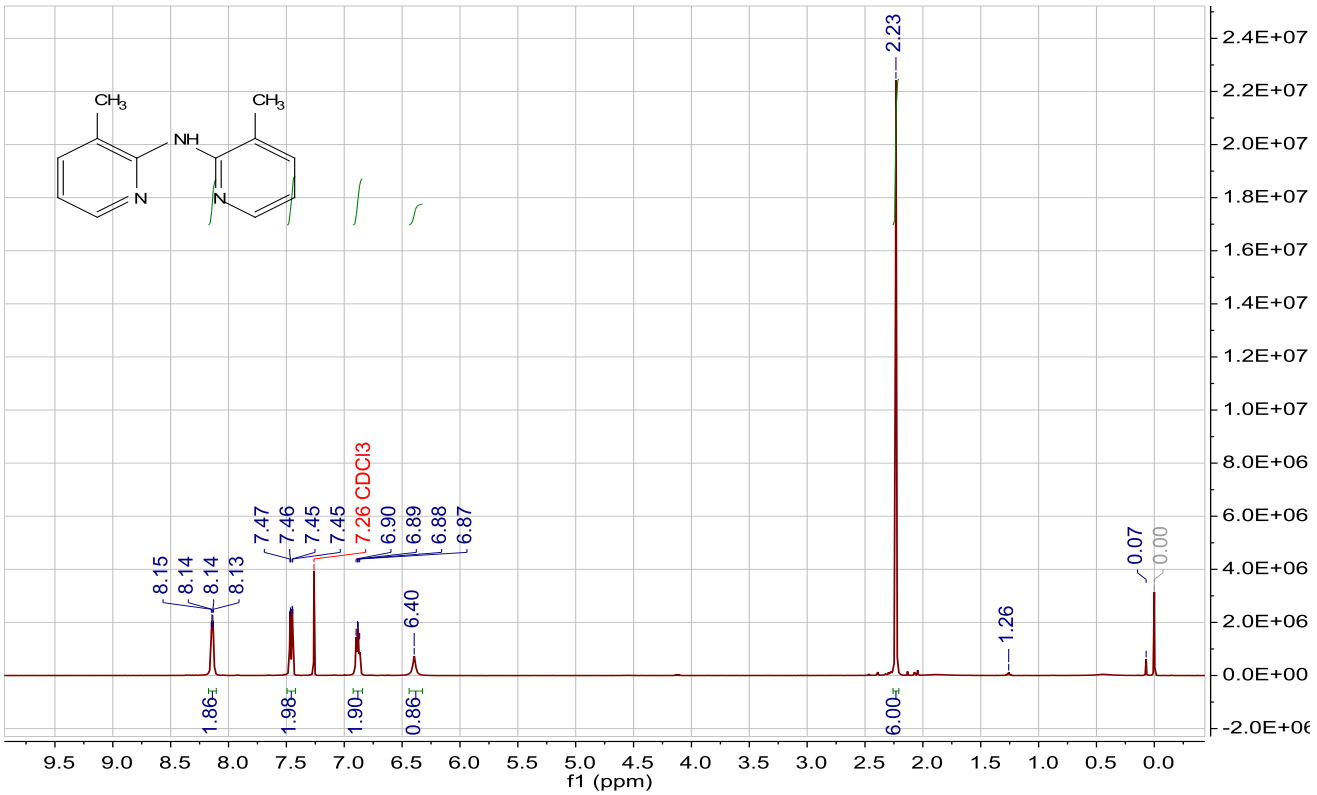


**Figure S23**. $^{1}$H NMR spectrum of 3,3'-$Me_2$Hdpa in $CDCl_3$

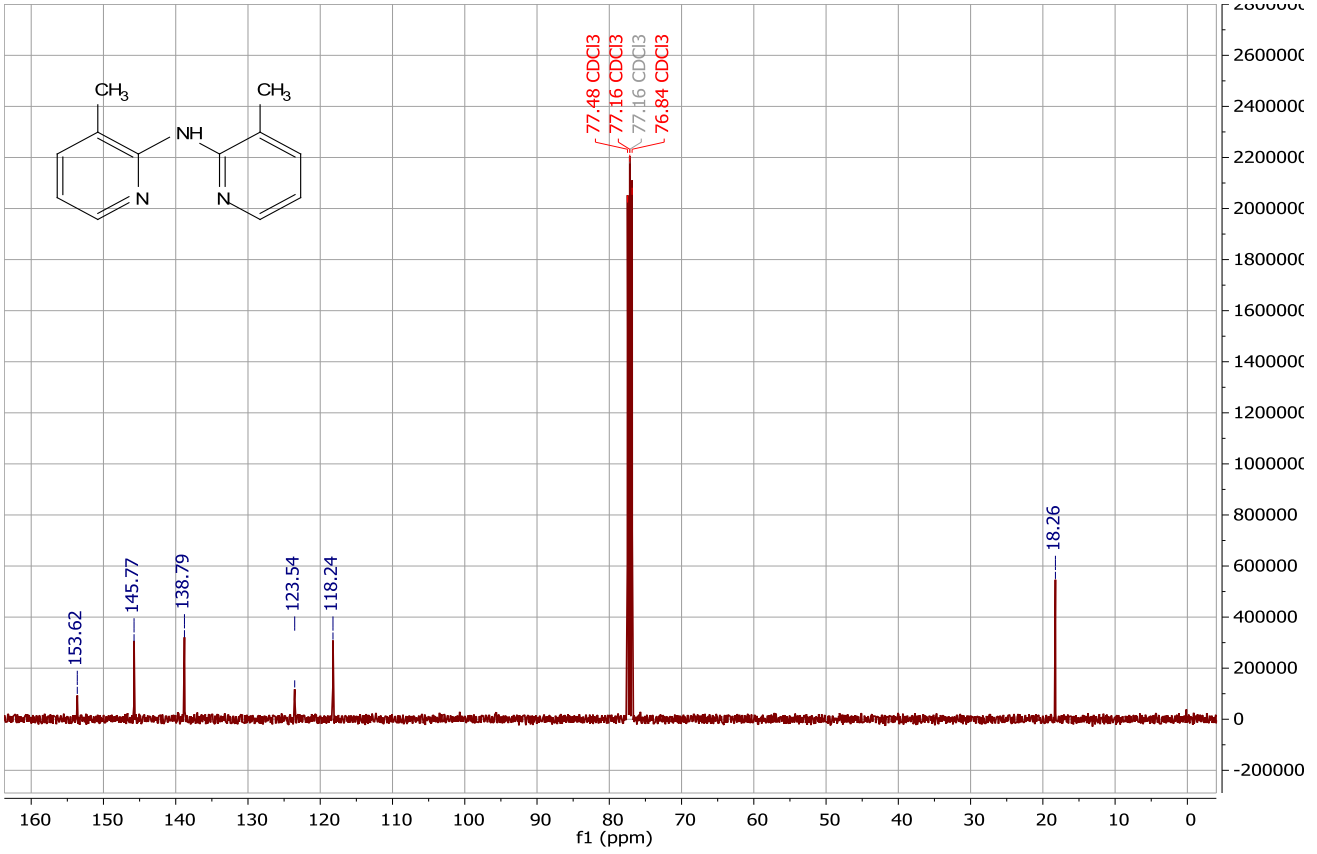


**Figure S24**. $^{13}$C NMR spectrum of 3,3'-$Me_2$Hdpa in $CDCl_3$

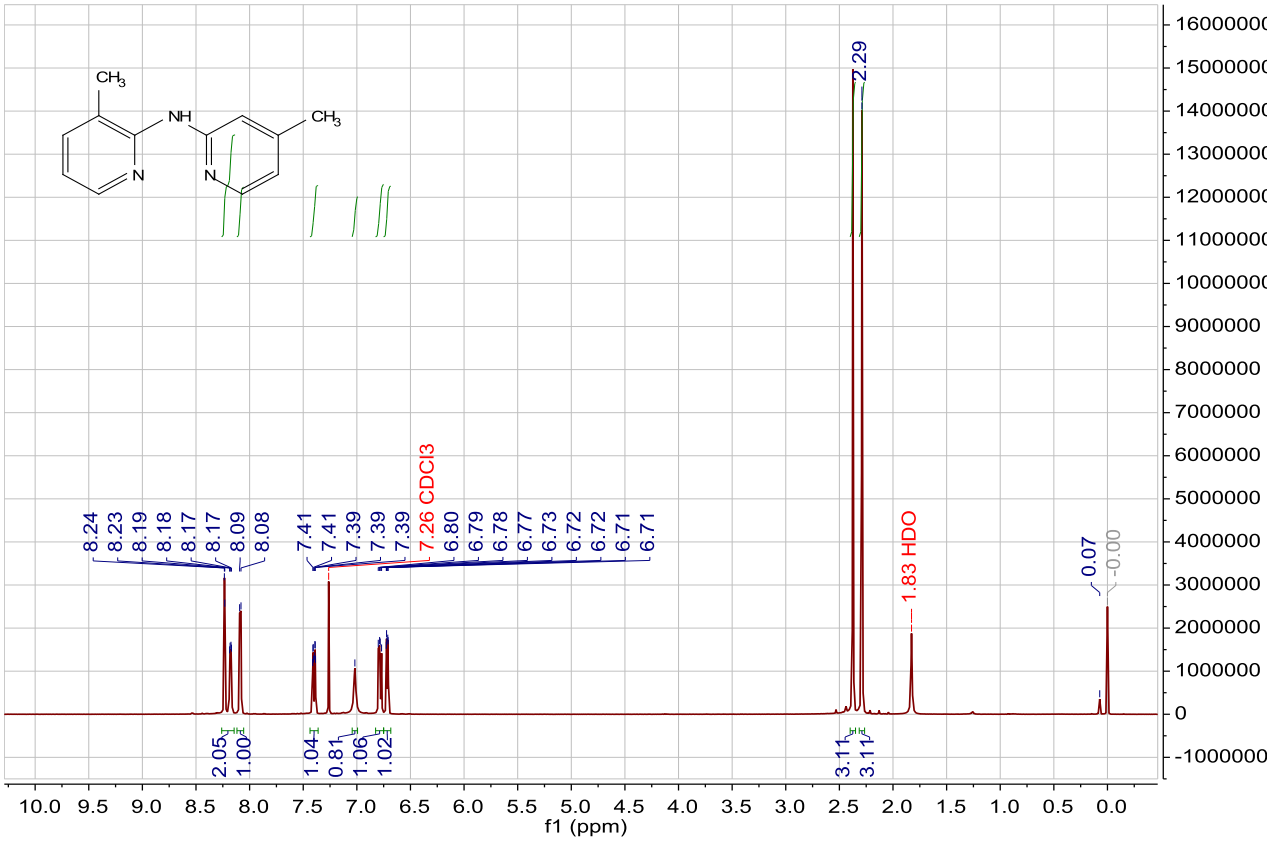


**Figure S25**. $^{1}$H NMR spectrum of 3,4'-$Me_2$Hdpa in $CDCl_3$

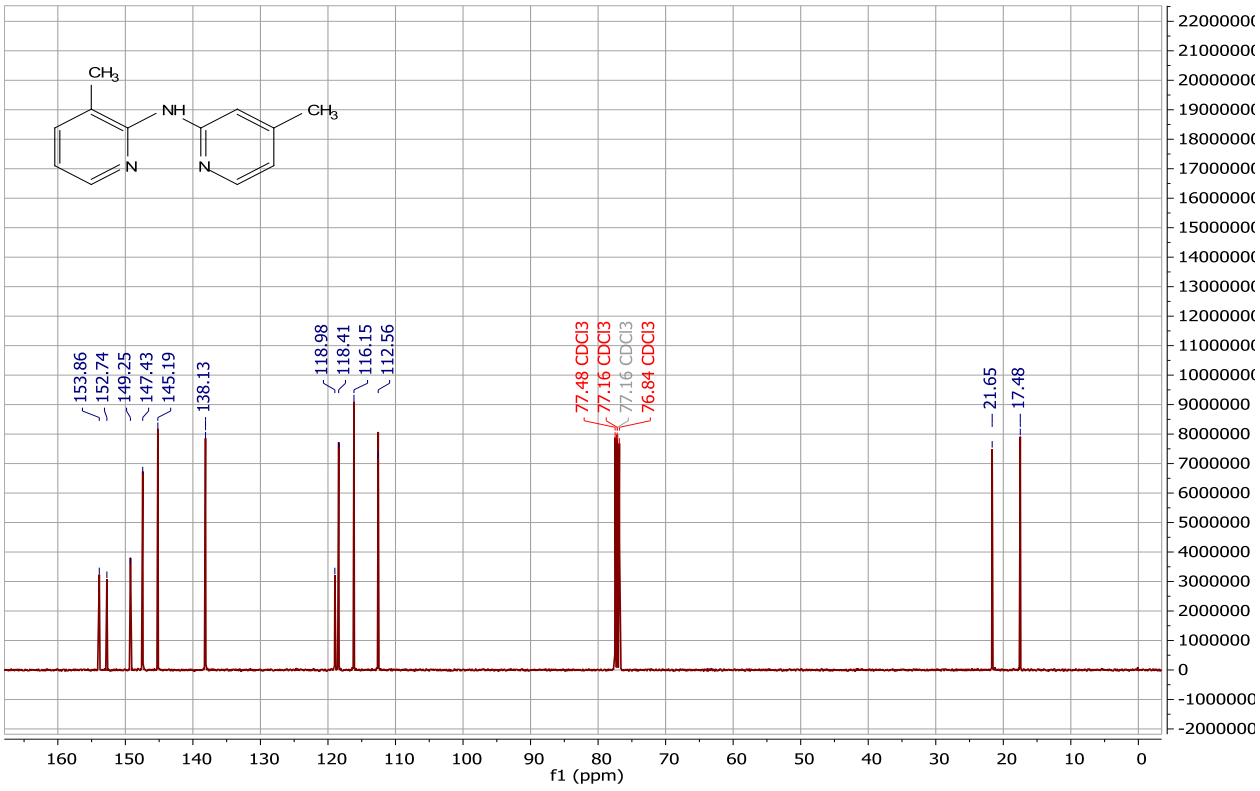


**Figure S26**. $^{13}$C NMR spectrum of 3,4'-$Me_2$Hdpa in $CDCl_3$

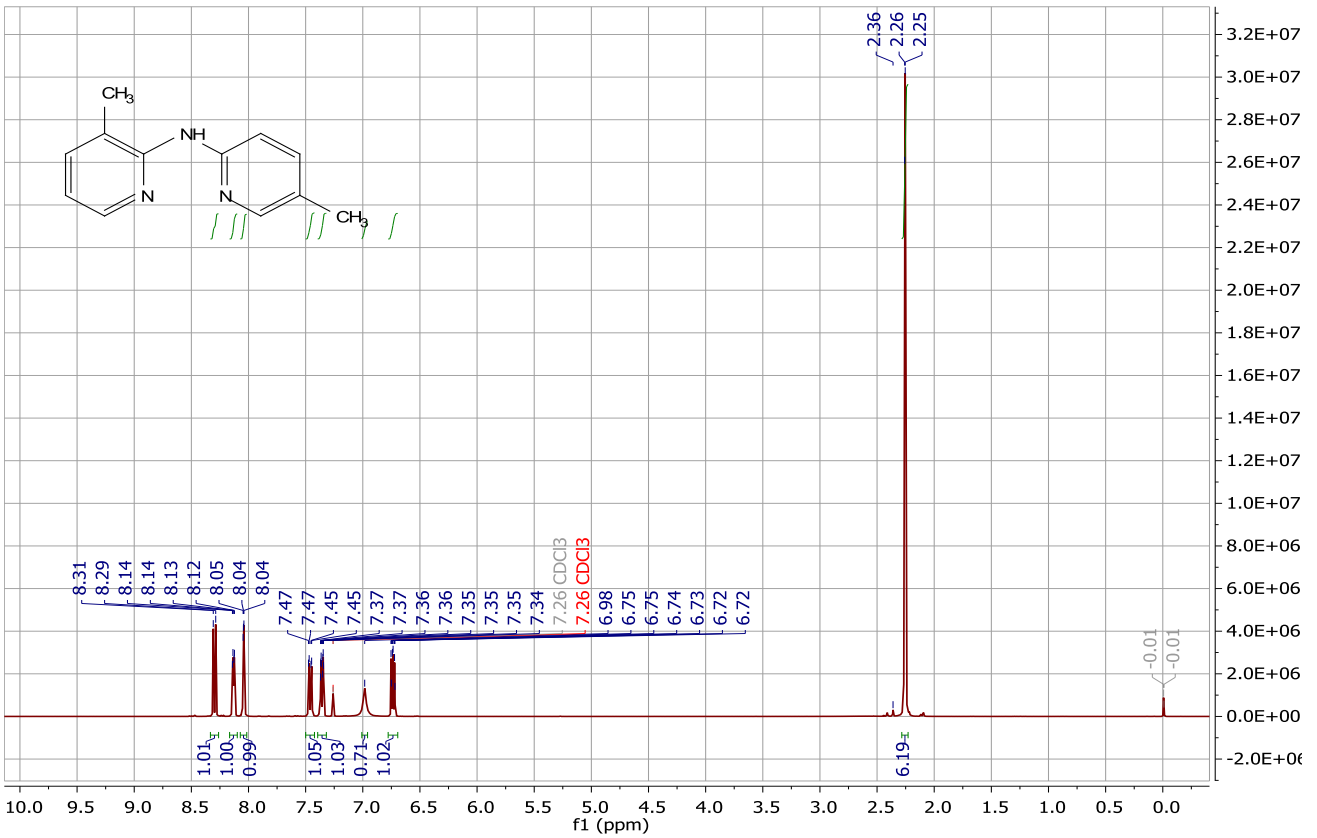


**Figure S27**. $^{1}$H NMR spectrum of 3,5'-$Me_2$Hdpa in $CDCl_3$

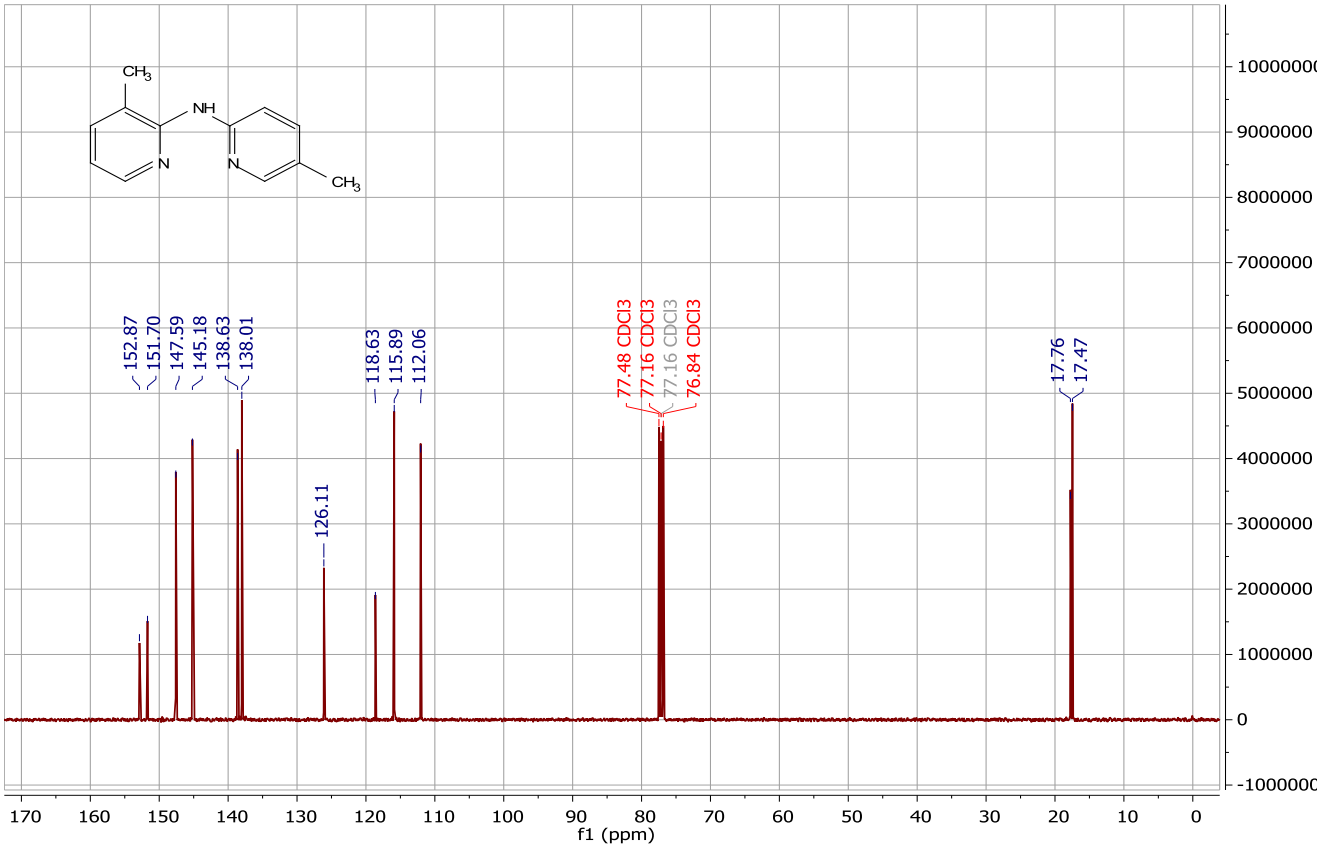


**Figure S28**. $^{13}$C NMR spectrum of 3,5'-$Me_2$Hdpa in $CDCl_3$

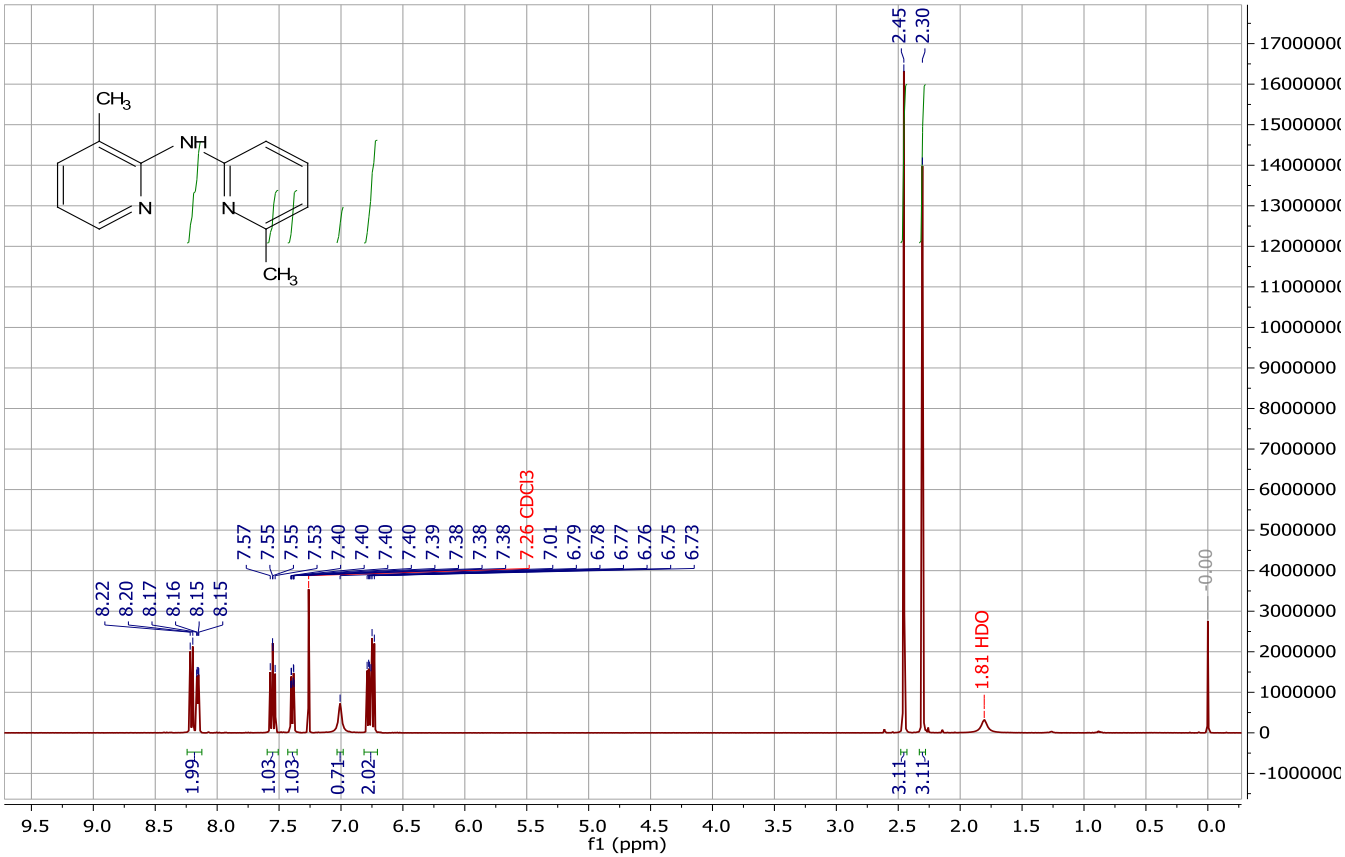


**Figure S29**. $^{1}$H NMR spectrum of 3,6'-$Me_2$Hdpa in $CDCl_3$

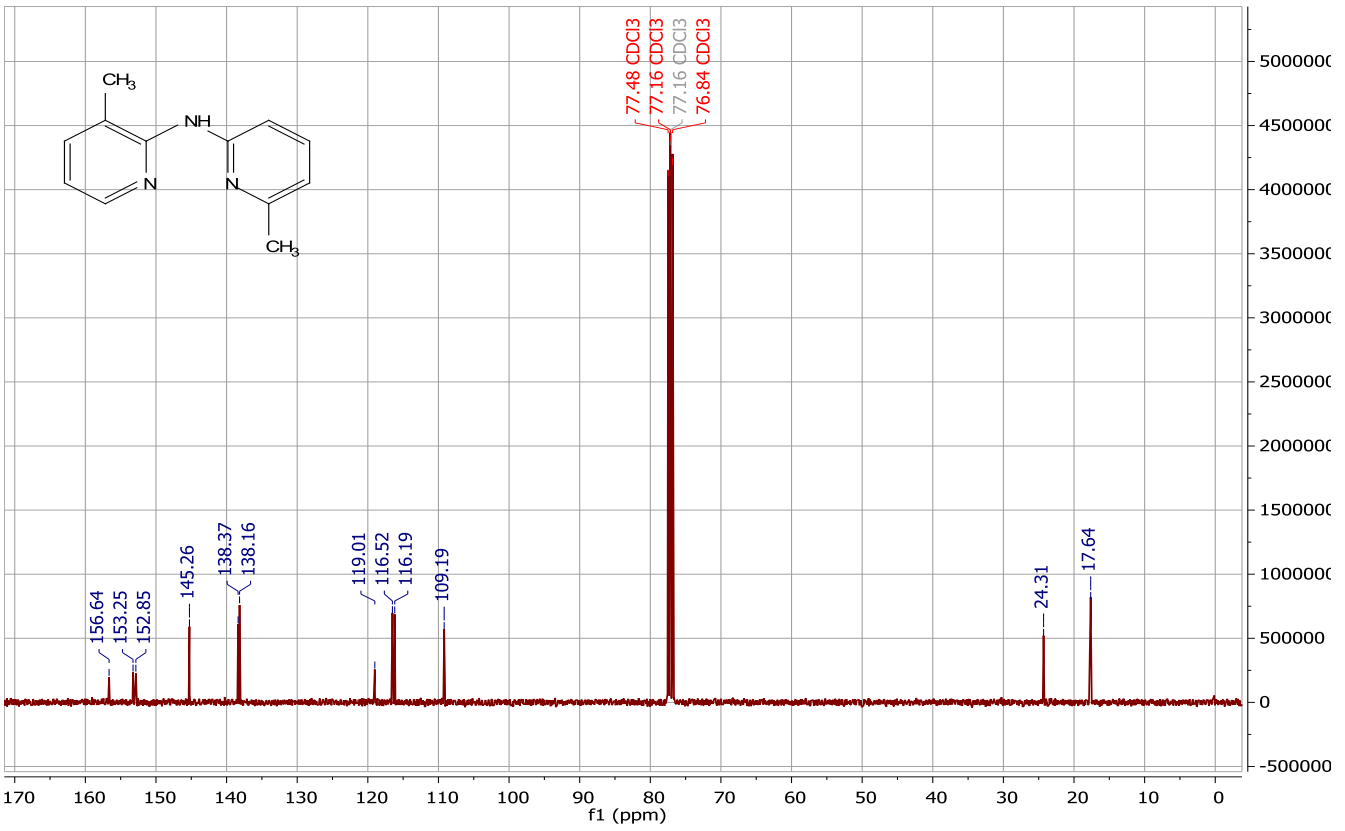


**Figure S30**. $^{13}$C NMR spectrum of 3,6'-$Me_2$Hdpa in $CDCl_3$

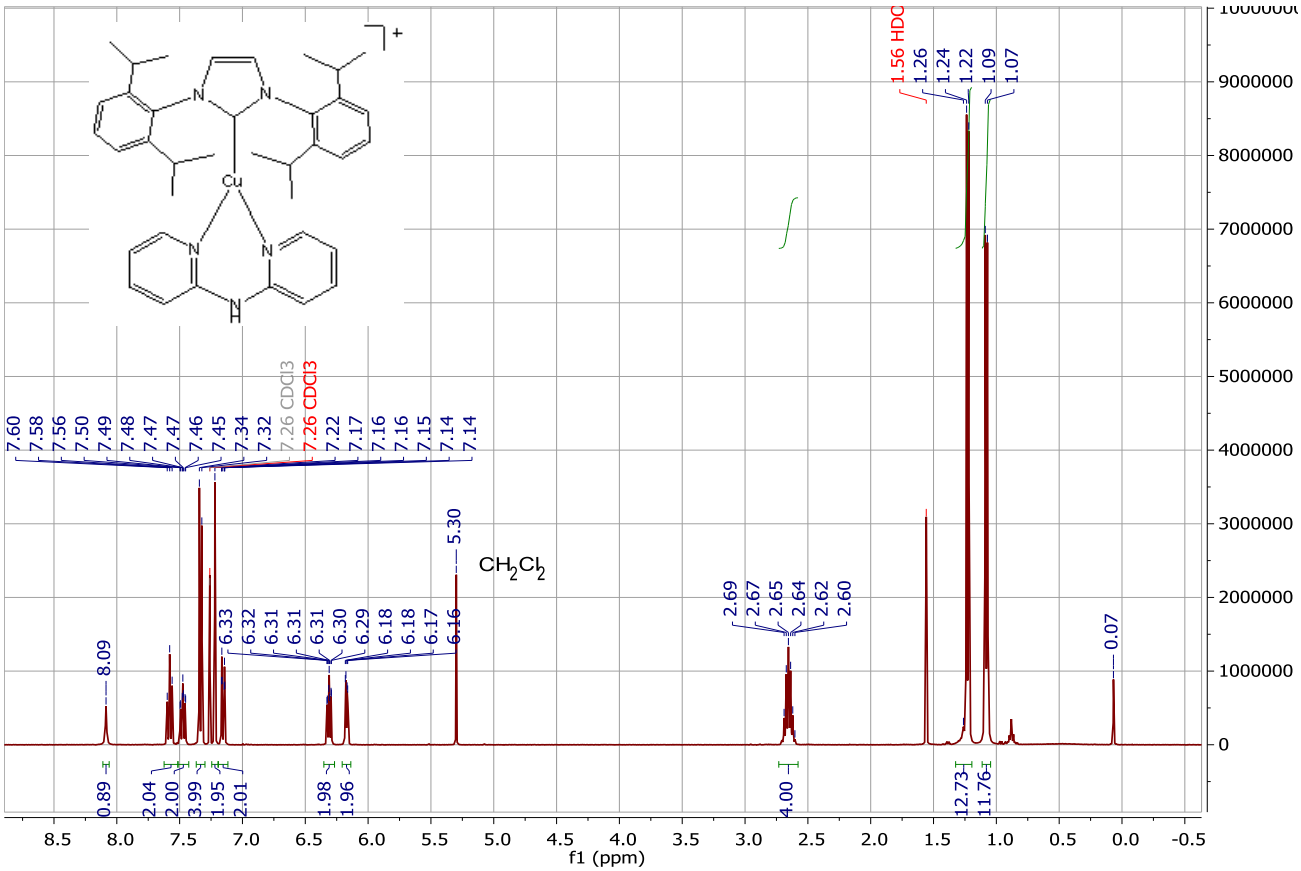


**Figure S31**. $^{1}$H NMR spectrum of [Cu(IPr)(Hdpa)]$PF_6$ (**4**) in $CDCl_3$

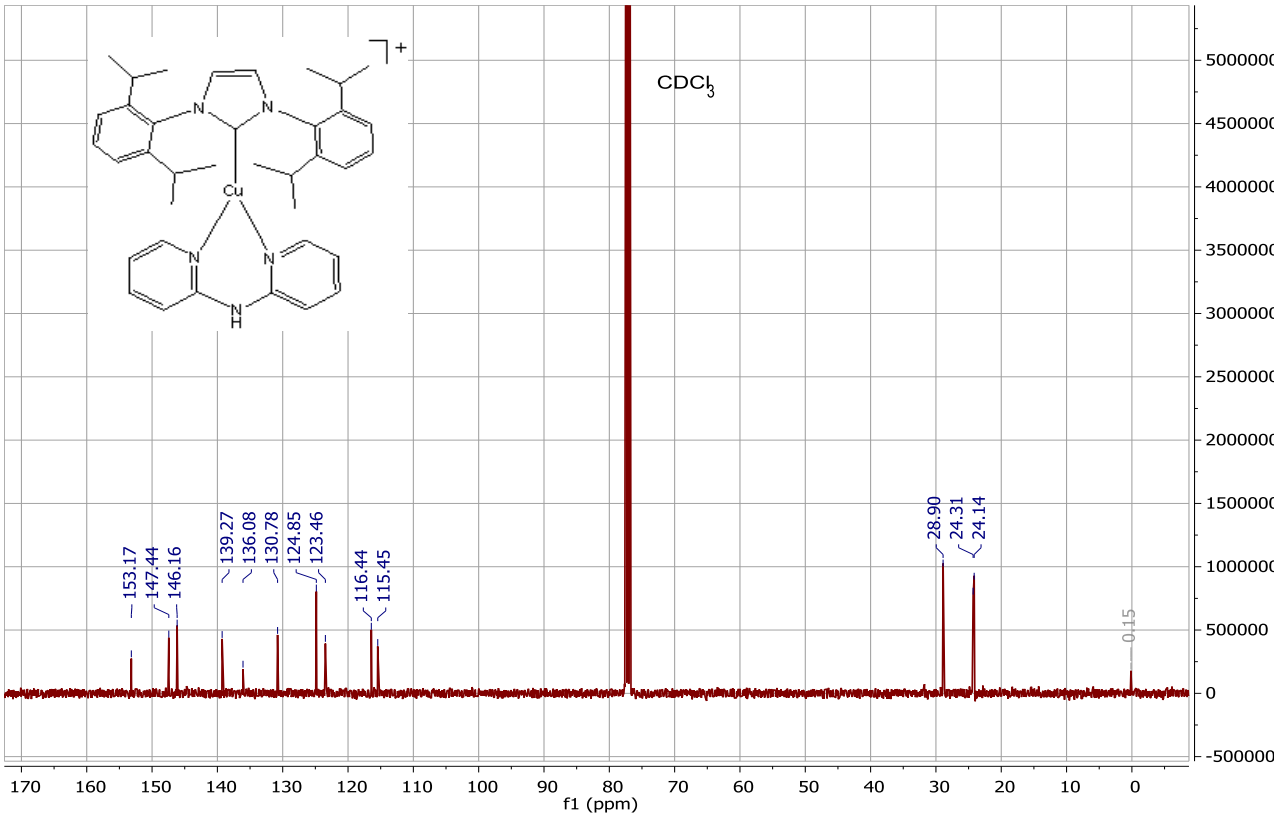


**Figure S32**. $^{13}$C NMR spectrum of [Cu(IPr)(Hdpa)]$PF_6$ (**4**) in $CDCl_3$

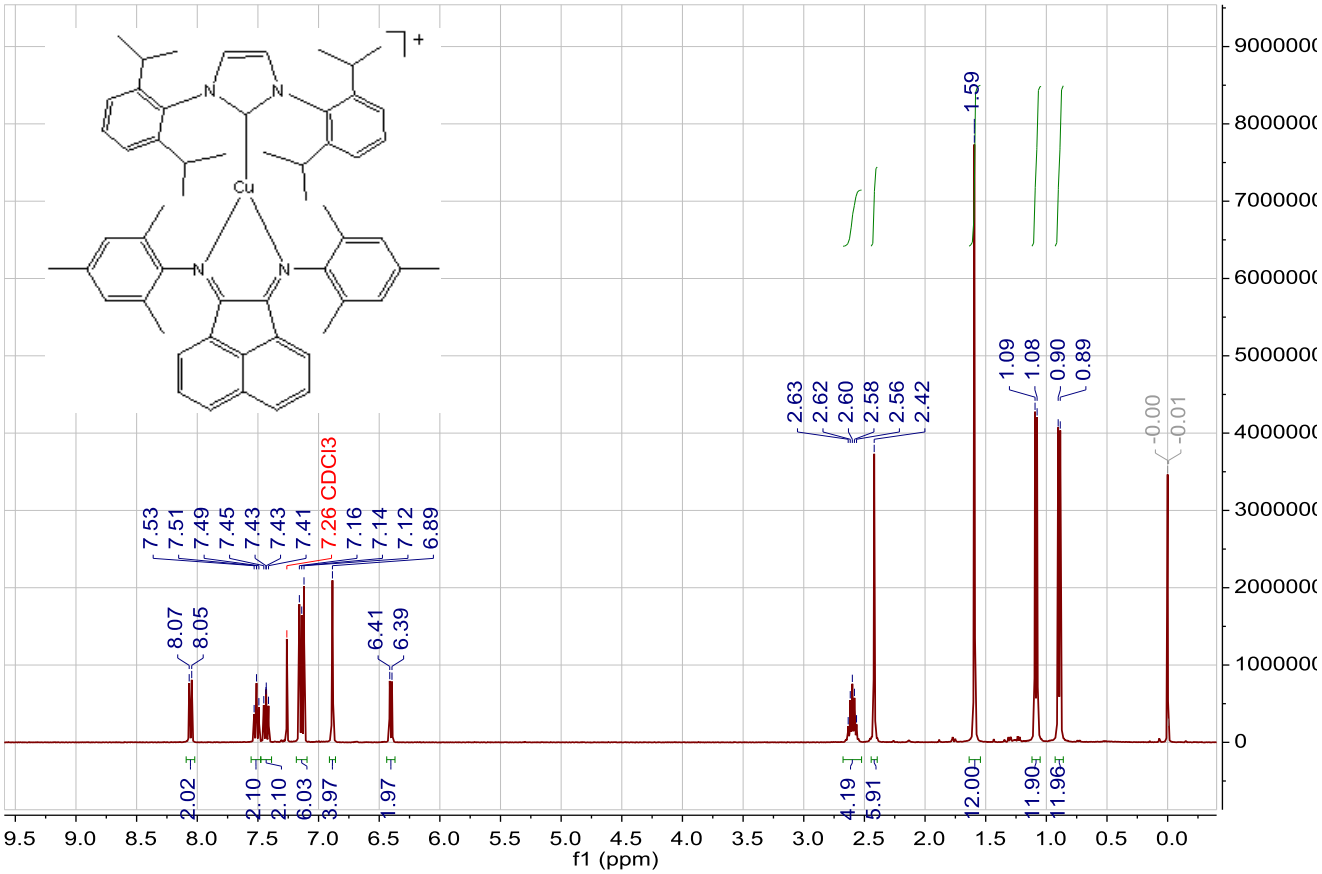


**Figure S33**. $^{1}$H NMR spectrum of [Cu(IPr)(mesBIAN)]$PF_6$ (**6**) in $CDCl_3$

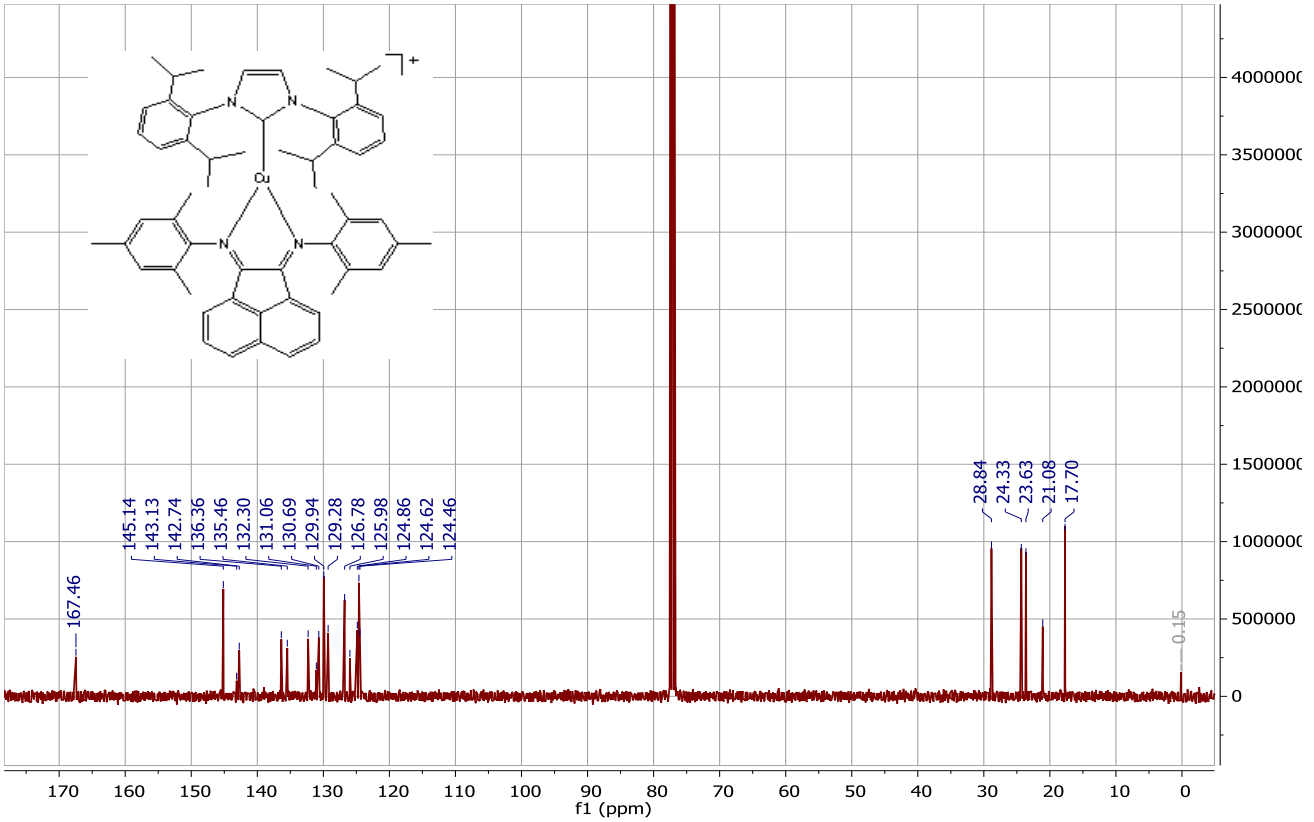


**Figure S34**. $^{13}$C NMR spectrum of [Cu(IPr)(mesBIAN)]$PF_6$ (**6**) in $CDCl_3$

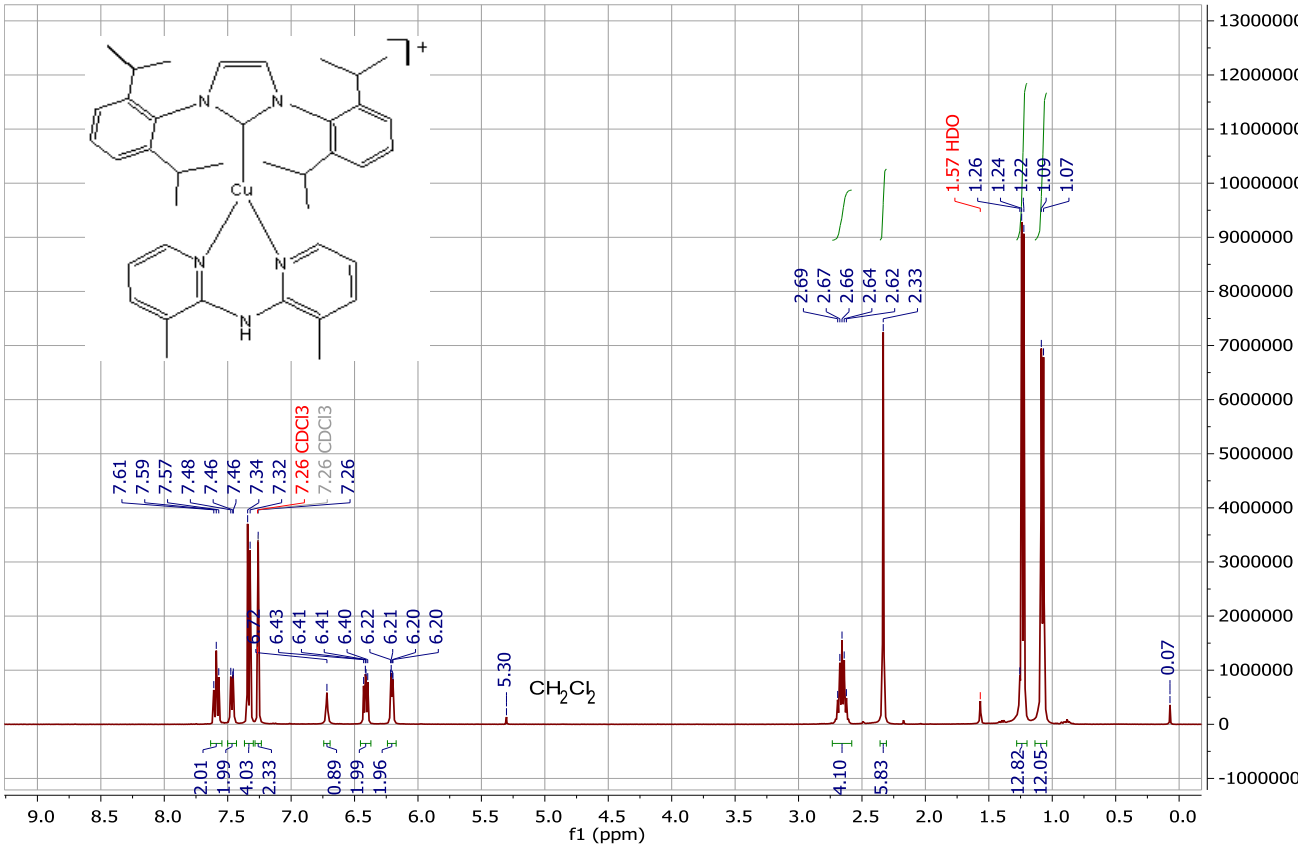


**Figure S35**. $^{1}$H NMR spectrum of [Cu(IPr)(3,3'-$Me_2$Hdpa)]$PF_6$ (**5**) in $CDCl_3$

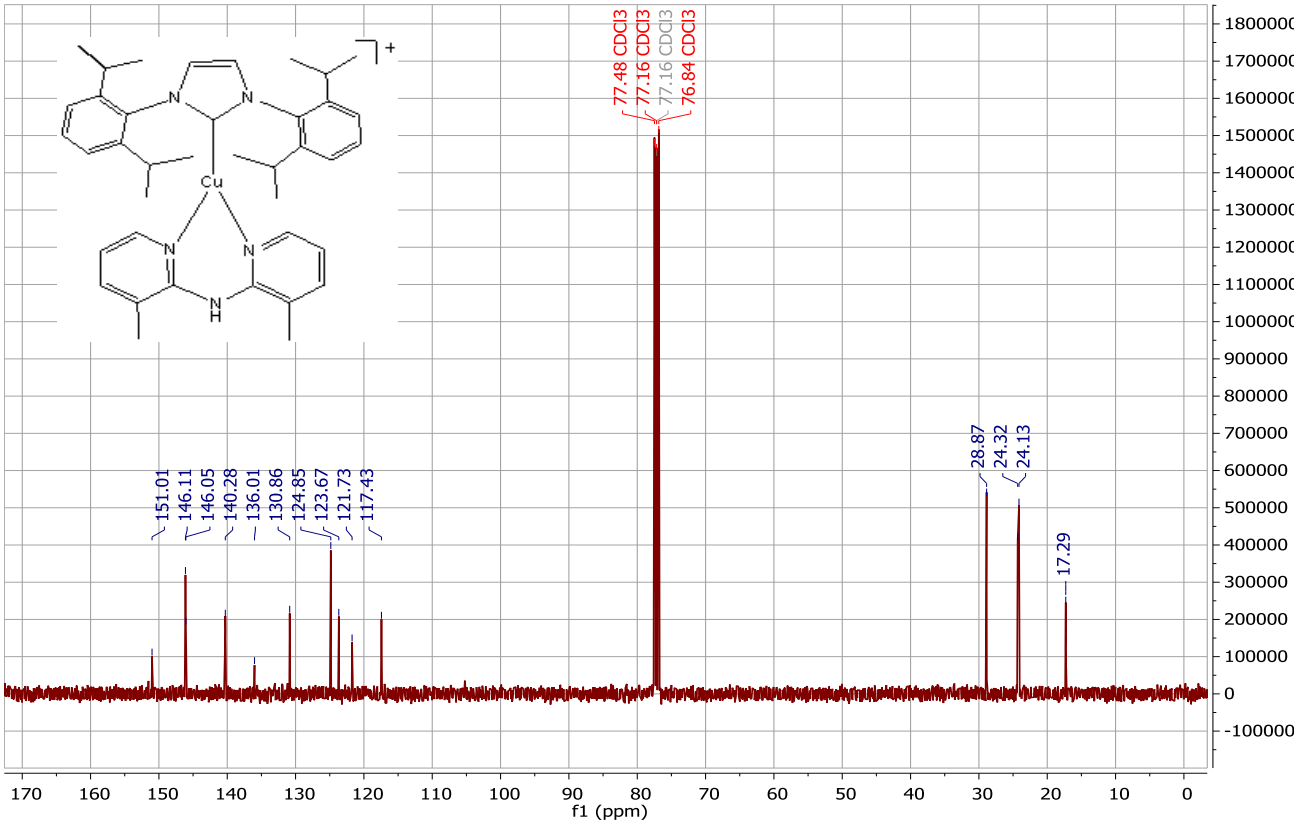


**Figure S36**. $^{13}$C NMR spectrum of [Cu(IPr)(3,3'-$Me_2$Hdpa)]$PF_6$ (**5**) in $CDCl_3$

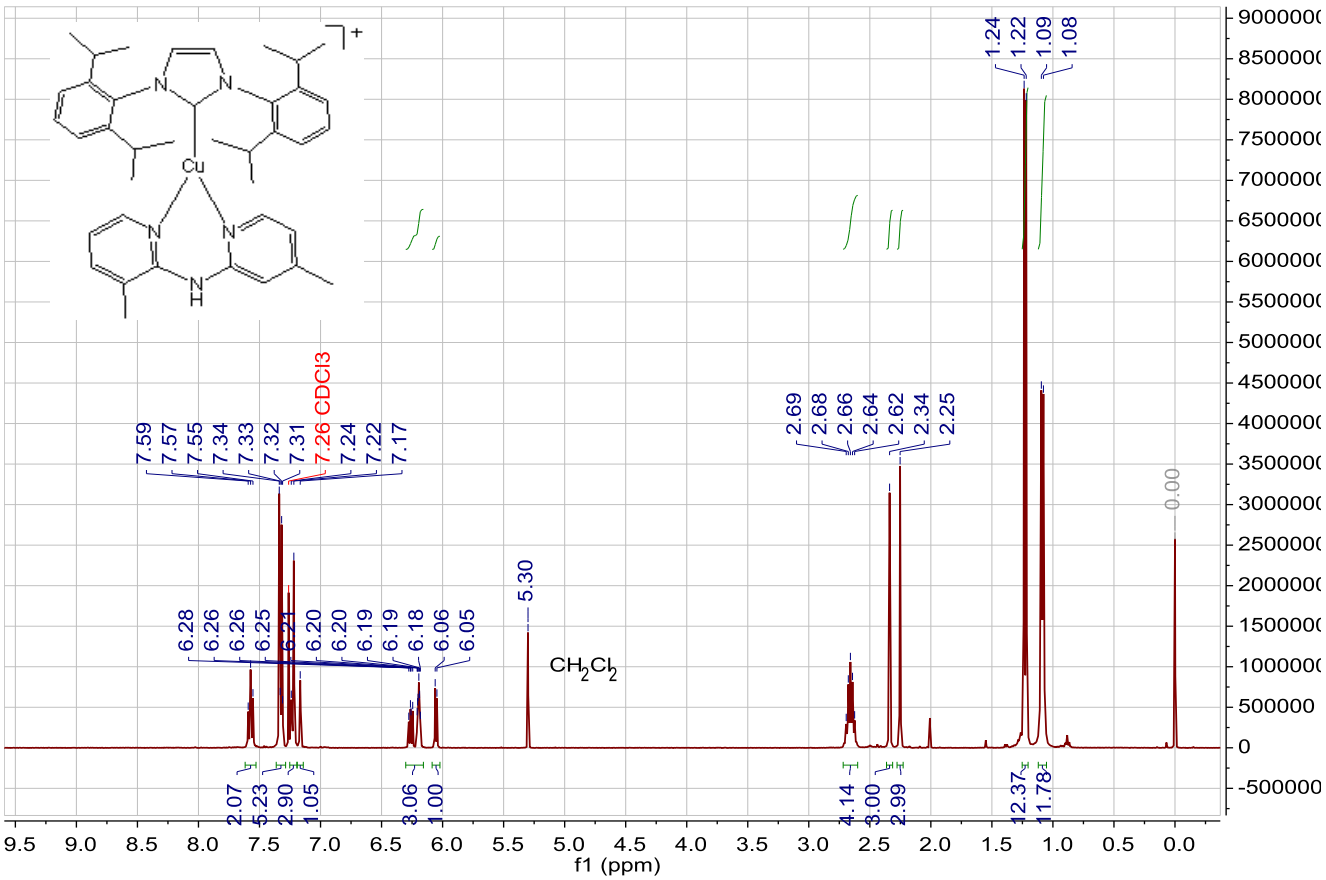


**Figure S37**. $^{1}$H NMR spectrum of [Cu(IPr)(3,4'-$Me_2$Hdpa)]$PF_6$ (**1**) in $CDCl_3$

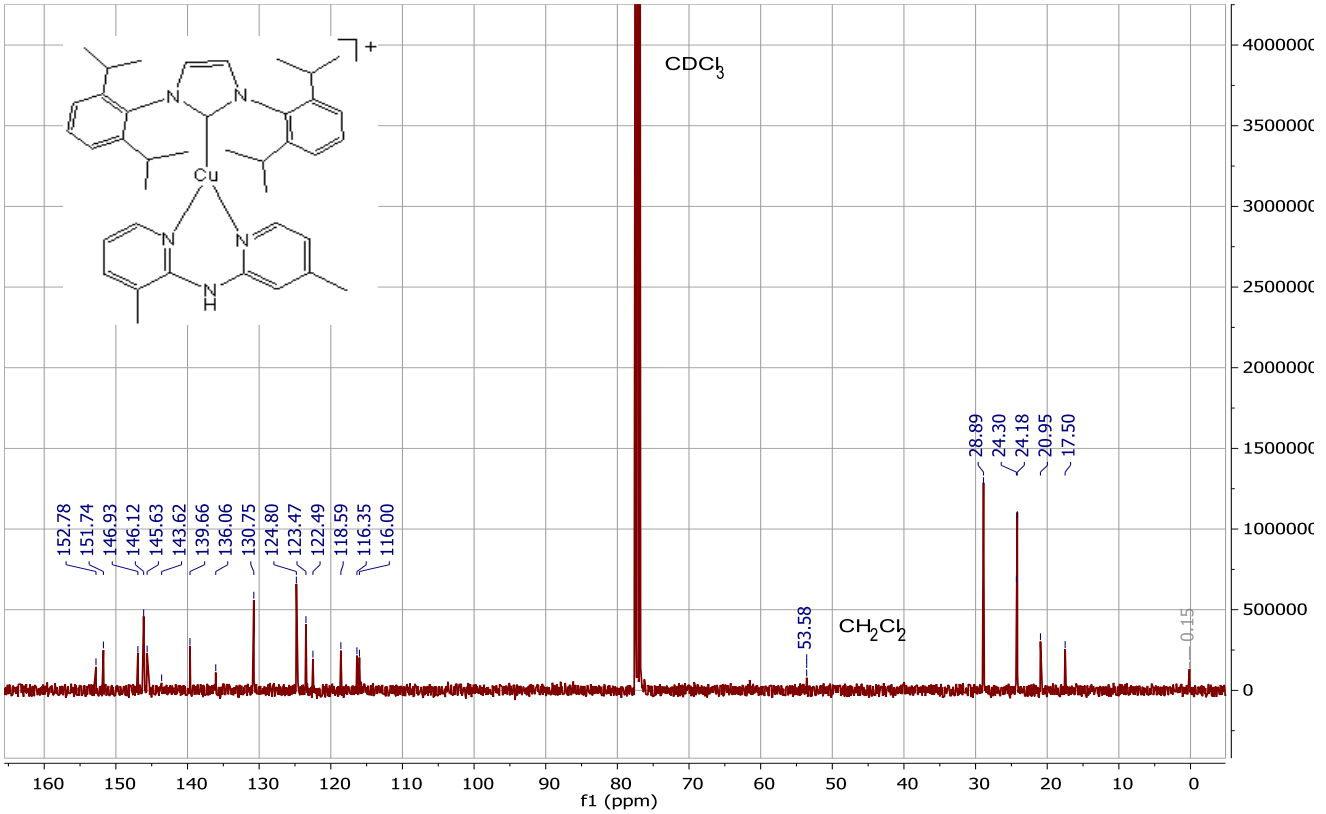


**Figure S38**. $^{13}$C NMR spectrum of [Cu(IPr)(3,4'-$Me_2$Hdpa)]$PF_6$ (**1**) in $CDCl_3$

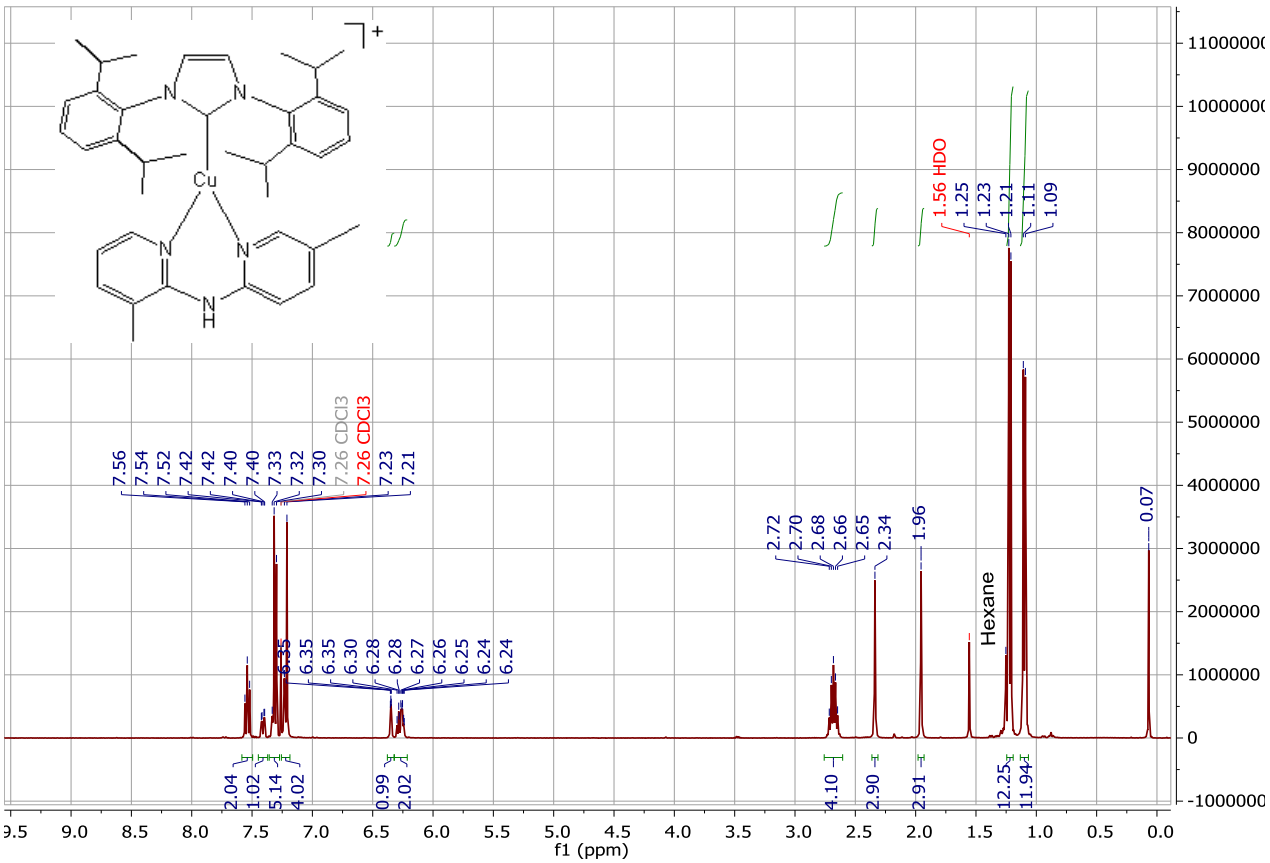


**Figure S39**. $^{1}$H NMR spectrum of [Cu(IPr)(3,5'-Me$_2$Hdpa)]PF$_6$ (**2**) in CDCl$_3$

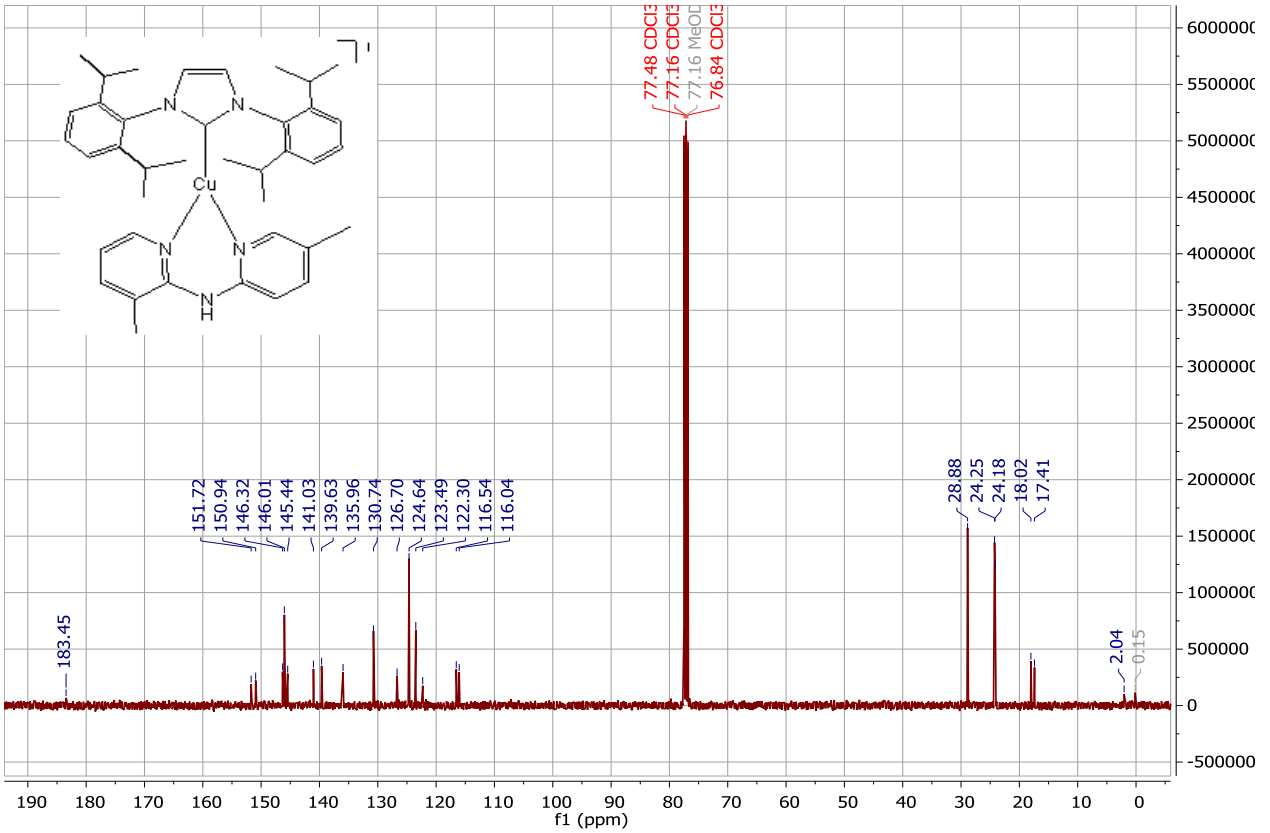


**Figure S40**. $^{13}$C NMR spectrum of [Cu(IPr)(3,5'-Me$_2$Hdpa)]PF$_6$ (**2**) in CDCl$_3$

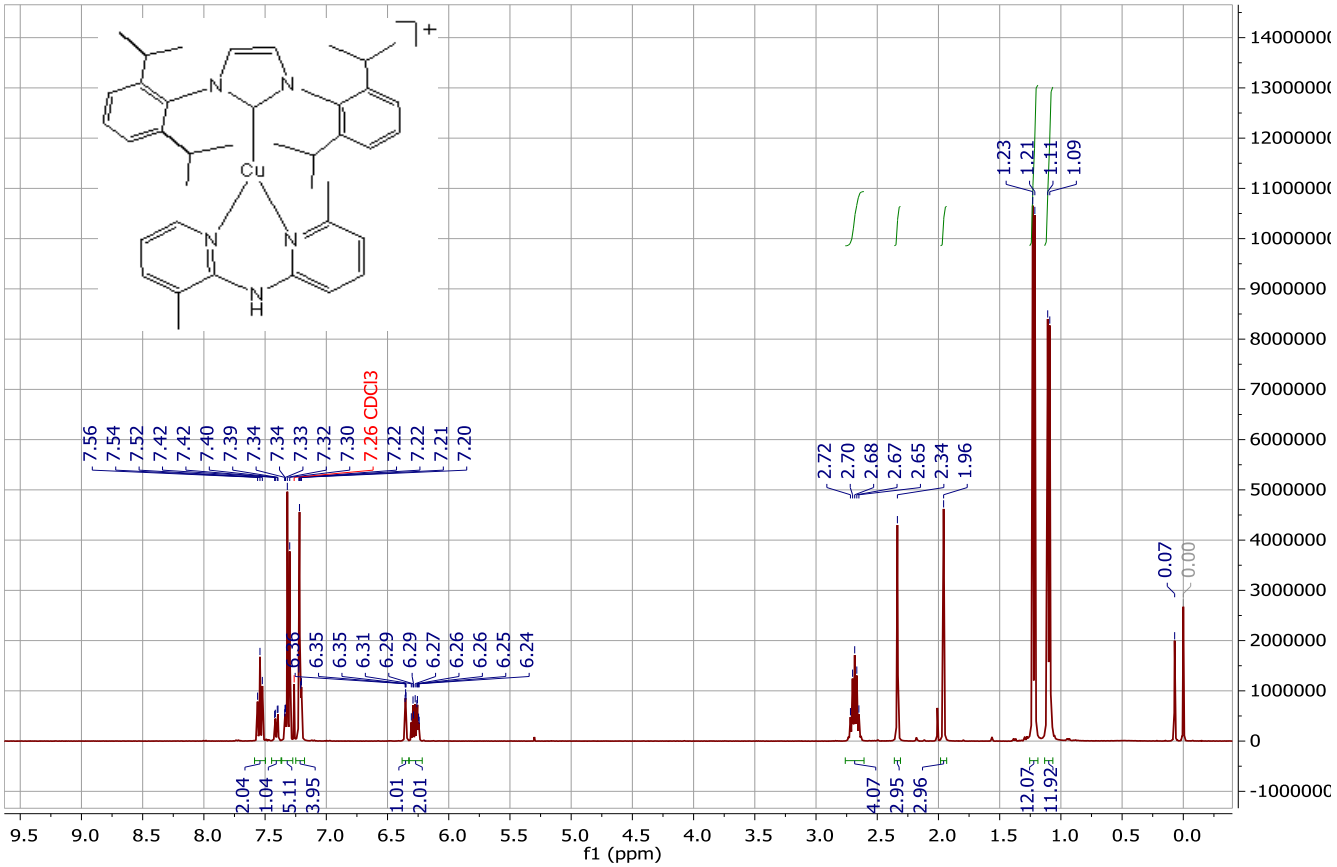


**Figure S41**. $^{1}$H NMR spectrum of [Cu(IPr)(3,6'-$Me_2$Hdpa)]$PF_6$ (**3**) in $CDCl_3$

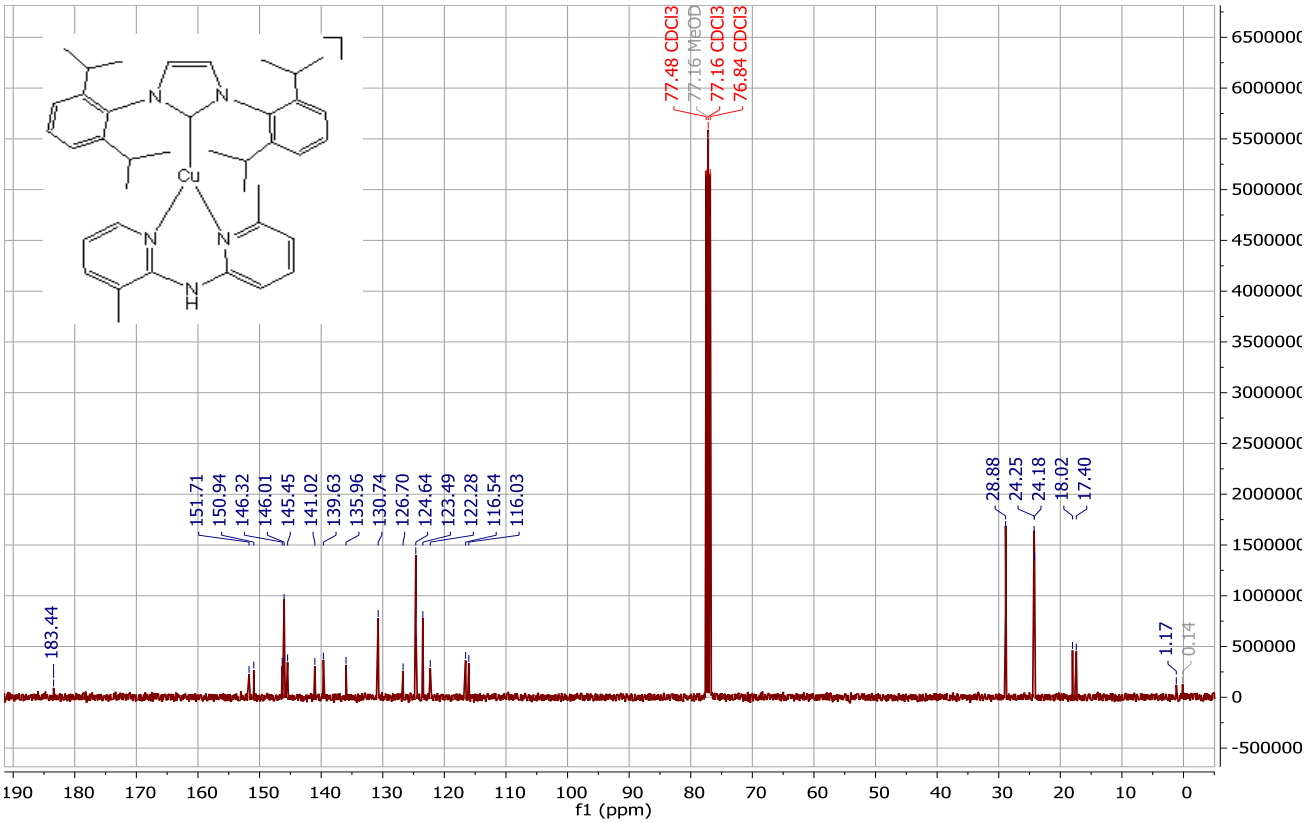


**Figure S42**. $^{13}$C NMR spectrum of [Cu(IPr)(3,6'-$Me_2$Hdpa)]$PF_6$ (**3**) in $CDCl_3$

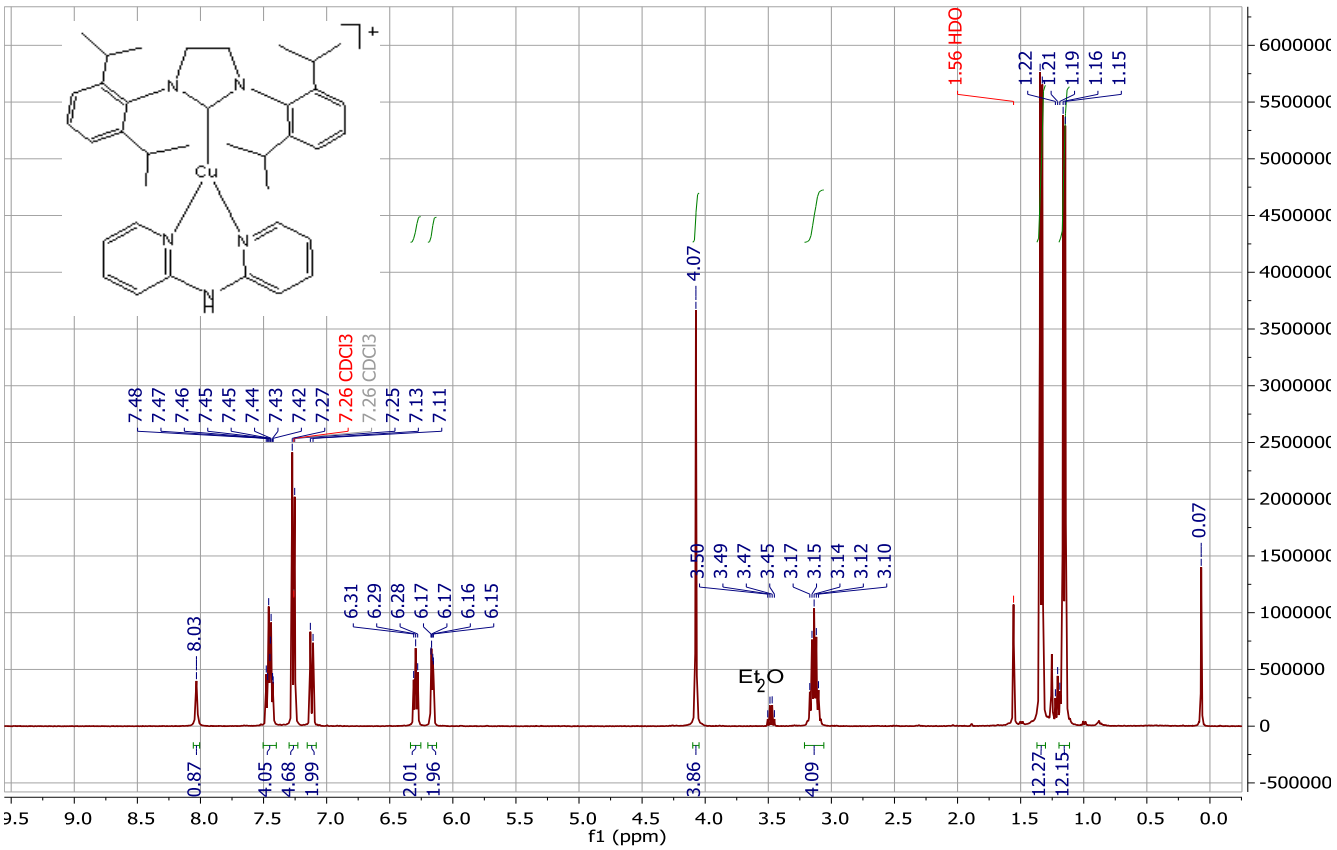


**Figure S43**. $^{1}$H NMR spectrum of [Cu(SIPr)(Hdpa)]$PF_6$ (**10**) in $CDCl_3$

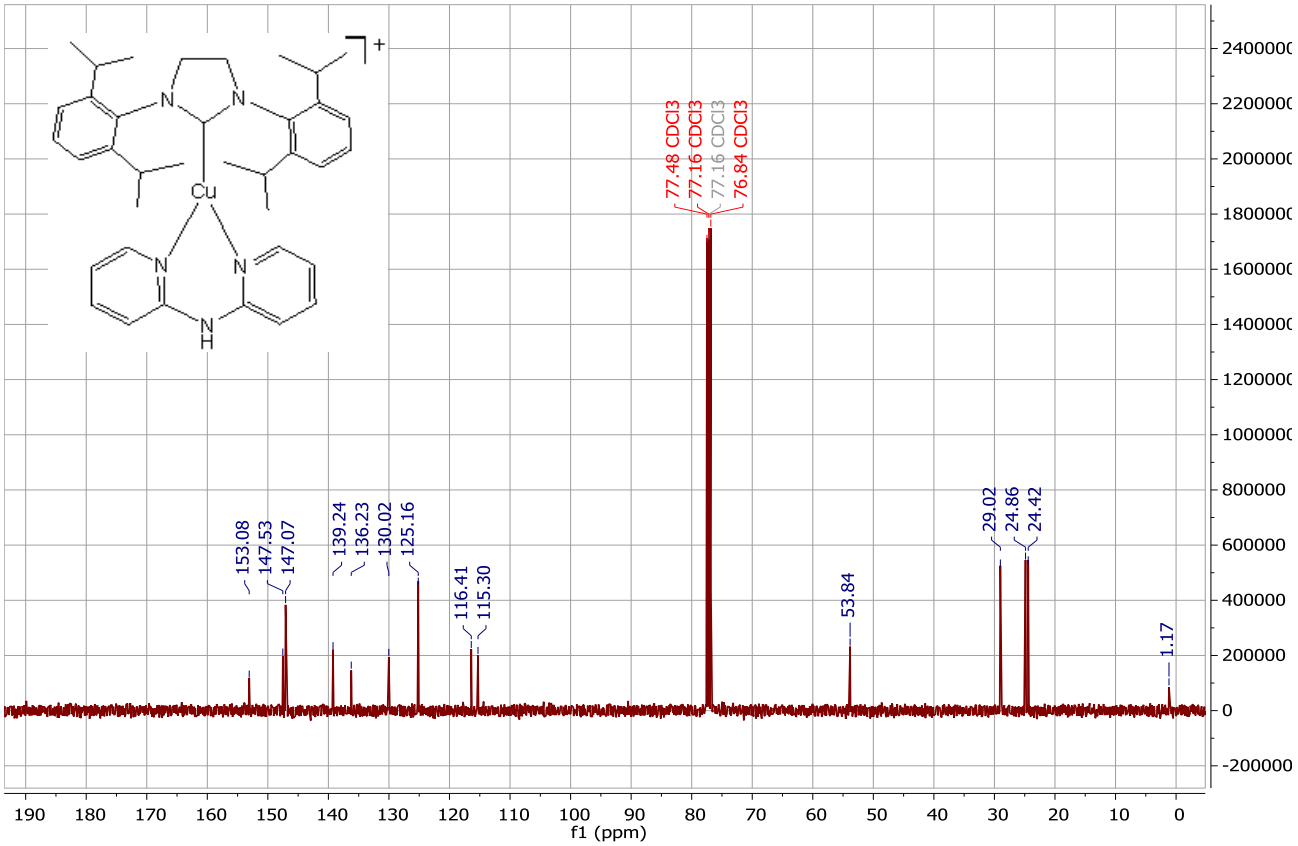


**Figure S44**. $^{13}$C NMR spectrum of [Cu(SIPr)(Hdpa)]$PF_6$ (**10**) in $CDCl_3$

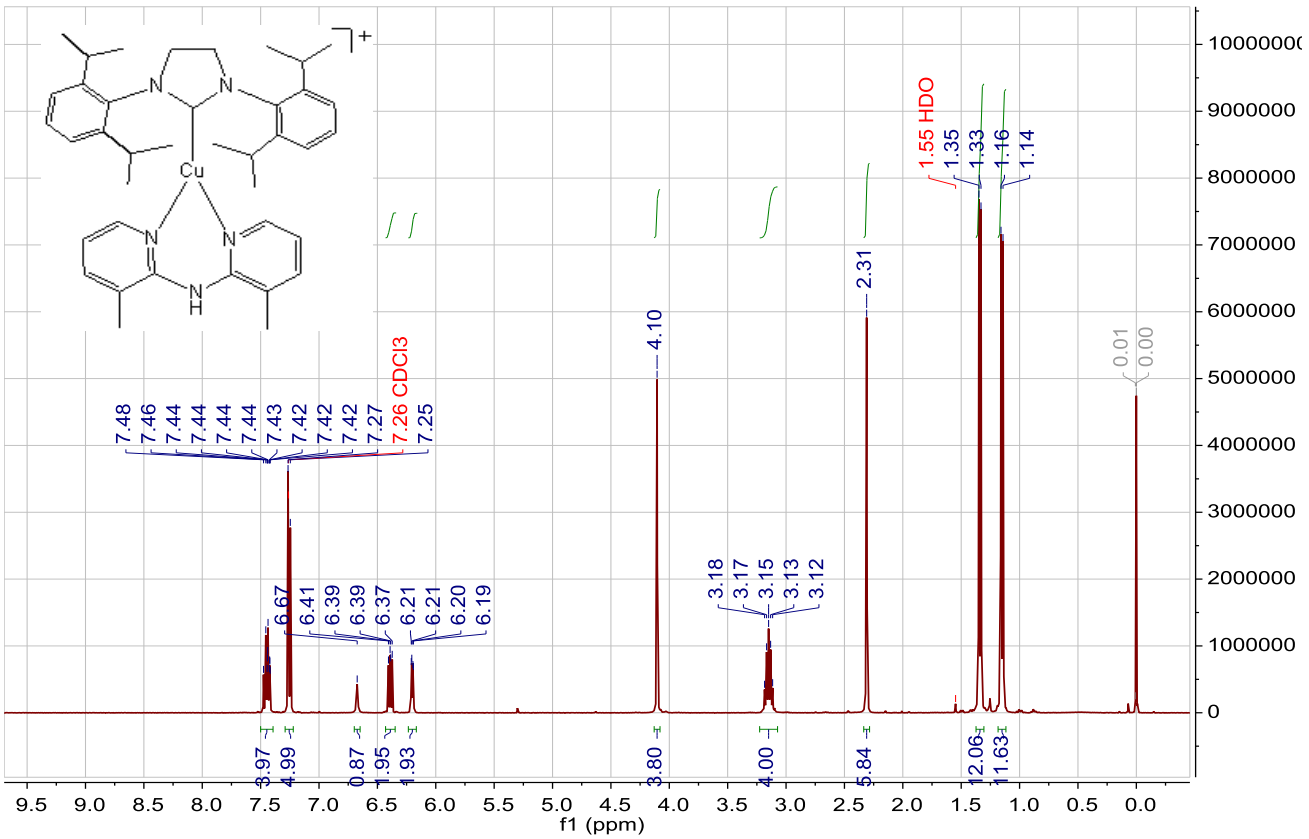


**Figure S45**. $^{1}$H NMR spectrum of [Cu(SIPr)(3,3'-$Me_2$Hdpa)]$PF_6$ (**11**) in $CDCl_3$

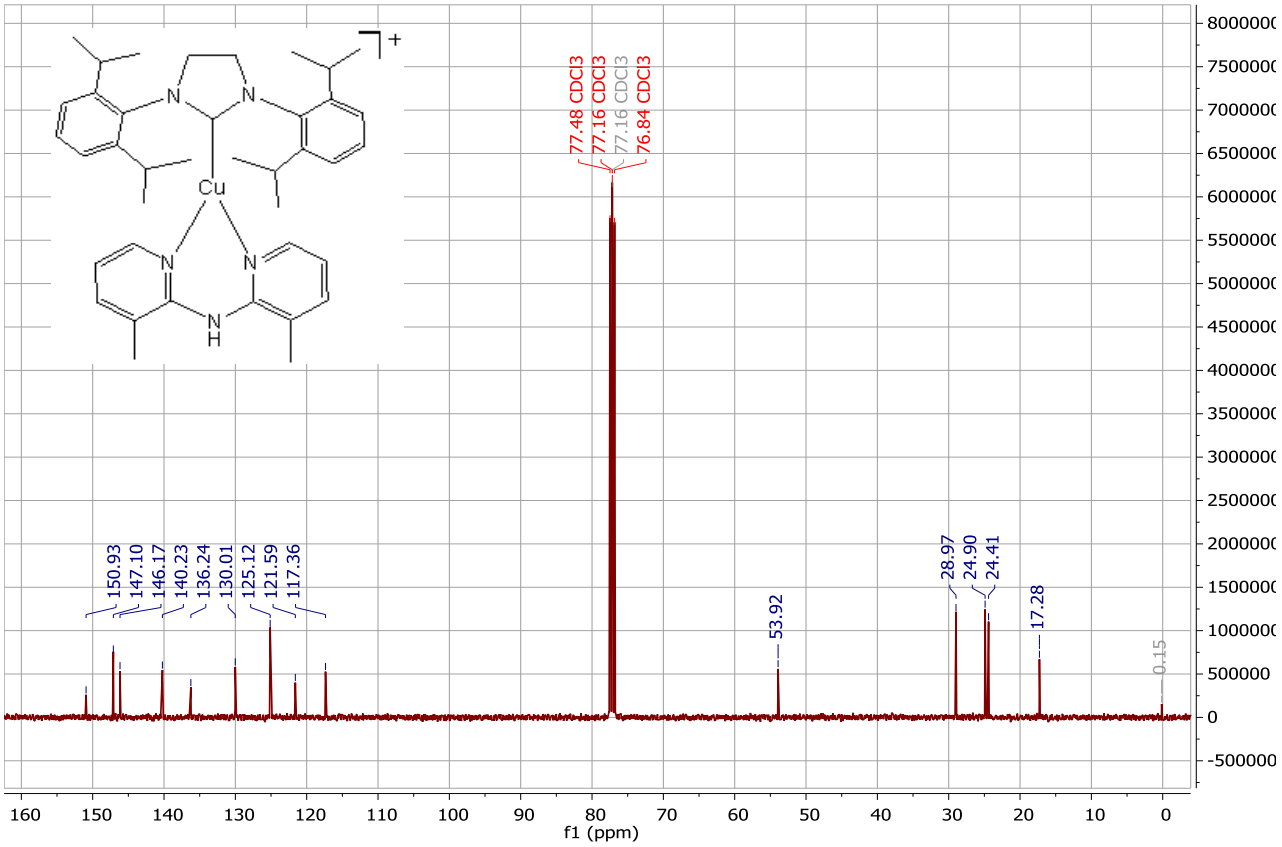


**Figure S46**. $^{13}$C NMR spectrum of [Cu(SIPr)(3,3'-$Me_2$Hdpa)]$PF_6$ (**11**) in $CDCl_3$

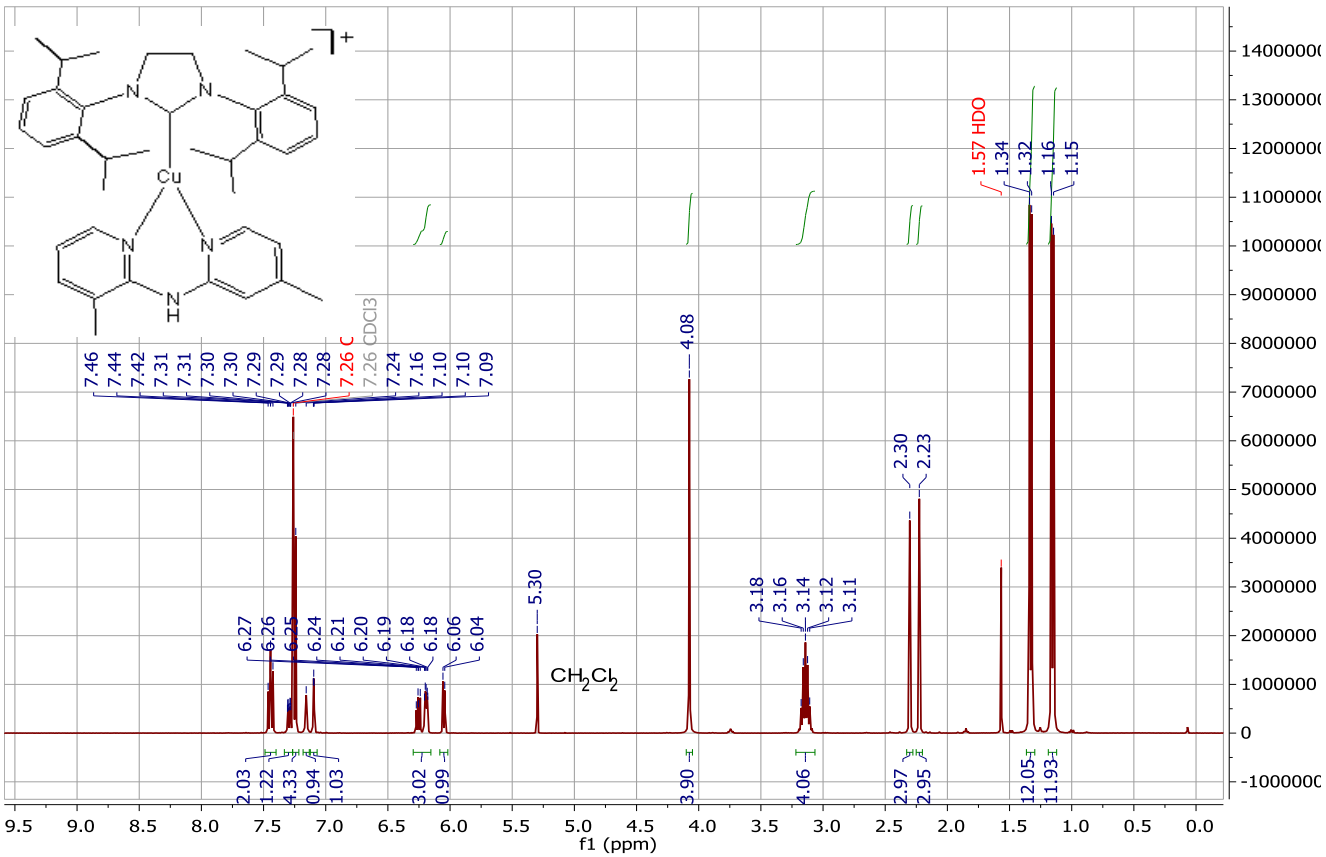


**Figure S47**. $^{1}$H NMR spectrum of [Cu(SIPr)(3,4'-Me$_2$Hdpa)]PF$_6$ (**7**) in CDCl$_3$

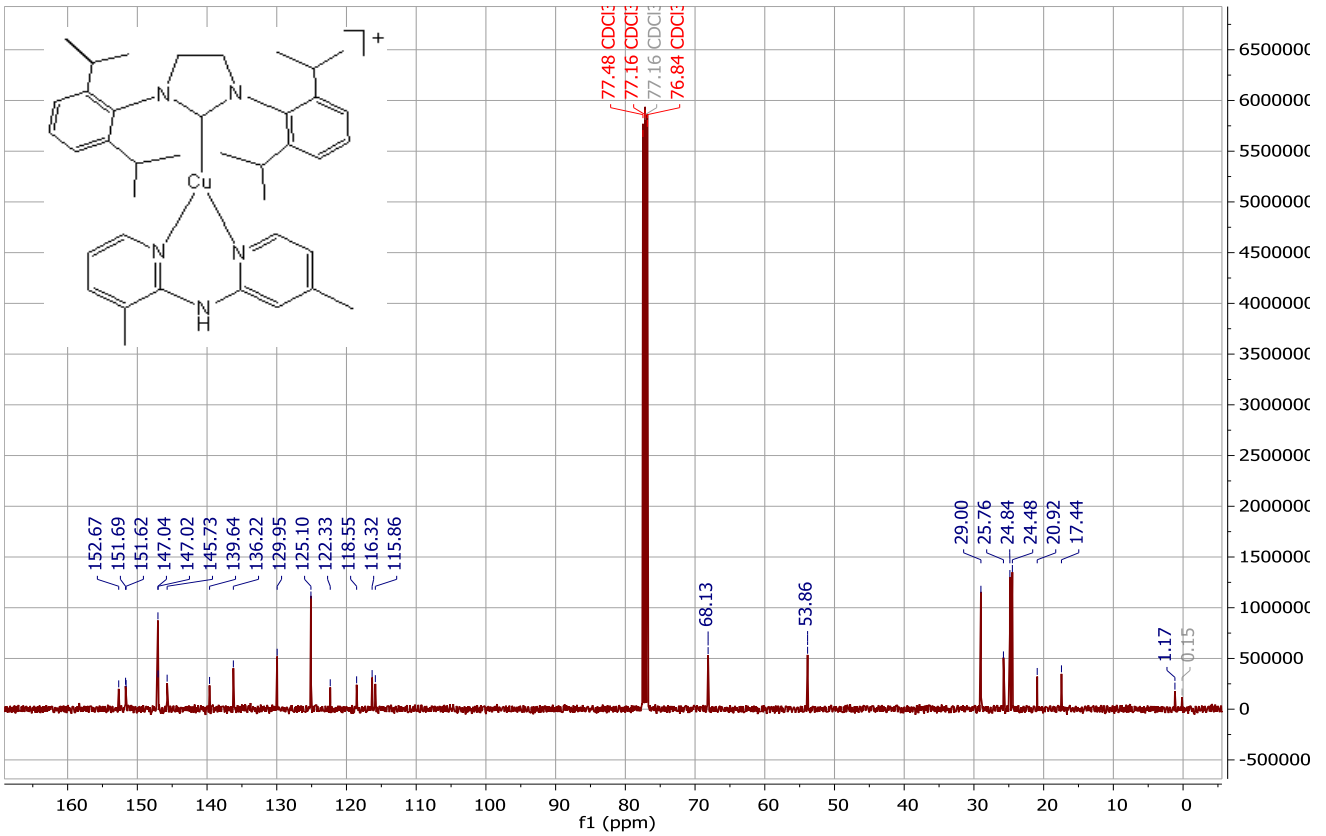


**Figure S48**. $^{13}$C NMR spectrum of [Cu(SIPr)(3,4'-Me$_2$Hdpa)]PF$_6$ (**7**) in CDCl$_3$

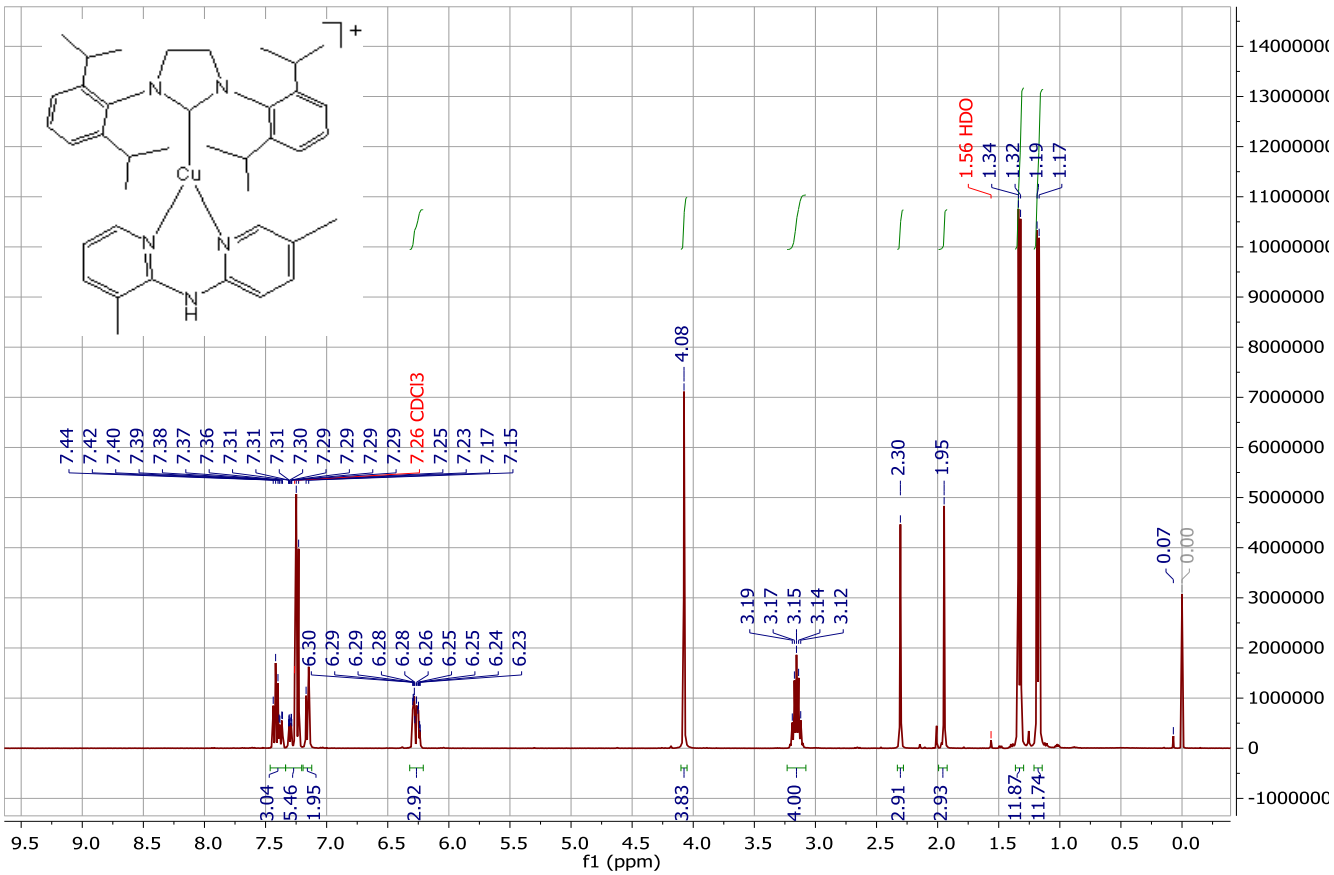


**Figure S49**. $^{1}$H NMR spectrum of [Cu(SIPr)(3,5'-Me$_2$Hdpa)]PF$_6$ (**8**) in CDCl$_3$

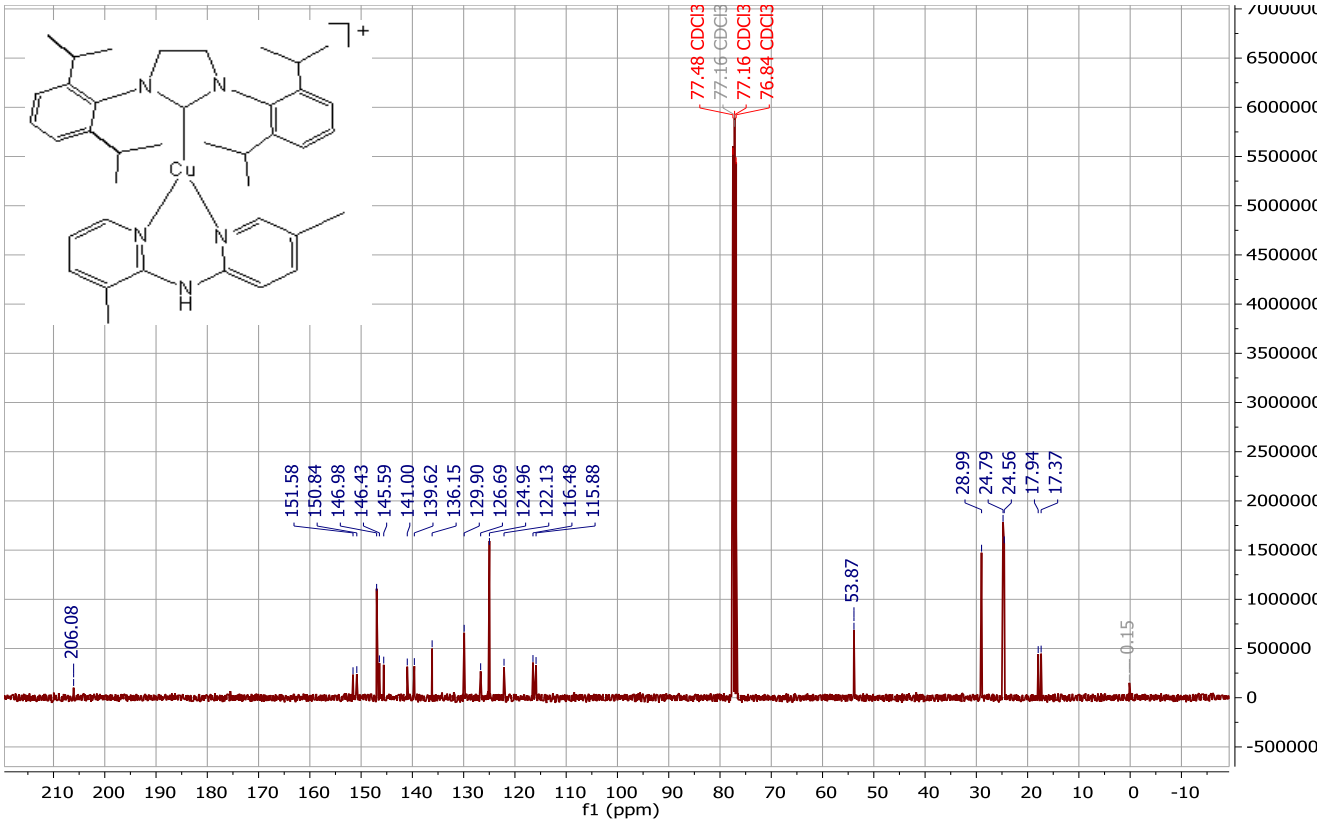


**Figure S50**. $^{13}$C NMR spectrum of [Cu(SIPr)(3,5'-Me$_2$Hdpa)]PF$_6$ (**8**) in CDCl$_3$

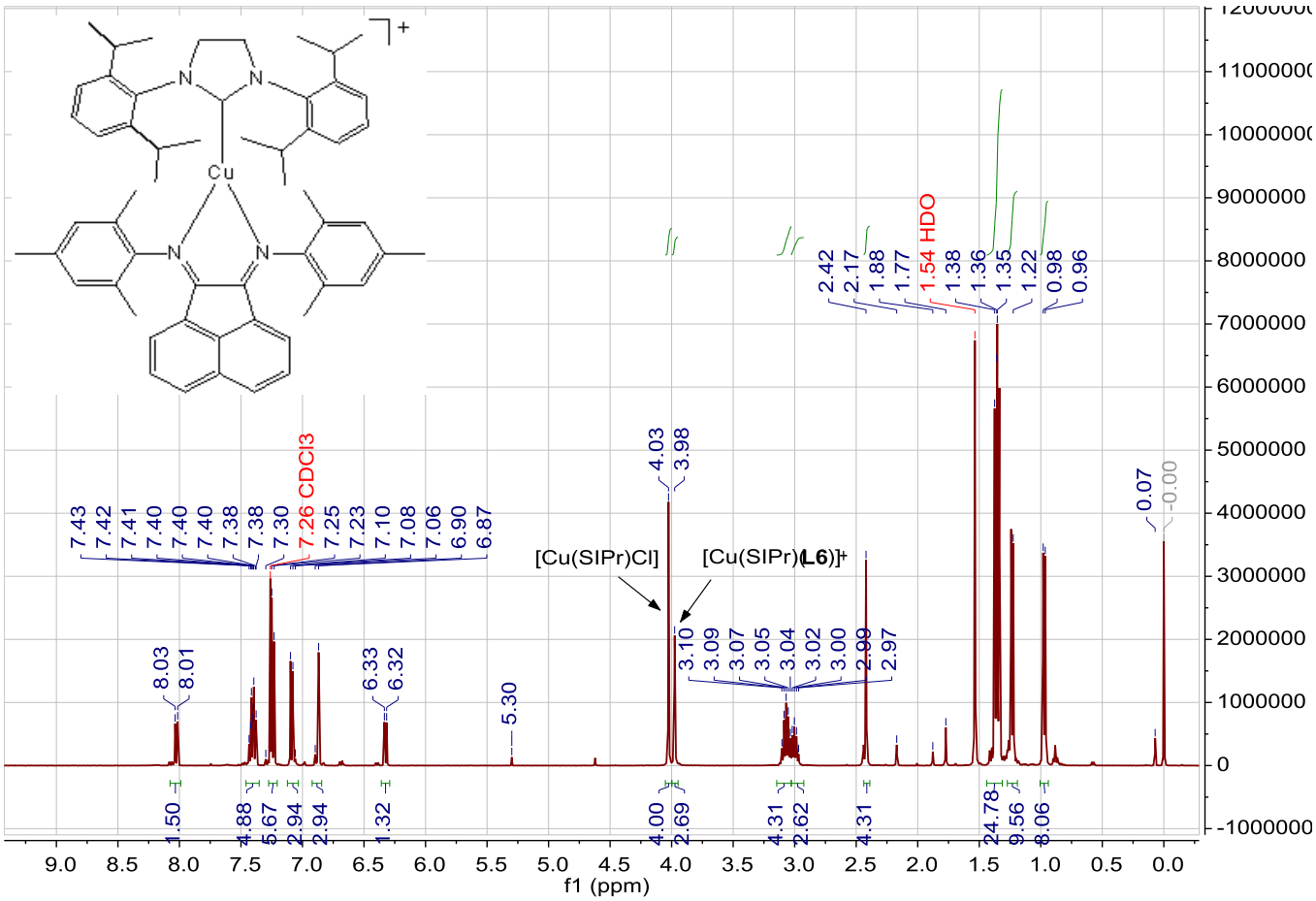


**Figure S51**. $^{1}$H NMR spectrum of a mixture of [Cu(SIPr)(mesBIAN)]$PF_6$ (**12**) and [Cu(SIPr)Cl] in $CDCl_3$

**References**


(1) APEX2, V., Bruker AXS, Madison, WI, USA, 2006.
(2) Bruker SAINT-plus; Version 6.29 ed.; Bruker AXS: Madison, WI, USA,: 2001.
(3) G. M. Sheldrick, S., Version 2.10, Bruker AXS Inc., Madison, WI, USA, 2000.
(4) G. M. Sheldrick, Version 6.14 ed.; Bruker AXS: Madison, WI, USA,: 2000.
(5) L. Farrugia, *J. Appl. Crystallogr.* 1997, **30**, 565.
(6) M. J. Frisch, G. W. Trucks, H. B. Schlegel, G. E. Scuseria, M. A. Robb0, J. R. Cheeseman, G. Scalmani, V. Barone, B. Mennucci, G. A. Petersson, H. Nakatsuji, M. Caricato, X. Li, H. P. Hratchian, A. F. Izmaylov, J. Bloino, G. Zheng, J. L. Sonnenberg, M. Hada, M. Ehara, K. Toyota, R. Fukuda, J. Hasegawa, M. Ishida, T. Nakajima, Y. Honda, O. Kitao, H. Nakai, T. Vreven, J. A., Jr. Montgomery, J. E. Peralta, F. Ogliaro, M. Bearpark, J. J. Heyd, E. Brothers, K. N. Kudin, V. N. Staroverov, R. Kobayashi, J. Normand, K. Raghavachari, A. Rendell, J. C. Burant, S. S. Iyengar, J. Tomasi, M. Cossi, N. Rega, N. J. Millam, M. Klene, J. E. Knox, J. B. Cross, V. Bakken, C. Adamo, J. Jaramillo, R. Gomperts, R. E. Stratmann, O. Yazyev, A. J. Austin, R. Cammi, C. Pomelli, J. W. Ochterski, R. L. Martin, K. Morokuma, V. G. Zakrzewski, G. A. Voth, P. Salvador, J. J. Dannenberg, S. Dapprich, A. D. Daniels, Ö. Farkas, J. B. Foresman, J. V. Ortiz, J. Cioslowski, D. J. Fox, Gaussian 09, Revision D.01; Gaussian, Inc.: Wallingford, CT, 2009.
(7) A. D. Becke, *J. Chem. Phys.*, 1993, **98**, 5648.
(8) Y. Zhao and D. G. Truhlar, Theor. Chem. Acc., 2008, **120**, 215-41.
(9) J.-D. Chai and M. Head-Gordon, *Phys. Chem. Chem. Phys.*, 2008, **10**, 6615-20.
(10) W. R. Wadt, P. J. Hay, *J. Chem. Phys*., 1985, **82**, 270 + 284 + 299
(11) W. J. Hehre, R. Ditchfield, J. A. Pople, *J. Chem. Phys*. 1972, **56**, 2257.
(12) P. C. Hariharan, J. A. Pople, *Theor. Chim. Acta* 1973, **28**, 213.
(13) V. A. Rassolov, J. A. Pople, M. A. Ratner, T. L. Windus, *J. Chem. Phys*. 1998, **109**, 1223.
(14) A. J. H. Wachters, *J. Chem. Phys*. 1970, **52**, 1033.
(15) P. J. Hay, *J. Chem. Phys*. 1977, **66**, 4377.
(16) K. Raghavachari, G. W. Trucks, *J. Chem. Phys*. 1989, **91**, 1062.
(17) T. Clark, J. Chandrasekhar, G. W. Spitznagel, P. V. R. Schleyer, *J. Comput. Chem*. 1983, **4**, 294.
(18) M. J. Frisch, J. A. Pople, J. S. Binkley, *J. Chem. Phys*. 1984, **80**, 3265.
(19) F. Weigend, R. Ahlrichs, *Phys. Chem. Chem. Phys*. 2005, **7**, 3297.
(20) L. Rustioni, F. Di Meo, M. Guillaume, O. Failla, P. Trouillas, *Food Chem*. 2013, **141**, 4349.